

Electronic Thesis and Dissertation Repository

4-21-2015 12:00 AM

A Comprehensive Study Of Esterification Of Free Fatty Acid To Biodiesel In a Simulated Moving Bed System

Nillohit Mitra Ray, *The University of Western Ontario*

Supervisor: Ajay K. Ray, *The University of Western Ontario*

A thesis submitted in partial fulfillment of the requirements for the Doctor of Philosophy degree in Chemical and Biochemical Engineering

© Nillohit Mitra Ray 2015

Follow this and additional works at: <https://ir.lib.uwo.ca/etd>



Part of the [Process Control and Systems Commons](#)

Recommended Citation

Mitra Ray, Nillohit, "A Comprehensive Study Of Esterification Of Free Fatty Acid To Biodiesel In a Simulated Moving Bed System" (2015). *Electronic Thesis and Dissertation Repository*. 2743.
<https://ir.lib.uwo.ca/etd/2743>

This Dissertation/Thesis is brought to you for free and open access by Scholarship@Western. It has been accepted for inclusion in Electronic Thesis and Dissertation Repository by an authorized administrator of Scholarship@Western. For more information, please contact wlsadmin@uwo.ca.

**A COMPREHENSIVE STUDY OF ESTERIFICATION OF FREE FATTY ACID
TO BIODIESEL IN A SIMULATED MOVING BED SYSTEM**

(Thesis format: Integrated Article)

by

NILLOHIT MITRA RAY

Graduate Program in Chemical and Biochemical Engineering

A thesis submitted in partial fulfillment
of the requirements for the degree of PhD

The School of Graduate and Postdoctoral Studies
The University of Western Ontario
London, Ontario, Canada

© Nillohit Mitra Ray, 2015

Abstract

Simulated Moving Bed (SMB) systems are used for separations that are difficult using traditional separation techniques. Due to the advantage of adsorption-based chromatographic separation, SMB has shown promising application in petrochemical and sugar industries, and of late, for chiral drug separations. In recent years, the concept of integration of reaction and in-situ separation in a single unit has achieved considerable attention. The simulated moving bed reactor (SMBR) couples both these unit operations bringing down the operation costs while improving the process performance, particularly for products that require mild operating conditions. However, its application has been limited due to complexity of the SMBR process. Hence, to successfully implement a reaction in SMB, a detailed understanding of the design and operating conditions of the SMBR corresponding to that particular reaction process is necessary.

Biodiesel has emerged as a viable alternative to petroleum-based diesel as a renewable energy source in recent years. Biodiesel can be produced by esterification of free fatty acids (present in large amounts in waste oil) with alcohol. The reaction is equilibrium-limited, and hence, to achieve high purity, additional purification steps increase the production cost. Therefore, combining reaction and separation in SMBR to produce high purity biodiesel is quite promising in terms of bringing down the production cost.

In this work, the reversible esterification reaction of oleic acid with methanol catalyzed by Amberlyst 15 resin to form methyl oleate (biodiesel) in SMBR has been investigated both theoretically and experimentally. First, the adsorption and kinetic constants were determined for the biodiesel synthesis reaction by performing experiments in a single column packed with Amberlyst 15, which acts as both adsorbent and catalyst. Thereafter, a rigorous model was used to describe the dynamic behaviour of multi-column SMBR followed by experimental verification of the mathematical model. Sensitivity analysis is done to determine robustness of the model. Finally, a few simple multi-objective optimization problems were solved that included both existing and design-stage SMBRs using non-dominated sorting genetic algorithm (NSGA). Pareto-optimal solutions were

obtained in both cases, and moreover, it was found that the performance of the SMBR could be improved significantly under optimal operating conditions.

Keywords

Simulated moving bed reactor, Modeling, Multi-objective optimization, Biodiesel, Integrated reactor-separator, Multi-functional reactor, Genetic algorithm.

Co-Authorship Statement

Chapters 3, 4 and 5 of this thesis have been submitted for publication to the Canadian Journal of Chemical Engineering.

Article title:

Determination of Adsorption and Kinetic Parameters for Methyl Oleate Esterification Reaction in a Plug Flow Reactor Catalyzed by Amberlyst 15

Authors:

Nillohit Mitra Ray, Ajay K. Ray

Status:

Submitted to Canadian Journal of Chemical Engineering (2015)

Individual contributions:

The manuscript was written by Nillohit Mitra Ray who also conducted experimental analysis and numerical simulations. The work was supervised by Ajay Ray.

Article title:

Modeling, Simulation and Experimental Study of a Simulated Moving Bed Reactor for the Synthesis of Biodiesel

Authors:

Nillohit Mitra Ray, Ajay K. Ray

Status:

Submitted to Canadian Journal of Chemical Engineering (2015)

Individual contributions:

The manuscript was written by Nillohit Mitra Ray who also conducted experimental analysis and numerical simulations. The work was supervised by Ajay Ray.

Article title:

Multi-objective Optimization of Biodiesel Synthesis in Simulated Moving Bed Reactor

Authors:

Nillohit Mitra Ray, Ajay K. Ray

Status:

Submitted to Canadian Journal of Chemical Engineering (2015)

Individual contributions:

The manuscript was written by Nillohit Mitra Ray who also conducted analysis and numerical simulations. The work was supervised by Ajay Ray.

Acknowledgments

I would like to thank my supervisor, Dr. Ajay Kumar Ray without whose constant support and guidance I would not have been able to undertake this long and arduous task of completing my PhD. He has supported me not only academically, but also in other aspects of life due to which I was able to keep myself together through the various highs and lows of my life in Canada. Throughout the entire course of PhD, he has been a friend, philosopher and guide to me. I extend my sincere and heartfelt gratitude to him.

I extend my sincere thanks to Pankaj Chowdhury, Krupal Pal, Housyn Mahmoud, Gureet Chandhok for endowing me both with their friendship and academic guidance from time to time. My gratitude also goes to Souheil Afara, Luis Pastor, José Munoz and Brian Dennis who helped me with the various technical aspects of the instruments I was working with. My thanks to my good colleagues; Ghodsieh Malekshoar, Shimin Mao, Noshin Hashim, Gloria Kumordzi, Kyriakos Manoli, Naeimeh Faraji for providing me with a nice working environment, and also their friendship.

My special thanks go to my friend and colleague, Pegah Saremirad who helped me during a crucial stage of experiment, thereby removing a very tricky roadblock. Thank you Pegah! for your help and mental support which you regularly provided me. It is very much appreciated and cherished.

Last but not at all the least, I extend my heartfelt gratitude to my parents; Dr. Swapan Kumar Mitra Ray & Ratna Mitra Ray, whose unconditional love and support has made me what I am today.

Table of Contents

Abstract	ii
Co-Authorship Statement.....	iv
Acknowledgments.....	vi
Table of Contents	vii
List of Tables	xii
List of Figures	xiii
List of appendices	xv
Chapter 1	1
1 Introduction.....	1
1.1 Background.....	1
1.2 Application of SMBR for Production of Biodiesel.....	3
1.3 Optimization of SMBR.....	4
1.4 Research objective	6
1.5 Thesis outline	6
1.6 References.....	8
Chapter 2.....	13
2 Literature review.....	13
2.1 Chromatography: A Brief Introduction	13

2.2 Chromatographic Reactor	14
2.3 Batch Chromatographic Reactor.....	15
2.4 Continuous Chromatographic Reactor.....	17
2.4.1 Annular Rotating Chromatographic Reactor	17
2.4.2 Countercurrent Chromatographic Reactor	19
2.4.2.1 True Countercurrent Moving Bed Chromatographic Reactor	19
2.4.2.2 Simulated Countercurrent Moving Bed Chromatographic Reactor.....	24
2.5 Design strategies proposed for Simulated Moving Bed systems.....	44
2.5.1 Theory proposed by research group at University of Minnesota.....	44
2.5.2 Theory proposed by research group at ETH, Zurich	46
2.5.2.1 Linear isotherm	48
2.5.2.2 Nonlinear isotherm.....	50
2.5.3 Standing Wave Theory proposed by research group at Purdue University	55
2.5.3.1 Neglecting axial dispersion and mass transfer resistance	58
2.5.3.2 Linear system with axial dispersion and mass transfer resistance	60
2.6 Biodiesel - A Brief Introduction	61
2.6.1 Current processes for biodiesel production.....	63
2.6.2 Choice of Catalyst: Homogenous vs. Heterogeneous.....	64
2.6.3 Amberlyst 15 as catalyst	65

2.6.4 Production of biodiesel by simulated moving bed technology, a reactive – separation method	67
2.7 References	69
Chapter 3	90
3 Determination of Adsorption and Kinetic Parameters for Methyl Oleate Esterification Reaction in a Plug Flow Reactor Catalyzed by Amberlyst 15	90
3.1 Introduction	90
3.2 Adsorbent and Catalyst	92
3.3 Reaction Kinetics	93
3.4 Kinetic Model	94
3.5 Experimental details	95
3.5.1 Materials used	95
3.5.2 Experimental set-up	95
3.5.3 Experimental procedure	96
3.5.4 Analysis	96
3.6 Mathematical model	96
3.7 Results and Discussion: Determination of Adsorption and Kinetic Parameters	98
3.7.1 Non-reactive breakthrough experiments	98
3.7.2 Reactive breakthrough experiments	101
3.7.3 Estimation of external and internal diffusion resistance	104
3.8 Conclusions	105

3.9	References.....	106
Chapter 4	109
4	Modeling, Simulation and Experimental Study of a Simulated Moving Bed Reactor for the Synthesis of Biodiesel.....	109
4.1	Introduction.....	109
4.2	Synthesis of Biodiesel in SMBR.....	110
4.3	Mathematical Model	113
4.4	Experimental Details.....	117
4.4.1	Materials Used	118
4.4.2	Experimental Set-up.....	119
4.5	Results and Discussion	120
4.5.1	Effect of Switching Time.....	122
4.5.2	Effect of Raffinate Flow Rate.....	126
4.5.3	Effect of Feed Flow Rate	130
4.6	Sensitivity Studies.....	133
4.7	Conclusions.....	135
4.8	References.....	136
Chapter 5	140
5	Multi-objective Optimization of Biodiesel Synthesis in Simulated Moving Bed Reactor	140
5.1	Introduction.....	140

5.2 Multi-objective Optimization.....	141
5.3 Optimization Methodology - Genetic Algorithm	142
5.4 Mathematical model of SMBR	147
5.5 Optimization of biodiesel production in SMB.....	151
5.6 Optimization of Existing Setup.....	155
5.7 Design stage optimization.....	162
5.8 Conclusions.....	167
5.9 References.....	167
Chapter 6.....	170
6 Conclusion and future recommendations.....	170
6.1 Conclusions.....	170
6.2 Major contributions of this research	172
6.3 Recommendations for future work	172
Appendices.....	175
Curriculum Vitae	187

List of Tables

Table 2.1 Description of various reactive systems on SMBR	28
Table 2.2 Biodiesel by reactive separation	67
Table 3.1 Properties of Amberlyst 15 dry.....	92
Table 3.2 Adsorption equilibrium constants and apparent dispersion coefficients of methyl oleate (MO) and water (WA).....	99
Table 3.3 Adsorption constant of Oleic Acid (K_{OA}), reaction rate constant (K_f) and equilibrium constant (K_{Eq}) for synthesis of Methyl Oleate from Oleic Acid	102
Table 4.1 Adsorption equilibrium constants and dispersion coefficients of methyl oleate (MO), water (W) and oleic acid (A) along with forward reaction rate constant and equilibrium constant.....	115
Table 4.2 Comparison of σ and V (cm/min) values of methyl oleate and water in various sections of SMBR under different experimental conditions.....	121
Table 5.1 Optimization problems along with their objective functions, constraints, decision variables and fixed parameters	154
Table 5.2 Numerical parameter values used in NSGA optimization.....	155

List of Figures

Figure 1.1 Concept of Pareto set.....	5
Figure 2.1 Operating principle of a batch chromatographic reactor	15
Figure 2.2 Annular rotating chromatographic reactor	18
Figure 2.3 True Countercurrent Moving Bed Reactor	22
Figure 2.4 Schematic diagram of a 4-section, 8-column SMBR system.....	25
Figure 2.5 Comparison of a 6-column SMBR with a 6-column VARICOL	27
Figure 2.6 System described by a Linear Adsorption Isotherm	50
Figure 2.7 Triangle theory described by nonlinear adsorption isotherm	51
Figure 2.8 Effect of overall feed concentration on the region of complete separation in the m_2 , m_3 plane	52
Figure 2.9 Application of triangle theory for optimal operating conditions in SMB	54
Figure 2.10 Standing wave theory for a linear TMB system	56
Figure 2.11 A general scheme for transesterification reaction	62
Figure 2.12 Amberlyst 15 polymer.....	66
Figure 3.1 Non-reactive breakthrough of Methyl Oleate - Water system	100
Figure 3.2 Reactive breakthrough of Oleic Acid – Methyl Oleate – Water system.	103
Figure 4.1 Schematic diagram of a SMBR system.....	110
Figure 4.2 Experimental setup of a 4-column SMBR system	119
Figure 4.3 Effect of switching time on SMBR performance	124

Figure 4.4 Effect of switching time on cyclic steady state concentration profiles of methyl oleate-water-oleic acid. (a) 12min, (b) 8min, (c) 17min	125
Figure 4.5 Effect of raffinate flow rate on SMBR performance.....	128
Figure 4.6 Effect of raffinate flow rate on cyclic steady state concentration profiles of methyl oleate-water-oleic acid. (a) $\beta Q_P = 1\text{ml/min}$, (b) $\beta Q_P = 1.66\text{ml/min}$, (c) $\beta Q_P = 2\text{ml/min}$	129
Figure 4.7 Effect of feed flow rate on SMBR performance	131
Figure 4.8 Effect of feed flow rate cyclic steady state concentration profiles of methyl oleate-water-oleic acid. (a) $\alpha Q_P = 0.05\text{ml/min}$, (b) $\alpha Q_P = 0.1\text{ml/min}$, (c) $\alpha Q_P = 0.2\text{ml/min}$	132
Figure 4.9 Sensitivity analysis of various process parameters on synthesis of methyl oleate	134
Figure 5.1 Schematic diagram of a 4-column SMBR.....	147
Figure 5.2 Pareto optimal solutions and corresponding operating variables for maximizing yield and purity of biodiesel	158
Figure 5.3 Steady state concentration profiles of methyl oleate-water-oleic acid system; (a) corresponding to point 1 & (b) corresponding to point 2 of figure 5.2a	159
Figure 5.4 Pareto optimal solutions and corresponding operating variables for maximizing purity and minimizing desorbent consumption	162
Figure 5.5 Pareto solutions for maximizing yield and purity with column length as a design stage parameter	164
Figure 5.6 Pareto solutions for maximizing purity and minimizing desorbent consumption	166

List of appendices

Appendix A: A schematic representation of NSGA.....	195
Appendix B: Raw data for non-reactive breakthrough experiments.....	196
Appendix C: Raw data for reactive breakthrough experiments.....	201

Nomenclature

a, OA	Oleic acid
c_i	Mobile phase concentration of component i [mol/lit]
D_i	Dispersion coefficient of component i [$\times 10^6$ m ² /sec]
F	Error function [mol ² /lit ²]
H	Henry's constant
K_{eq}	Reaction equilibrium constant [mol/lit]
K_f	Forward reaction rate constant [$\times 10^2$ /sec]
K_i	Adsorption equilibrium constant of component i
L	Length of section or column [m]
m	Flow rate ratio parameter
ME	Methyl Ester (or methyl oleate)
N	Sorption capacity, number of columns, number of switching
P_{ME}	Purity of methyl ester
p, q, r, s	Number of columns in sections P, Q, R and S respectively
q_i	Solid phase concentration of component i [mol/lit]
Q_P, Q_Q, Q_R, Q_S	Flow rates in sections P, Q, R and S respectively [lit/min]
t	Time [mins]
t_s	Switch time [mins]
u_g	Mobile phase velocity [m/sec]
u_s	Solid flow velocity [m/sec]
V_i	Velocity of component i [m/sec]
W	Water
Y_{ME}	Yield of methyl ester
z	Axial coordinate [m]
F, R, D, E	Feed flow rate, Raffinate flow rate, Desorbent flow rate and Extract flow rate respectively [lit/min]

Abbreviations

TMBR	True Moving Bed Reactor
SER	Sorption Enhanced Reaction
SMBR	Simulated Moving Bed Reactor
SCMCR	Simulated Countercurrent Moving Bed Reactor
GA	Genetic Algorithm
NSGA	Non-dominated Sorting Genetic Algorithm
FFA	Free Fatty Acid
PDE	Partial Differential Equation
FDM	Finite Difference Method
ODE-IVP	Ordinary Differential Equation of Initial Value Problem
IMSL	International Mathematics and Statistics Library

Greek letters

α	Ratio of feed flow rate to flow rate in section P
β	Ratio of raffinate flow rate to flow rate in section P
γ	Ratio of desorbent flow rate to flow rate in section P
ϕ	Section
ε	Void fraction
δ	Phase ratio
σ	Relative carrying capacity
ζ	Pseudo solid phase velocity [m/sec]
ρ	Resin density

Chapter 1

1 Introduction

1.1 Background

Separation processes are of significant importance in a wide variety of industrial applications. Integration of reaction and separation may significantly improve the efficiency of process industries. The integration of reaction and separation of the corresponding products in one single unit allows, in addition to obvious savings in equipment costs, significant improvements in process performance, particularly in the case of equilibrium limited reactions [1].

Currently, reactive distillation is the conventional method to carry out chemical reaction and separation simultaneously, which is extensively being used in the petrochemical industry as well as in a number of other industrial applications. However, there is a disadvantage of this process. It cannot be applied to reaction systems where the components involved are either non-volatile or heat sensitive. This is often the case in pharmaceutical and fine chemical industries.

Hence, an alternative to this problem is the use of an integrated chromatographic reactor, which couples reaction with chromatographic separation. The main working principle of the chromatographic reactor is the difference in the adsorption affinities of the various components present in the stationary phase. Preferential adsorption of one of the reaction products will result in the equilibrium being shifted towards the product phase [2]. This process has superior separating power, use of mild conditions and relatively low cost. Hence, it is quite competitive to other separation processes like membrane separation, extraction or crystallization. Also, if chromatographic separation has been used for separation of products before, the lengthy work for screening a suitable solvent is omitted [3]. Before the process is designed only the catalyst has to be chosen for the reaction system. Hence, the cost of process development is significantly reduced.

Since its development in 1960s, chromatographic reactor has been used for preparative as well as analytical purposes in either batch or continuous mode. Recently more importance has been given to the continuous mode, as it is highly efficient in using the stationary phase and lower amount of eluent consumption occurs as compared to the batch mode.

An effective way to design a continuous process is to achieve a countercurrent flow of solid and mobile phase. This concept is utilized in a True Countercurrent Moving Bed Reactor (TMBR). Both irreversible [4-6] and reversible [7-8] reactions systems have been studied in true countercurrent moving bed reactors and high conversion much greater than the equilibrium along with high product purity has been reported in these studies. However, it is quite difficult to carry out reactions when there is actual movement of solid phase. During scaling up to a column of larger diameter, many problems arise; such as adsorbent attrition, fines removal, mechanical difficulties in moving the solid bed, expansion of bed, channeling of the reactor etc. So to bypass these problems, the Simulated Moving Bed (SMB) technology is used. The SMB was first introduced by Chicago-based Universal Oil Products (UOP) in the 1960s [9]. In this technology, the countercurrent movement of the solid-phase and the fluid-phase is simulated (mimicked) by switching the inlet and withdrawal ports simultaneously (synchronously) in the direction of the fluid movement, along a series of fixed columns. This switching is done at a fixed time interval which is determined by the user. For convenience of operation, the SMB system is divided into sections; with each section containing a number of columns, the number being determined depending on the application (based on degree of difficulty of separation) of the system.

The applicability of SMBR has been studied for various reaction systems, for example; reversible reactions [10-13], irreversible reactions [14-17], esterification reactions [18-21], inversion of sugar [22-25], and isomerization reactions [26-28]. These studies show that higher product purity and favorable equilibrium shifts can be obtained in SMBR; hence it has high potential for application to fine chemical and pharmaceutical industries. To increase the flexibility of the process, a modified version of the SMB known as VARICOL [29, 30] was developed which involves non-synchronous switching of the

inlet and outlet ports within a global switching period. Hence, the number of columns in any particular section of the SMBR varies within a switching time interval. This has led to more flexibility in the separation process by allowing better utilization of the stationary phase than the conventional rigid SMB process.

1.2 Application of SMBR for Production of Biodiesel

The continuous increasing demand for energy and the diminishing tendency of petroleum resources has led to the search for alternative renewable and sustainable fuel. Biodiesel is a biodegradable and renewable fuel, emerging as a viable alternative to petroleum diesel. It is a good substitute for petro-diesel and also is most advantageous for its environmental friendliness, particularly due to its good quality exhaust [31]. It is a fatty acid ester produced by either transesterification reaction of triglycerides present in animal fats and vegetable oils with alcohol, or by esterification of free fatty acid present in waste oils with alcohol. This reaction is equilibrium-limited and endothermic; hence it takes place in the presence of acidic or basic catalysts and high temperature. Due to very high purity requirements ($\approx 96.5\%$) [31, 32], additional separation and refining steps are required which increases the cost of biodiesel production. Hence, studies have focused on the application of process intensification to improve the mass transfer, conversion, and product purity, minimization of wastes and usage of energy, and downsizing of equipment in biodiesel systems [2]. This can be achieved by integrating the reaction and separation in a single unit. In this regard, membrane reactors, reactive distillation, reactive adsorption etc. have been employed. While membrane reactors have enhance the rate of reaction by removing products from the reaction mixture and maintaining a reasonable heat and mass transfer between the immiscible phases [33, 34]; reactive distillation combines esterification reaction between fatty acid and methanol and separation by removal of the byproduct water [35, 36], in a single unit for biodiesel production [2].

Another pathway for high conversion is reactive adsorption; also known as sorption enhanced reaction (SER) or chromatographic reactor. It works by shifting the equilibrium

toward the right by preferential adsorption of one of the products. This can be brought about in an SMBR, thus producing high quality biodiesel without the use of extreme temperature and/or pressure. Simulation studies have shown that high purity biodiesel production in SMBR is possible [2], hence SMB technology must be further investigated in this regard. However, due to complexity of SMBR process, it has limited application in industry. For practical and large scale application of this technology, a detailed understanding of its operating conditions is required; followed by optimization of its operating conditions and design parameters.

1.3 Optimization of SMBR

Optimization of SMBR is necessary to realize its true economic potential and for realization of potential industrial application. A few studies were done involving single-objective optimization of SMBR [20] [37-39]. But in practical scenario, optimization of single-objective function is not sufficient, because the various operating parameters of a complex SMB system often act in conflicting ways. Hence, a desirable change in one objective function worsens another objective function [40]. Therefore, for the meaningful design of a SMBR, simultaneous optimization of more than one objective function is highly desirable.

In multi-objective optimization, for conflicting objective functions, one obtains a set of equally good solutions; known as Pareto optimal solutions. In a Pareto set, no single solution can be considered superior to the other solutions with respect to all objective functions. Each solution is better than the other with respect to one objective, but worse with respect to other objectives. Hence, selection of the ‘best’ optimal solution depends on the decision makers and the auxiliary information provided by the user.

Figure 1.1 shows a set of solutions obtained for a process where the yield of the product and its purity act in a conflicting manner. As one move from point P to point Q, both yield and purity increase, hence the solution at point Q is always better than that at point P or for any points between P and Q. But, while moving from Q to R, the yield decreases

and the purity increases. Hence, when all the solution points which lie between Q and R are considered, no single solution can be asserted as better than the other with respect to both objectives. These points thus constitute a non-dominating Pareto set. If more yield is desired, one moves towards R, whereas for more purity, solutions near point R are preferred. Thus, multi-objective optimization is quite different from single objective optimization; the goal in the latter being to obtain the best solution which is the global minimum or the global maximum although may not be the ‘best meaningful’ optimal solution.

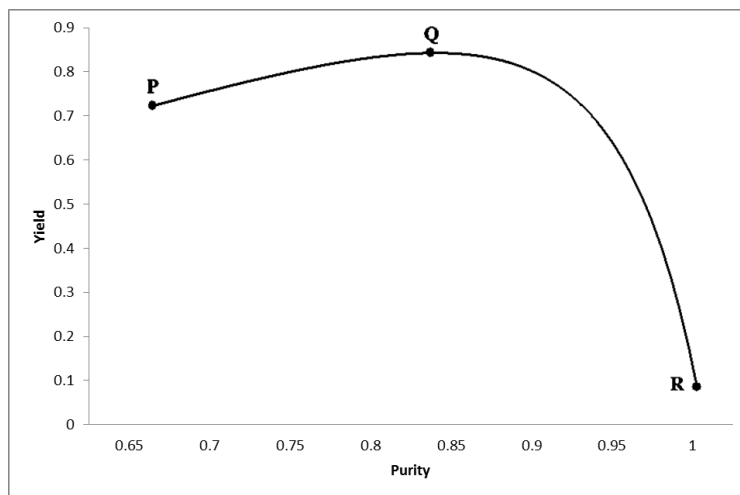


Figure 1.1 Concept of Pareto set

Multi-objective optimization problem can be solved by various techniques, such as the ϵ -constraint method [41], goal attainment method [42], or the non-dominated sorting genetic algorithm (NSGA) method [43]. Out of these, the NSGA technique has become quite popular in chemical engineering [44-53]. This technique is relatively insensitive to the shape of the Pareto optimal front, hence more efficient than the competitive methods. Also, one run is enough to generate the entire Pareto set [44, 54]. Multi-objective optimization using NSGA has been successfully implemented for SMBR [17, 25, 30, 40, 55, 56]. Hence, NSGA has also been applied in this work for optimizing biodiesel production in SMBR.

1.4 Research objective

The objective of this research work is to investigate the reversible esterification reaction of free fatty acid and methanol catalyzed by Amberlyst 15 to produce biodiesel in a simulated moving bed system, and to gain a deeper insight of the process dynamics. In this work, the performance of SMBR for biodiesel production was thoroughly investigated by numerical simulation as well as experimental verification of the simulation results. Thereafter, a novel optimization strategy, the multi-objective optimization using NSGA, was applied to further improve the performance of SMBR.

1.5 Thesis outline

This thesis is organized into six chapters.

Chapter 1 gives an introductory background and a general outline of the entire thesis dissertation.

Chapter 2 represents a generalized background of the chromatographic reactor, its applications, the various design strategies of SMB systems and its justification for production of biodiesel.

Chapter 3 presents the determination of adsorption equilibrium constants, dispersion coefficients and kinetic parameters for the reversible reaction involving synthesis of biodiesel from free fatty acid and alcohol catalyzed by Amberlyst 15. Experiments were conducted in a single column packed bed reactor packed with Amberlyst 15 which acted as both catalyst and adsorbent. All the experiments were carried out at room temperature using a rectangular pulse input. An equilibrium dispersive mathematical model was used for the single column reactor. Quasi-homogenous reaction kinetics and linear adsorption isotherm were used for the model. Both reactive and non-reactive breakthrough experiments were performed. The adsorption and kinetic parameters as well as dispersion coefficients were determined by tuning the model simulation results with the experimentally obtained breakthrough curves of the reactants (free fatty acid and alcohol)

and the products (biodiesel and water). The curve-fitting was done using the state-of-art-optimization technique, Genetic Algorithm (GA). Further validation of the mathematical model was done by carrying out experiments at different flow rates, feed concentrations and pulse input. The yield and purity of the biodiesel formed was also determined. The kinetic parameters were obtained under conditions free of both internal and external mass transfer resistance. It was observed that the model predicted the experimental results reasonably well.

Chapter 4 deals with the evaluation of the SMBR performance for synthesis of biodiesel from free fatty acid and alcohol catalyzed by Amberlyst 15. The SMBR performance was evaluated both numerically and experimentally. To describe the dynamic behavior of SMBR, a rigorous mathematical model was developed. Experiments were done at different operating conditions to validate the model. The yield and purity of the biodiesel formed was determined; it was observed the yield and purity of the biodiesel to be greater than those obtained during single column experiment. It was found that the experimental results agree reasonably well with the model predicted results. The effects of various operating parameters like feed flow rate, switching time, and raffinate flow rate as well as other variables on the SMBR performance was evaluated by performing a sensitivity analysis. The results from the sensitivity analysis indicated that further improvement in SMBR performance is possible by doing multiple-objective optimization of the design and process parameters as some variables act in conflicting ways.

Chapter 5 aims at optimizing the SMBR performance; the optimization being performed based on the experimentally verified mathematical model presented in Chapter 4. Multi-objective optimization was performed using state-of-art-algorithm, the non-dominated sorting genetic algorithm (NSGA). Optimization problems for both existing setup and design-stage of SMBR were performed. The objective functions considered were maximization of yield and purity of biodiesel and minimization of desorbent consumption. The decision variables for the optimization problems were based on the sensitivity studies mentioned in chapter 4. It was observed that even higher yield and purity of biodiesel using less desorbent can be obtained by through systematic multiple-objective optimization of the SMBR system.

Finally, in Chapter 6, conclusions of the present work and recommendations for further studies are mentioned.

1.6 References

1. Lode F, Mazzotti M, Morbidelli M. A new reaction-separation unit: The simulated moving bed reactor. *Chimia (Aarau)*. 2001;55:883-886.
<http://www.scopus.com/inward/record.url?eid=2-s2.0-0035648308&partnerID=tZOtx3y1>.
2. Kapil A, Bhat S a., Sadhukhan J. Dynamic Simulation of Sorption Enhanced Reaction Processes for Biodiesel Production. *Ind Eng Chem Res*. 2010;49(5):2326-2335.
doi:10.1021/ie901225u.
3. Fricke J, Meurer M, Schmidt-Traub H. Design and Layout of Simulated-Moving-Bed Chromatographic Reactors. *Chem Eng Technol*. 1999;22(10):835-839.
doi:10.1002/(SICI)1521-4125(199910)22:10<835::AID-CEAT835>3.0.CO;2-0.
4. Viswanathan S, Aris R. Countercurrent Moving Bed Chromatographic Reactors. *Adv Chem Ser*. 1974;(13):191-204.
5. Takeuchi K, Uraguchi Y. Basic Design of Chromatographic Moving Bed Reactors for Product Refining. *Chem Eng Jap*. 1976;9:246-248.
6. Takeuchi K, Uraguchi Y. Separation Conditions of the Reactant and the Product with a Chromatographic Moving Bed Reactor. *Chem Eng Jap*. 1976;(9):164-166.
7. Petroulas T, Aris R, Carr RW. Analysis and performance of a countercurrent moving-bed chromatographic reactor. *Chem Eng Sci*. 1985;40(12):2233-2240.
8. Fish B. The continuous countercurrent moving bed chromatographic reactor. *Chem Eng Sci*. 1986;41:661-668.
9. Broughton, D.B., Gerhold CG. broughton and gold 1961.pdf. 1961.
10. Ray AK, Tonkovich AL, Aris R, Carr RW. The Simulated Countercurrent Moving Bed Chromatographic Reactor. *Chem Eng Sci*. 1990;45(8):2431-2437.
11. Ray AK, Carr RW, Aris R. The Simulated Countercurrent Moving Bed Chromatographic Reactor: A Novel Reactor - Separator. *Chem Eng Sci*. 1994;49(4):469-480.

12. Ray AK, Carr RW. Experimental study of a laboratory scale simulated countercurrent moving bed chromatographic reactor. *Chem Eng Sci.* 1995;50:2195-2202. [http://www.eng.uwo.ca/people/array/Ajay Publications PDF files/A5 SMB Minn Expt CES 1995.pdf](http://www.eng.uwo.ca/people/array/Ajay%20Publications%20PDF%20files/A5%20SMB%20Minn%20Expt%20CES%201995.pdf).
13. Ray AK, Carr RW. Numerical simulation of a simulated countercurrent moving bed chromatographic reactor. *Chem Eng Sci.* 1995;50:3033-3041. doi:10.1016/0009-2509(95)00135-R.
14. Tonkovich ALY, Carr RW. A simulated countercurrent moving-bed chromatographic reactor for the oxidative coupling of methane: Experimental results. *Chem Eng Sci.* 1994;49:4647-4656. doi:10.1016/S0009-2509(05)80048-X.
15. Bjorklund MC, Carr RW. The simulated countercurrent moving bed chromatographic reactor: a catalytic and separative reactor. *Catal Today.* 1995;25:159-168. doi:10.1016/0920-5861(95)00105-O.
16. Kruglov A V., Bjorklund MC, Carr RW. Optimization of the simulated countercurrent moving-bed chromatographic reactor for the oxidative coupling of methane. *Chem Eng Sci.* 1996;51(11):2945-2950. doi:10.1016/0009-2509(96)00179-0.
17. Kundu PK, Ray AK, Elkamel A. Numerical simulation and optimisation of unconventional three-section simulated countercurrent moving bed chromatographic reactor for oxidative coupling of methane reaction. *Can J Chem Eng.* 2012;90:1502-1513. doi:10.1002/cjce.20663.
18. Mazzotti M, Kruglov A, Neri B, Gelosa D, Morbidelli M. A continuous chromatographic reactor: SMBR. *Chem Eng Sci.* 1996;51:1827-1836. doi:10.1016/0009-2509(96)00041-3.
19. Kawase M, Suzuki T Ben, Inoue K, Yoshimoto K, Hashimoto K. Increased esterification conversion by application of the simulated moving-bed reactor. *Chem Eng Sci.* 1996;51:2971-2976. doi:10.1016/0009-2509(96)00183-2.
20. Lode F, Houmard M, Migliorini C, Mazzotti M, Morbidelli M. Continuous reactive chromatography. *Chem Eng Sci.* 2001;56(2):269-291. doi:10.1016/S0009-2509(00)00229-3.
21. Yu W, Hidajat K, Ray AK. Modeling, Simulation, and Experimental Study of a Simulated Moving Bed Reactor for the Synthesis of Methyl Acetate Ester. *Ind Eng Chem Res.* 2003;42(26):6743-6754. doi:10.1021/ie0302241.
22. Ganetsos G, Barker PE, Ajongwen JN. Batch and continuous chromatographic systems as combined bioreactor-separators. In: *Preparative and Production Scale Chromatography*. Vol 40.; 1993:375-394.

23. Meurer M, Altenhöner U, Strube J, Untiedt A, Schmidt-Traub H. Dynamic simulation of a simulated moving-bed chromatographic reactor for the inversion of sucrose. *Starch/Staerke*. 1996;48:452-457. doi:DOI 10.1002/star.19960481113.
24. Ching C, Lu Z. Simulated moving-bed reactor: application in bioreaction and separation. *Ind Eng Chem Res*. 1997;36:152-159. doi:Doi 10.1021/Ie9603171.
25. Kurup AS, Subramani HJ, Hidajat K, Ray AK. Optimal design and operation of SMB bioreactor for sucrose inversion. *Chem Eng J*. 2005;108(1-2):19-33. doi:10.1016/j.cej.2004.12.034.
26. Hashimoto NK, Adachi S. Models For the Separation of Glucose/Fructose Mixture Using a Simulated Moving-Bed Adsorber. *J Chem Eng Japan*. 1983;16(5).
27. Borges da Silva EA, Ulson de Souza AA, de Souza SGU, Rodrigues AE. Analysis of the high-fructose syrup production using reactive SMB technology. *Chem Eng J*. 2006;118:167-181. doi:10.1016/j.cej.2006.02.007.
28. Zhang Y, Hidajat K, Ray AK. Modified reactive SMB for production of high concentrated fructose syrup by isomerization of glucose to fructose. *Biochem Eng J*. 2007;35:341-351. doi:10.1016/j.bej.2007.01.026.
29. LUDEMANN-HOMBOURGER O, NICOUD RM, BAILLY M. The "VARICOL" Process: A New Multicolumn Continuous Chromatographic Process. *Sep Sci Technol*. 2000;35(12):1829-1862. doi:10.1081/SS-100100622.
30. Yu W, Hidajat K, Ray AK. Optimization of reactive simulated moving bed and Varicol systems for hydrolysis of methyl acetate. *Chem Eng J*. 2005;112(1-3):57-72. doi:10.1016/j.cej.2005.06.008.
31. Atadashi IM, Aroua MK, Aziz a. A. High quality biodiesel and its diesel engine application: A review. *Renew Sustain Energy Rev*. 2010;14(7):1999-2008. doi:10.1016/j.rser.2010.03.020.
32. Karaosmanoglu F, Cigizoglu K, Tuter M, Ertekin S. Investigation of the refining step of biodiesel production. *Energy & Fuels*. 1996;10:890-895. doi:10.1021/ef9502214.
33. Dubé MA, Tremblay AY, Liu J. Biodiesel production using a membrane reactor. *Bioresour Technol*. 2007;98:639-647. doi:10.1016/j.biortech.2006.02.019.
34. Cao P, Dubé MA, Tremblay AY. High-purity fatty acid methyl ester production from canola, soybean, palm, and yellow grease lipids by means of a membrane reactor. *Biomass and Bioenergy*. 2008;32:1028-1036. doi:10.1016/j.biombioe.2008.01.020.

35. Kiss AA, Dimian AC, Rothenberg G. Biodiesel production by heat-integrated reactive distillation. *Comput Aided Chem Eng.* 2008;25:775-780. doi:10.1016/S1570-7946(08)80135-6.
36. Dimian AC, Bildea CS, Omota F, Kiss AA. Innovative process for fatty acid esters by dual reactive distillation. *Comput Chem Eng.* 2009;33:743-750. doi:10.1016/j.compchemeng.2008.09.020.
37. Migliorini C, Fillinger M, Mazzotti M, Morbidelli M. Analysis of simulated moving-bed reactors. *Chem Eng Sci.* 1999;54:2475-2480. doi:10.1016/S0009-2509(98)00487-4.
38. Dunnebie G, Fricke J, Klatt KU. Optimal design and operation of simulated moving bed chromatographic reactors. *Ind Eng Chem Res.* 2000;39:2290-2304. doi:10.1021/ie990820o.
39. Azevedo DCS, Rodrigues AE. Design methodology and operation of a simulated moving bed reactor for the inversion of sucrose and glucose-fructose separation. *Chem Eng J.* 2001;82:95-107. doi:10.1016/S1385-8947(00)00359-4.
40. Yu W, Hidajat K, Ray AK. Application of Multiobjective Optimization in the Design and Operation of Reactive SMB and Its Experimental Verification. *Ind Eng Chem Res.* 2003;42:6823-6831. doi:10.1021/ie030387p.
41. Changkong V, Haimes YY. *Multiobjective Decision Making: Theory and Methodology.* New York: North Holland; 1983.
42. Fonseca CM, Fleming PJ. Multiobjective optimization and multiple constraint handling with evolutionary algorithms. I. A unified formulation. *IEEE Trans Syst Man, Cybern - Part A Syst Humans.* 1998;28(1):26-37. doi:10.1109/3468.650319.
43. Srinivas N, Deb K. Multiobjective Optimization Using Nondominated Sorting in Genetic Algorithms. *Evol Comput.* 1994;2:221-248. doi:10.1162/evco.1994.2.3.221.
44. Bhaskar V, Gupta SK, Ray AK. Applications of multiobjective optimization in chemical engineering. *Rev Chem Eng.* 2000;16:1-54.
45. Bhaskar V, Gupta SK, Ray AK. Multiobjective optimization of an industrial wiped film poly(ethylene terephthalate) reactor: Some further insights. *Comput Chem Eng.* 2001;25:391-407. doi:10.1016/S0098-1354(00)00665-7.
46. Rajesh JK, Gupta SK, Rangaiah GP, Ray AK. Multiobjective Optimization of Steam Reformer Performance Using Genetic Algorithm. *Ind Eng Chem Res.* 2000;39:706-717. doi:10.1021/ie9905409.

47. Tarafder A, Rangaiah GP, Ray AK. Multiobjective optimization of an industrial styrene monomer manufacturing process. *Chem Eng Sci.* 2005;60:347-363. doi:10.1016/j.ces.2004.07.120.
48. Sankararao B, Gupta SK. Multiobjective optimization of the dynamic operation of an industrial steam reformer using the jumping gene adaptations of simulated annealing. *Asia-Pacific J Chem Eng.* 2006;1:21-31. doi:10.1002/apj.4.
49. Abraham A, Jain L. Evolutionary multiobjective optimization. *Evol Multiobjective Optim.* 2005:313. doi:10.1007/1-84628-137-7.
50. Mitra K, Gopinath R. Multiobjective optimization of an industrial grinding operation using elitist nondominated sorting genetic algorithm. *Chem Eng Sci.* 2004;59:385-396. doi:10.1016/j.ces.2003.09.036.
51. Yee AKY, Ray AK, Rangaiah GP. Multiobjective optimization of an industrial styrene reactor. *Comput Chem Eng.* 2003;27:111-130. doi:10.1016/S0098-1354(02)00163-1.
52. Massebeuf S, Fonteix C, Hoppe S, Pla F. Development of new concepts for the control of polymerization processes: Multiobjective optimization and decision engineering. I. Application to emulsion homopolymerization of styrene. *J Appl Polym Sci.* 2003;87:2383-2396. doi:10.1002/app.12026.
53. Mazumder J, Zhu J, Bassi AS, Ray AK. Multiobjective optimization of the operation of a liquid-solid circulating fluidized bed ion-exchange system for continuous protein recovery. *Biotechnol Bioeng.* 2009;103:873-890. doi:10.1002/bit.22328.
54. Nandasana AD, Ray AK, Gupta SK. Applications of the Non-Dominated Sorting Genetic Algorithm (NSGA) in Chemical Reaction Engineering Applications of the Non-Dominated Sorting Genetic Algorithm (NSGA) in Chemical Reaction Engineering. *Int J Chem React Eng.* 2003;1.
55. Ziyang Z, Hidajat K, Ray AK. Multiobjective Optimization of Simulated Countercurrent Moving Bed Chromatographic Reactor (SCMCR) for MTBE Synthesis. *Ind Eng Chem Res.* 2002;41(13):3213-3232. doi:10.1021/ie0106940.
56. Zhang Y, Hidajat K, Ray AK. Multi-objective optimization of simulated moving bed and Varicol processes for enantio-separation of racemic pindolol. *Sep Purif Technol.* 2009;65:311-321. doi:10.1016/j.seppur.2008.10.050.

Chapter 2

2 Literature review

2.1 Chromatography: A Brief Introduction

Separation process is essential to every chemical manufacturing operation to obtain a product of desired purity. This process is thermodynamically unfavorable, as it is the opposite of mixing. Hence, the efficiency and economics of these processes are of significant impact on both the product quality and cost. There are various separation technologies like distillation, extraction, sublimation, stripping, membrane separation etc. However, these conventional processes are not very effective for separation of chemically similar components like amino acids, proteins, complex hydrocarbons and other heat sensitive substances. In such cases, the mentioned conventional separation methods do not apply. The solution to this problem is given by adsorption, as it offers a good approach in dealing with difficult separations. This is because adsorbents are much more selective in their affinity for various materials than any known solvent. This adsorption principle is used in chromatography. Thus, we can say that chromatography is the answer to difficult separation methods.

The term ‘Chromatography’ literally means ‘color writing’. It is composed of two terms – in Greek “Chroma” means “color” and “Graphein” means “to write”. The process was used in the first decade of 20th century, primarily for separation of plant pigments such as chlorophyll. Although some related techniques were developed in the 19th century, the first true chromatography was carried out by the Russian botanist Mikhail Semyonovich Tswett. He used calcium carbonate columns to separate plant pigments for his research on chlorophyll.

Chromatography is the collective term given to a set of laboratory techniques for the separation of mixtures. The mixture to be separated is dissolved in a mobile phase and then the mobile phase is passed through a stationary phase. The stationary phase then separates the different components of the mixture based on the differential partitioning of

the individual components between the two phases. Hence it depends on the partition coefficient of the various components in the mixture. This technique offers the advantages of superior separating power, high selectivity, low energy cost and mild operating conditions as compared to other separation technologies. It can also be used for coupling reactions. Chromatography can be used for either preparative or analytical purposes.

2.2 Chromatographic Reactor

The integration of any unit operation with chemical reaction into one single apparatus allows for significant improvement in process performance [1]. Not only it improves process intensification, but also enhances conversion in case of equilibrium limited reactions by in-situ removal of one or more products as soon as they are formed. Thus a combination of chemical reaction and separation also improves their efficiency [2]. By properly separating reaction products, one can improve process selectivity and eliminate the need for expensive recycles between reaction and separation units [3]. Reactive distillation is one such process which integrates reaction-separation. It has a major advantage over conventional processes as it is possible to tune the concentration profiles within the unit to overcome a chemical equilibrium limitation. However, one major drawback is that that it cannot be used for heat-sensitive components, which often occur in fine chemical or pharmaceutical industries.

A suitable alternative to reactive distillation is the chromatographic reactor, which utilizes differences in the adsorptivity of different components rather than differences in their volatility. Hence it can be used for separating non - volatile and heat sensitive components [1, 2].

2.3 Batch Chromatographic Reactor

The basic concept of a chromatographic reactor can be understood when we look at a single chromatographic column, operating in a conventional batch mode. Let us assume an equilibrium limited reaction: $A \leftrightarrow B + C$. the reactant A is mixed with an inert solvent/desorbent and it is injected as a pulse into a fixed bed comprised of a catalyst and an adsorbent having a high affinity towards B, but lower affinities towards A and C. As the reaction proceeds, both reactant and products migrate through the reactor with different velocities, with B being retained more strongly than A and C and thus staying behind the reactive front. This is shown in Figure 2.1. This continuous separation of products suppresses the backward reaction, thus allowing the equilibrium limited reaction to proceed towards completion and enabling the collection of high purity product fraction at the reactor outlet.

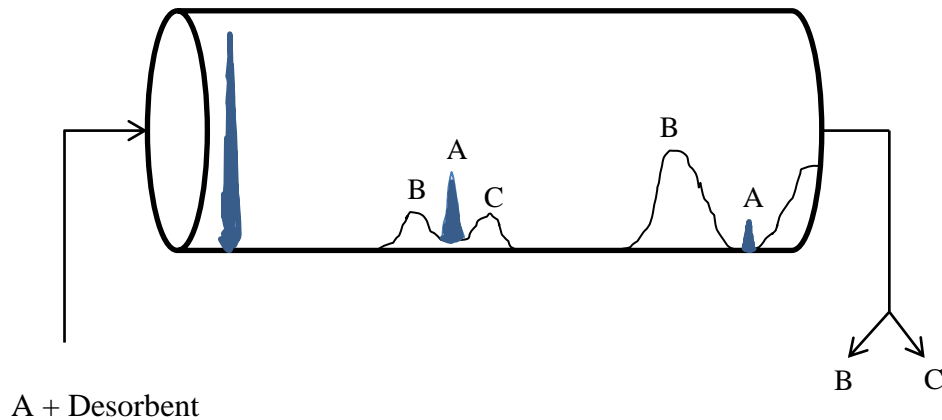


Figure 2.1 Operating principle of a batch chromatographic reactor [4]

However, in the case of bimolecular reactions, separation of reactants has to be avoided by choosing a suitable stationary phase and solvent, as well as proper operating conditions. This can be achieved by using one of the reactants as the solvent so as to

ensure its availability to the reaction locus [5, 6]. The batch chromatographic reactor was developed by Roginskii et al. [7, 8] and Magee [9]. It has been investigated by many researchers;

- (1) Gore (1967) compared the performance of a chromatographic reactor having cyclic feed with a steady flow reactor and reported that the chromatographic reactor gave better conversion but needed more catalyst per unit volume to reach equilibrium [10].
- (2) Chu and Tsang (1971) used a Langmuir- Hinshelwood isotherm to account for competitive adsorption on the catalyst surface in a chromatographic reactor [11].
- (3) Langer and Patton (1973) characterized a general idealized chromatographic reactor that has the following features [12]:
 - (a) A pulse of reactants as it travels through the column, reaction occurs and the products are instantaneously separated from each other
 - (b) The mass transfer and adsorption rates are non-limiting, the reaction is limiting
 - (c) Adsorption isotherms are linear
 - (d) Axial dispersions and band spreading are negligible
 - (e) The mobile phase is incompressible and the stationary phase is uniformly packed
 - (f) The heating effects are negligible, i.e. the column is isothermally packed
- (4) Wetherold et al. (1974) studied the liquid phase hydrolysis reaction of methyl formate. They achieved conversions excess of equilibrium and compared the results with those obtained by simulation of mathematical model based on Freundlich adsorption isotherm [13].

(5) Schweich and Villermaux (1978) proposed a model which assumed a fast reaction rate as compared to the residence times of the components in the column. They investigated the dehydrogenation of cyclohexane and compared the experimentally measured conversion with the mathematical model. They found out that to accurately describe the adsorption isotherm for gas phase reactions, variations in the volumetric flow rate due to chemical expansion has to be taken into account [14].

However, there are several drawbacks of a batch chromatographic reactor. Periodic injection of reactants results in low throughput. There is low efficiency in utilizing the stationary phase and large eluent consumption resulting in product dilution.

In order to counter these problems the continuous chromatographic reactor was developed in the 1970s.

2.4 Continuous Chromatographic Reactor

This type of reactor has several advantages, like continuous operation, constant product quality, limited or no recycling, better utilization of the available mass transfer area. The operation of this reactor type falls mainly under two categories: concurrent operation (annular rotating chromatographic reactor) and countercurrent operation (true moving bed reactor & simulated moving bed reactor).

2.4.1 Annular Rotating Chromatographic Reactor

Figure 2.2 shows a diagram of a rotating annular chromatographic reactor. The stationary phase is contained between two concentrically arranged cylinders, rotating about their common axis. The solvent is fed into the unit from the top along the whole circumsection, but the feed is introduced only at a fixed point. The compounds are adsorbed in the stationary phase, where the reaction takes place. Due to the circumvential displacement of the adsorbed compounds, the species to be separated leave the reactor at

different angles, which depend on the affinity towards the stationary phase. Thus the more strongly adsorbed component travels for a longer time and thus exits at large angle compared to the fixed feed port. At steady state it is possible to collect different fractions at various angular positions along the outlet circumference at the bottom of the cylinder [15].

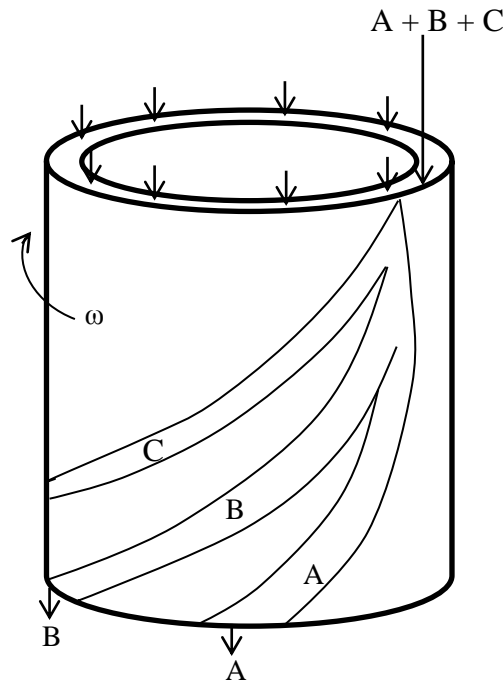


Figure 2.2 Annular rotating chromatographic reactor [16]

This type of reactor has been applied experimentally applied to study many reactive systems. Example: hydrolysis of methyl formate on activated charcoal [17], gas phase catalytic dehydrogenation of cyclohexane [8], biochemical reactions like sachcharification of starch [18] ,inversion of sucrose [19], protein purification [20, 21].

However, several criteria have to be met for the reaction to suitably take place in the annular chromatographic reactor [16]:

- (1) The reaction should be of type: $A \leftrightarrow B + C$

- (2) Forward reaction rate should be sufficiently large to keep the reactor at reasonable length
- (3) Reaction equilibrium constant should be small enough to allow significant yield improvement
- (4) Adsorption of A, B and C on the stationary phase should differ largely for good separation.

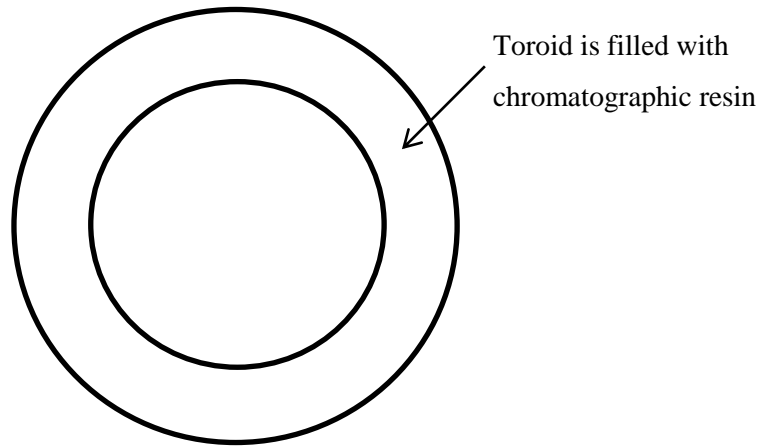
2.4.2 Countercurrent Chromatographic Reactor

This reactor is different from concurrent operation in the sense that the solid phase and the mobile phase move in opposite directions with respect to each other. It is of two types: the true countercurrent moving bed reactor and the simulated moving bed reactor.

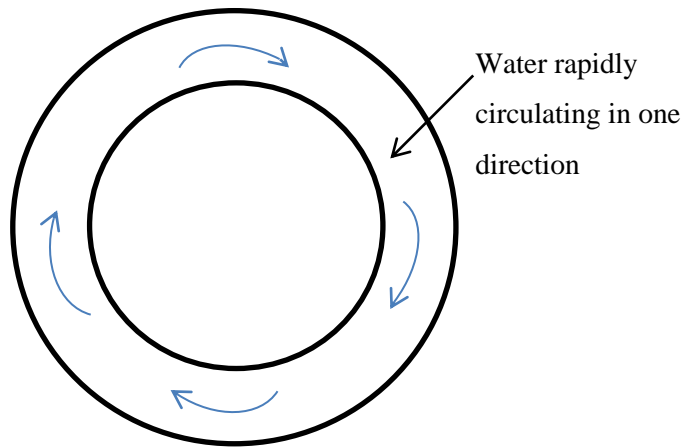
2.4.2.1 True Countercurrent Moving Bed Chromatographic Reactor

As the name suggests, in this type of reactor, there is actual countercurrent movement of the solid phase with respect to the mobile phase. The following series of diagrams will help in explaining the concept of a true moving bed reactor:

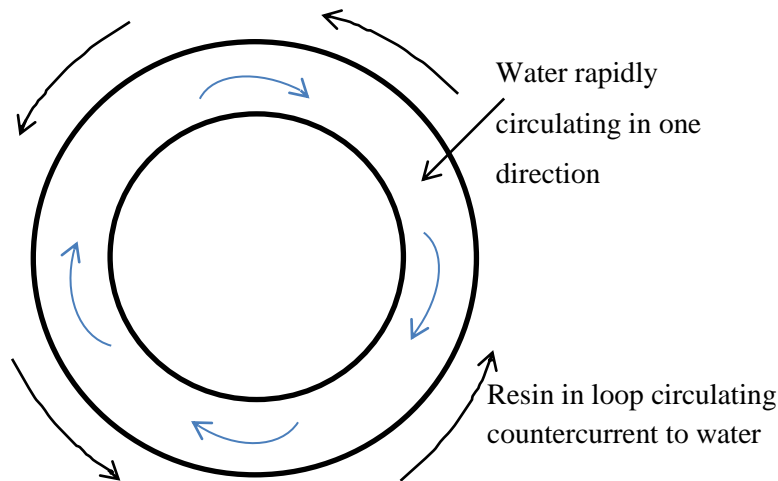
Let us imagine a resin filled column in the form of a toroid [22]:



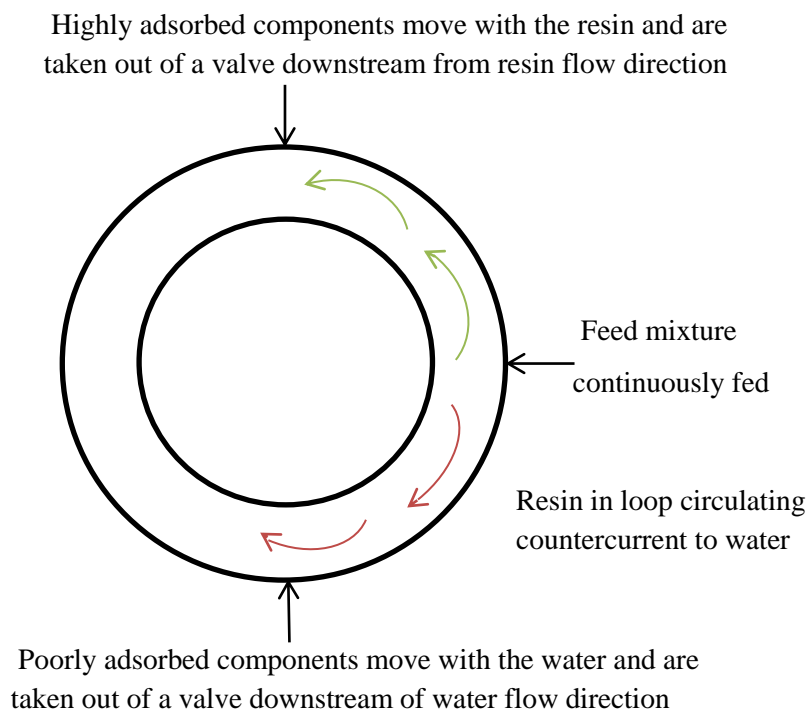
Now we assume a rapid, continuous flow of water (eluent) in one direction inside the loop [22]:



Now, we assume that the resin is circulating in the opposite direction to that of water[22]:



Now a binary mixture is added continuously at one point of the loop, so that the component more readily adsorbed by the resin will tend to move with it, and the lesser adsorbed component will tend to move with water [22]:



Thus, by balancing the two opposing internal flows, the two components are continuously separated and recovered. So we have true moving bed continuous chromatography. This concept is brought into practice in a true Countercurrent Moving Bed Chromatographic Reactor (CMCR), a typical configuration of which is given below:

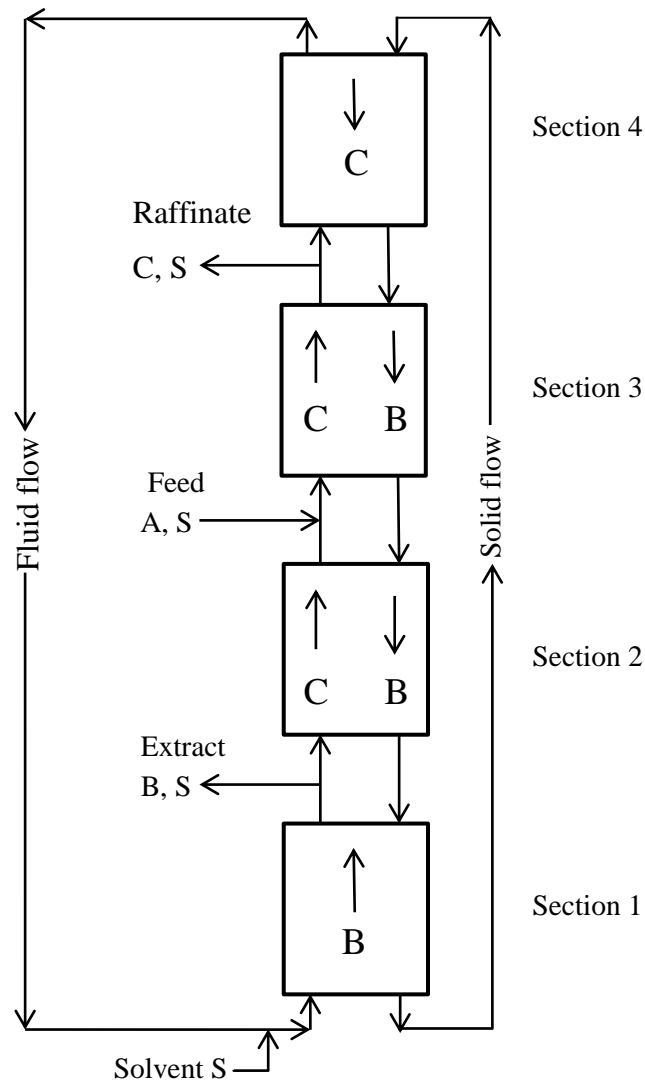


Figure 2.3 True Countercurrent Moving Bed Reactor [15]

The above unit is divided into four sections. The solid phase is introduced at the top of the reactor and moves downwards, whereas the fluid phase is introduced at the reactor bottom and moves upwards. Hence countercurrent flow is achieved.

We consider a reaction: $A \rightarrow B + C$. A is diluted with solvent (S) and fed in between the two central sections (between sections 3 and 2). Upon entering the reactor, A is transported towards section 3 (raffinate port) by the fluid flow, whereas it is also carried to section 2 by solid movement. Hence, chemical reaction takes place in both sections 2 and 3 to produce the products B and C. while B is more adsorbed by the solid phase; C is comparatively less adsorbed and tends to remain in the fluid phase. To obtain complete conversion of A, the flow rates within section 2 have to be adjusted in such a way that C is completely desorbed from the solid phase before it reaches the extract port, while the more adsorbed B has a net flow in the direction of the solid phase.

In section 3, flow conditions must favor the adsorption of B in the solid phase, so that when it reaches the raffinate port in section 4, only C is present in the fluid phase and taken out from the raffinate port. In section 1, regeneration of the adsorbent is done by the incoming desorbent and in section 4, removal of the raffinate C is done to ensure solvent recycling [23]. Moreover, the flow rates in sections 2 and 3 should be adjusted not only to ensure separation but also to allow sufficient time for reactant A to be completely consumed.

Certain variations to the above set up can be done, depending on the reactive system studied. For example, if C is hardly adsorbed at all, solvent recycling is not possible; hence section 4 can be omitted [6]. If for desorption of B, a change in temperature, pressure or other operating conditions is required, section 1 may be decoupled from the central sections and solid phase regeneration may be separately carried out [24]. However, there are many problems associated with a true moving bed. When scaling up to a column of large diameter, mechanical difficulties like moving the solid, fines removal, solvent attrition, expansion of bed, channeling of reactor etc. occur.

Various studies have been performed with the true countercurrent moving bed reactor; for example, Study of first order irreversible reaction [25-27] , Study of reversible reaction [28, 29] , and development of mathematical model for consecutive and reversible reactions in CMCR [30].

2.4.2.2 Simulated Countercurrent Moving Bed Chromatographic Reactor

In recent years, researchers have focused on development of Simulated Countercurrent Moving Bed Chromatographic Reactor (SCMCR) systems, which preserve the inherent advantages of continuous countercurrent operation and at the same time avoiding the problems associated with a true moving bed reactor [31]. In a simulated moving bed, the process aspects of the countercurrent moving bed are simulated by successively switching the feed inlet and product take-off streams through a series of inlets located at timed intervals along a fixed bed [32]. The shifting of the feed and product positions in the direction of the fluid flow mimics the movement of solids in the opposite direction [33].

Hence, in SCMCR, the advantages of high product purity and favorable equilibrium shifts offered by the true moving bed process are retained while avoiding a number of problems of the true moving bed. There are two configurations for this system: one is the single column configuration in which one column is subdivided into a number of compartments. Another is the multiple column configuration, which consists of a number of columns connected in series.

For laboratory investigations, the multiple column configuration is more suitable [34]. The multiple column configuration consists of columns of uniform cross section connected in series in a circular array. Figure 2.4 represents a system with eight column setup. There are two incoming fluid streams (feed and eluent) and two outgoing fluid streams (raffinate and extract). As illustrated in the figure, these four ports divide the system into four sections, with two columns in each section, corresponding to the column configuration 2/2/2/2. After a time interval known as switch time (t_s), the inlet and withdrawal ports are advanced in the same direction of the fluid flow, column by column. In this way simulation of countercurrent movement of the solid and fluid phase is achieved. The switching time and column configuration in this system are decided beforehand and remain constant during the entire process [35].

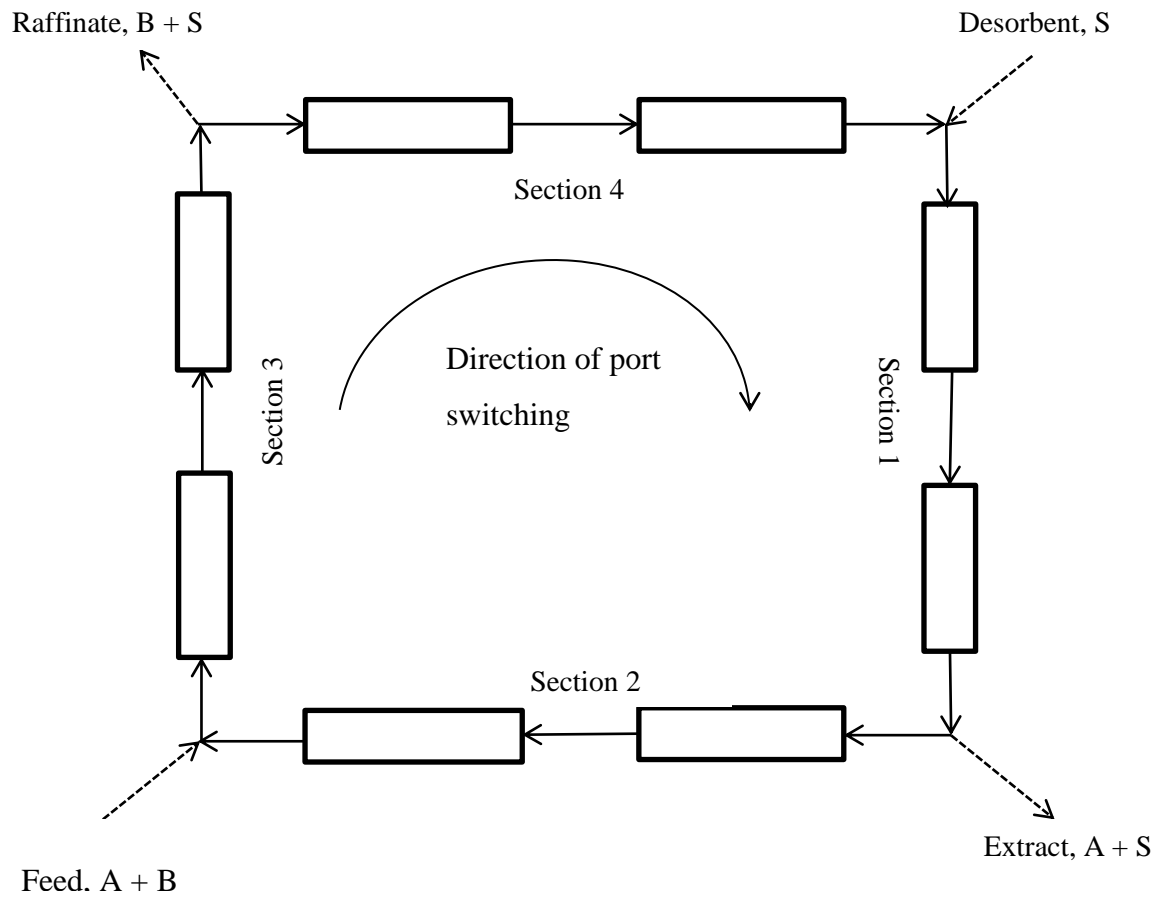


Figure 2.4 Schematic diagram of a 4-section, 8-column SMBR system

A significant improvement over the conventional SMB process is known as the Varicol, which was patented by Adam et al. in 1998. In contrast to the SMB, Varicol process is based on non-synchronous and unequal shift of the inlet and outlet ports. The concept and principle of Varicol operation alongwith an equivalent SMB process is described in Figure 2.5. The figure illustrates the working of a six column SMB (column configuration 2/1/1/2) and a six column Varicol, both of them having switch time t_s . Within this switching time, the Varicol is divided into four subintervals: 0 to $t_s/4$, $t_s/4$ to $t_s/2$, $t_s/2$ to $t_s \cdot 3/4$ and $t_s \cdot 3/4$ to t_s . Within each of these four subintervals, the column configuration of the Varicol changes, whereas that of SMB remains constant. Initially,

both the SMB and the Varicol have column configuration 2/1/1/2. In the 2nd subinterval, the extract port of the varicol is shifted one column forward and the column configuration becomes 2/1/2/1. In the 3rd subinterval, the feed port in Varicol is shifted one column forward and the column configuration becomes 1/1/2/2. In the 4th and final subinterval, the extract port is shifted one column forward and the column configuration becomes 1/2/1/2. Finally in the next switching cycle, the raffinate port is shifted one column forward to return to the original configuration of 2/1/1/2. Thus there is non-synchronous shifting of ports within a global switching time. Whereas in SMB, no such non-synchronous shift occurs. At the end of the switching time, all the ports are switched one column forward in SMB, so that the original column configuration of 2/1/1/2 is maintained all the time.

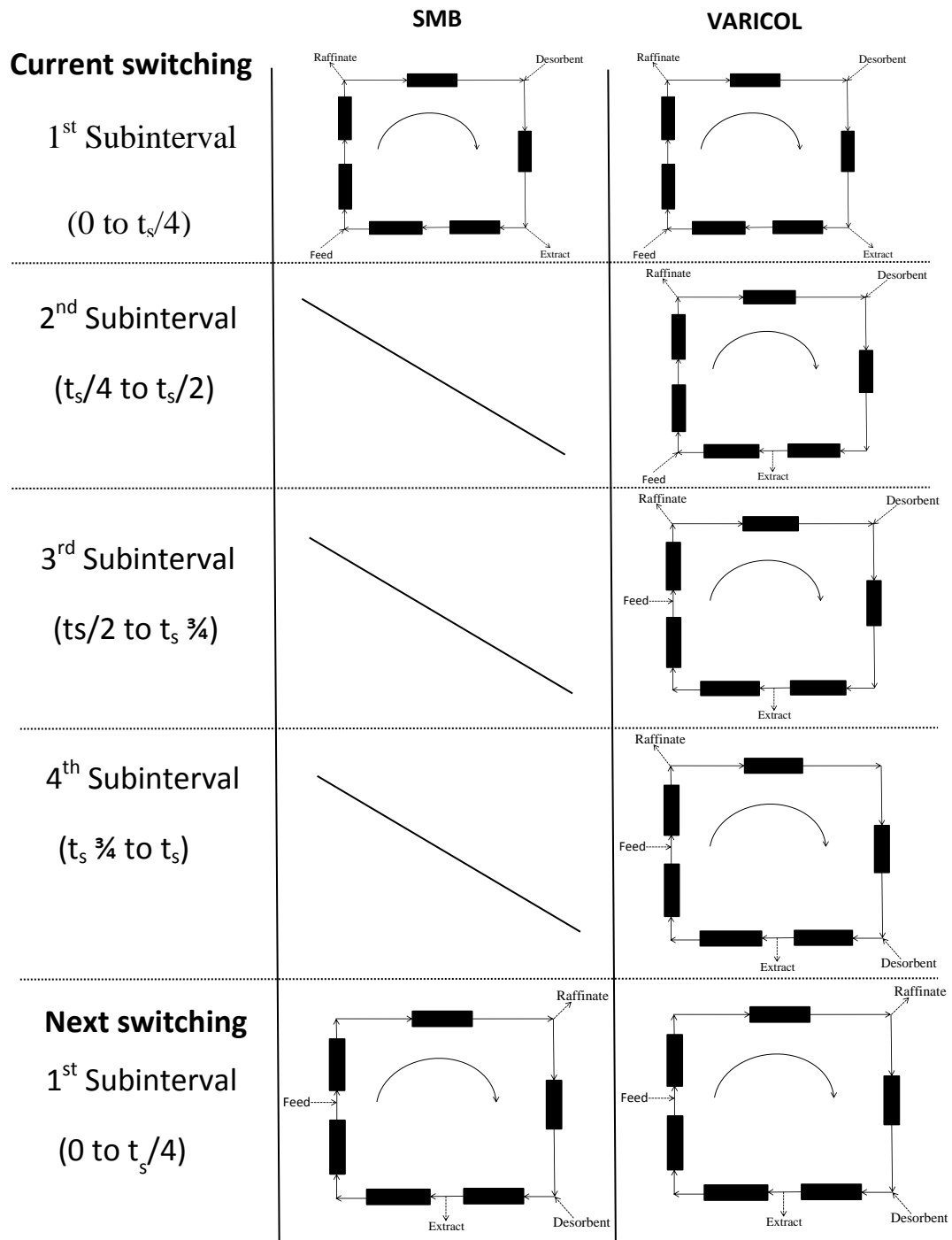


Figure 2.5 Comparison of a 6-column SMBR with a 6-column VARICOL [36]

The SMB system has been evaluated in quite a number of studies in the last couple of decades. Various classes of both chemical and biochemical reactions have been studied in a SMBR. Table 2.1 gives a brief and comprehensible account of the reaction systems studied in a SMBR.

Table 2.1 Description of various reactive systems on SMBR

Author: Ray, A.K., A. Tonkovich, Carr, R.W., Aris, R.(1990) [34]

Name of the paper: The simulated countercurrent moving bed chromatographic reactor

System investigated: Hydrogenation of 1,3,5 Trimethylbenzene (mesitylene) to 1,3,5 Trimethylcyclohexane

Description of Work done: Simulation studies were done to evaluate SMBR performance. Two configurations were studied; single column having multiple ports for feed & product, and multiple columns interconnected with inlet and outlet ports. Catalyst and adsorbent were packed together in columns. An equilibrium stage model was developed for SMBR. It predicted almost complete conversion of the reaction which would otherwise be equilibrium limited at 62% at 463K.

Author: Ray, A.K., A. Tonkovich, Carr, R.W., Aris, R.(1994) [37]

Name of the paper: The simulated countercurrent moving bed chromatographic reactor – A novel reactor-separator

System investigated: Hydrogenation of 1,3,5 Trimethylbenzene (mesitylene) to 1,3,5 Trimethylcyclohexane

Description of Work done: Simulation studies were done to evaluate SMBR performance and compare it with that of a Fixed Bed Reactor. The SMBR configuration was that of a single column with multiple ports for feed and product. Catalyst and adsorbent were packed together in columns. Equilibrium stage model was considered for SMBR, and almost complete conversion and purity for the reaction was predicted.

Author: Ray, A.K. and Carr, R.W. (1995a) [38]

Name of the paper: Experimental study of a laboratory-scale simulated countercurrent moving bed chromatographic reactor

System investigated: Hydrogenation of 1,3,5 Trimethylbenzene (mesitylene) to 1,3,5

Trimethylcyclohexane

Description of Work done: Experimental investigation of a 5-column SMBR was carried out. Catalyst (10% Pt/Al₂O₃) and adsorbent (Chromosorb 106) were packed together in columns A product purity of 96% and conversion of 83% was obtained under proper operating conditions; this conversion was in excess of 40% equilibrium conversion that would be obtained in a non separative reactor.

Author: Ray, A.K. and Carr, R.W. (1995b) [39]

Name of the paper: Numerical simulation of a simulated countercurrent moving bed chromatographic reactor

System investigated: Hydrogenation of 1,3,5 Trimethylbenzene (mesitylene) to 1,3,5 Trimethylcyclohexane

Description of Work done: Model was developed for prediction of SMBR behaviour. Partial differential equations were solved by finite elements method for the simulations. Reactant conversion of 83% and product purity of 98% – 99% was reported. Simulation results were similar to prediction by equilibrium stage model for SMBR.

Author: Tonkovich, A.L. and Carr, R.W.(1994a) [40]

Name of the paper: A simulated countercurrent moving-bed chromatographic reactor for the oxidative coupling of methane

System investigated: Oxidative coupling of methane

Description of Work done: Experimental investigation of ethylene production was carried out in a 4-section SMBR. Each section had 1 reactor and 2 separator columns. Catalyst (samarium oxide) and adsorbent (activated charcoal) were used. Effects of temperature, switch time and methane to oxygen feed ratio were studied. Irreversible reaction-kinetics was followed. SMBR experiments showed a conversion of 60% as compared to 10% conversion in single pass in a microreactor.

Author: Tonkovich, A.L. and Carr, R.W.(1994b) [41]

Name of the paper: Modeling of the simulated countercurrent moving-bed chromatographic reactor used for the oxidative coupling of methane

System investigated: Oxidative coupling of methane

Description of Work done: A simple equilibrium stage model for SMBR was proposed. Reversible reaction kinetics was followed for the production of ethane and ethylene. Effects of switching time and makeup feed rate were studied. Experimental and predicted values were compared.

Author: Bjorklund, M.C. and Carr, R.W.(1995) [42]

Name of the paper: The simulated countercurrent moving bed chromatographic reactor: a catalytic and separative reactor

System investigated: Oxidative coupling of methane

Description of Work done: Experimental study of production of ethane and ethylene were carried out. Two SMBR configurations, a single fixed bed having a series of inlets and outlets along its length, and a series of columns with an inlet or outlet between each, were considered. SMBR performance was enhanced by modifying its configuration. 4 reactors and 4 short & 2 long separators were used in the SMBR setup. Catalyst (samarium oxide) and adsorbent (activated charcoal) were used. A 12 fold increase in conversion and 2 fold increase in yield for oxidative coupling of methane was observed as compared to conventional reactors.

Author: Kruglov, A.V., Bjorklund, M.C., Carr, R.W.(1996) [43]

Name of the paper: Optimization of the simulated countercurrent moving bed chromatographic reactor for the oxidative coupling of methane

System investigated: Oxidative coupling of methane

Description of Work done: SMBR was designed based on its performance sensitivity to the operating parameters. A 4-section SMBR was used with 1 reactor and 2 separator columns in each section. Different adsorbents (activated charcoal, zeolite 7 hydrophobic CMS) as well as catalysts ($Y_1Ba_2Zr_3O_{9.5}$, $Y_1Ba_2Ge_3O_{3.5}$, Sm_2O_3) were characterized. CMS and $Y_1Ba_2Zr_3O_{9.5}$ were found to be most suitable. Effects of feed ratio and switching time were analyzed. An axial dispersion plug flow model was used.

Author: Bjorklund, M.C., Kruglov, A.V., Carr, R.W.(2001) [44]

Name of the paper: Further studies of the oxidative coupling of methane to ethane and ethylene in a simulated countercurrent moving bed chromatographic reactor

System investigated: Oxidative coupling of methane

Description of Work done: SMBR modeling and experimental model verification were carried out for the reaction. A 3-zone SMBR was used with only 1 reactor in the set up and two adsorbers in each section. $Y_1Ba_2Zr_3O_{9.5}$ was used as catalyst and activated charcoal was used as adsorbent. Axial dispersion plug flow model was used. Effects of switching time and feed ratio were studied. Experimental and simulation results were in good agreement

Author: Kundu, P.K., Zhang, Y., Ray, A.K.(2009) [45]

Name of the paper: Modeling and simulation of simulated countercurrent moving bed chromatographic reactor for oxidative coupling of methane

System investigated: Oxidative coupling of methane

Description of Work done: Mathematical modeling of a five section SMBR was done. A realistic and rigorous kinetic model was developed. Adsorption isotherm parameters were then derived based on the experimental breakthrough curves acquired using single adsorption column. The proposed mathematical model demonstrated extremely good predictions of the experimental results. Finally, effects of operating parameters, such as switching time, methane/oxygen feed ratio, raffinate flow rate, eluent flow rate, etc., on the behavior of the SMBR were studied.

Author: Kundu, P.K., Ray, A.K., Elkamel, A.(2012) [46]

Name of the paper: Numerical simulation and optimization of unconventional three-section simulated countercurrent moving bed chromatographic reactor for oxidative coupling of methane reaction

System investigated: Oxidative coupling of methane

Description of Work done: A mathematical model of an unconventional three-section SCMCR for the reaction was first developed and solved using numerically tuned kinetic and adsorption parameters. The model predictions showed good agreement with available experimental results. Effects of several process parameters on the performance of SMBR were investigated. A multi-objective optimization problem was solved at the operating stage using state-of-the-art AI-based non-dominated sorting genetic algorithm with jumping genes adaptations (NSGA-II-JG), which resulted in Pareto Optimal solutions. It was found that the performance of the SMBR could be significantly improved under optimal operating conditions.

Author: Bjorklund, M.C. and Carr, R.W.(2002) [47]

Name of the paper: Enhanced methanol yields from the direct partial oxidation of methane in a simulated countercurrent moving bed chromatographic reactor

System investigated: Methanol synthesis

Description of Work done: A laboratory-scale SMBR for the direct, homogeneous partial oxidation of methane to methanol was constructed and tested. Reaction conditions were evaluated from independent experiments with a single-pass tubular reactor. Separation was effected by gas-liquid partition chromatography with 10% Carbowax on Supelcoport. At the optimal reaction conditions, the methane conversion was 50%, selectivity was 50%, and yield was 25%. Factors affecting methane conversion were investigated.

Author: Kruglov, A.V. (1994) [48]

Name of the paper: Methanol synthesis in a simulated countercurrent moving-bed adsorptive catalytic reactor

System investigated: Methanol synthesis

Description of Work done: Synthesis of methanol from syngas in SMBR was studied by numerical modeling. Two different reactor configurations were considered. In the first, operating under adiabatic conditions, the fixed bed consisted of a catalyst (Cu/ZnO/Al₂O₃) and adsorbent (silica-alumina) mixed together. In the other one, operating isothermally, the catalyst and adsorbent were alternately packed in beds containing catalyst or adsorbent and only adsorber sections participated in countercurrent movement. Performances of the two reactors were compared. Operating conditions were determined for 96-99% carbon monoxide conversion in a single-pass operation.

Author: Ganetsos, G., Barker, P.E., Ajongwen, J.N.(1993) [49]

Name of the paper: Batch and continuous chromatographic systems as combined bioreactor-separators

System investigated: Inversion of sucrose into glucose and fructose using Invertase enzyme

Description of Work done: A novel SMBR setup was proposed for inversion of sucrose. The SMBR consisted of 12 columns with calcium charged resin as adsorbent. High purity of glucose and fructose was obtained alongwith high enzyme productivity. Substrate inhibition was minimized using SMBR.

Author: Meurer, M., Altenhoner, U., Strube, J., Untiedt, A., Schmidt-Traub, H.(1997) [50]

Name of the paper: Dynamic simulation of a simulated-moving-bed chromatographic reactor for inversion of sucrose, starch

System investigated: Inversion of sucrose into glucose and fructose using Invertase enzyme

Description of Work done: An 8-column SMBR with DOWEX 99/Ca cation exchange resin as adsorbent was used. Equilibrium dispersive model was applied and dynamic simulation studies were done to compare its performance with that of conventional chromatographic processes. Optimization was done with switching time, enzyme concentration and flow rates acting as process parameters.

Author: Ching, C.B., & Lu, Z.P.(1997) [51]

Name of the paper: Simulated moving bed reactor: application in bioreaction and separation

System investigated: Inversion of sucrose into glucose and fructose using Invertase enzyme

Description of Work done: A 3 zone SMBR was used with 1, 5 and 6 adsorbers in sections 1, 2 and 3 respectively. Axial dispersion plug flow model was applied. Enzymatic reaction occurred in the fluid phase, the SMBR performance was evaluated based on rigorous modeling and simulation studies.

Author: Dunnebier, G., Fricke, J., Klatt, K.U.(2000) [52]

Name of the paper: Optimal design and operation of simulated moving bed chromatographic reactors

System investigated: Inversion of sucrose into glucose and fructose using Invertase enzyme

Description of Work done: A novel optimization strategy was proposed considering a 4-section SMBR with 2 columns in each section. A standard successive quadratic programming (SQP) algorithm was used for optimization. The SMBR model took into account convection, axial dispersion, mass transfer resistance, particle diffusion and adsorption kinetics. Desorbent consumption was indirectly saved by upto 56%.

Author: Azevedo, D.C. & Rodrigues, A.(2001) [53]

Name of the paper: Design methodology and operation of a simulated moving bed reactor for the inversion of sucrose and glucose-fructose separation

System investigated: Inversion of sucrose into glucose and fructose using Invertase enzyme

Description of Work done: Rigorous modeling and experimental verification of a bio-SMBR was done. A 4 – section, 12 column SMBR was set up, with DOWEX 99/Ca cation exchange resin used as adsorbent. Michaelis-Menten kinetic model was used. Optimization study was done which involved minimization of column length and enzyme concentration for a given feed flow rate. The effect of safety margin was also investigated.

Author: Kurup, A.S., Subramani, H.J., Hidajat, K., Ray, A.K.(2005) [54]

Name of the paper: Optimal design and operation of SMB bioreactor for sucrose inversion

System investigated: Inversion of sucrose into glucose and fructose using Invertase enzyme

Description of Work done: Systematic multi-objective optimization studies for the inversion of sucrose to produce high fructose syrup were carried out. Optimal operating conditions for both an existing system as well as at the design stage were determined for maximum production of at least 60% concentrated fructose while using minimum solvent. Effect of two modifications of traditional SMB, namely distributed feed and non-synchronous switching (Varicol process) were studied to determine the extent of performance improvement compared to the SMBR system. Optimization was performed using a new state-of-the-art AI-based non-traditional but robust optimization technique based on genetic algorithm, the Non-dominated sorting genetic algorithm with jumping genes (NSGA-II-JG). Pareto-optimal solutions were obtained in all cases and the results showed that significant improvement is possible, particularly for distributed feed and Varicol operation.

Author: Borges da Silva, E.A., Souza, D.P., Ulson de Souza, A.A., Guelli U. Souza, S.A., Rodrigues, A.E.(2005) [55]

Name of the paper: Analysis of the behavior of the simulated moving bed reactor in the sucrose inversion process

System investigated: Inversion of sucrose into glucose and fructose using Invertase enzyme

Description of Work done: A mathematical model was presented to predict the behavior of the SMBR in the sucrose inversion process. For this process, the triangular region which defines operating conditions to recover high-purity products in SMBR was obtained using two modeling strategies. The set of partial differential equations was solved by finite volume method. The influence of some operating conditions on the reactor performance was analyzed.

Author: Minceva, M., & Rodrigues, A.E.(2005) [56]

Name of the paper: Simulated moving-bed reactor: reactive-separation regions

System investigated: Inversion of sucrose into glucose and fructose using Invertase enzyme

Description of Work done: A reactive SMBR was designed for sucrose inversion. The reactive-separation regions were determined for two reactive systems: (1) inversion of sucrose, with enzyme introduced in the unit through the eluent stream and Michaelis-Menten reaction kinetics, and (2) $A \rightarrow B + C$ reaction, with immobilized enzyme and linear reaction kinetic law. In both systems the reaction species exhibit linear adsorption isotherms. TMBR analogy was applied in the algorithm used for determination of the reactive-separation regions. The influence of the mass-transfer limitation, reaction rate, product purities, reactant Henry constant, and SMBR configuration on the shape and position of reactive-separation regions was analyzed. It was shown that in certain conditions the reactive-separation regions extended out of the separation regions obtained for nonreactive SMB for product separation.

Author: Hashimoto et al.(1983,1993) [57, 58]

Name of the paper: A new process combining adsorption and enzyme reaction for producing higher-fructose syrup; Models for the separation of glucose/fructose mixture using a simulated moving-bed adsorber

System investigated: Isomerization of glucose into fructose

Description of Work done: A novel reactor-separator for glucose isomerization was proposed. An SMBR setup having 16 adsorbers and 7 reactors was used. Calcium ion form of Y zeolite was the adsorbent and glucose isomerase was the catalyst/enzyme. SMBR performance was analyzed both experimentally and by simulation and was compared with conventional processes. High fructose purity (65%) was obtained. the desorbent requirement was less than the equivalent fixed-bed process

Author: Ching, C.B., & Lu, Z.P.(1997) [51]

Name of the paper: Simulated moving bed reactor: application in bioreaction and separation

System investigated: Isomerization of glucose into fructose

Description of Work done: Modeling and simulation was done for a 3-zone SMBR. The setup consisted of 14 adsorbers and 7 reactors. Axial dispersion plug flow model of an equivalent TMBR was applied.

Author: Borges da Silva, E.A., Souza, D.P., Ulson de Souza, A.A., Guelli U. Souza, S.A., Rodrigues, A.E.(2006) [59]

Name of the paper: Analysis of the high-fructose syrup production using reactive SMB technology

System investigated: Isomerization of glucose into fructose

Description of Work done: A SMBR configuration for glucose isomerization was proposed .The isomerization kinetics was experimentally determined at 328 K by the Lineweaver-Burk technique. Basic adsorption data for the sugar isomers (glucose and fructose) were obtained with cationic exchange resin as adsorbent. A mathematical model based on the analogy with true moving bed reactor and its numerical solution based on finite volume method were used for the prediction of the SMBR behavior and performance.

Author: Zhang, Y., Hidajat, K., Ray, A.K.(2007) [60]

Name of the paper: Modified reactive SMB for production of high concentrated fructose syrup by isomerization of glucose to fructose

System investigated: Isomerization of glucose into fructose

Description of Work done: Modifications to Hashimoto's hybrid SMBR system were done which was used to produce 55% high fructose syrup (HFS55). Two different configurations of modified system were studied: the first configuration was a 4-zone SMB with one reactor column and 16 adsorption columns, while the other had 14 adsorption columns and one reactor. A new SMB operation known as the Varicol was applied to the second SMB configuration. A state-of-the-art optimization technique, the non-dominated sorting genetic algorithm (NSGA) was applied to for optimizing the modified reactive SMB and Varicol processes. Compared with Hashimoto's system, high

productivity and purity of fructose was achieved in using lesser number of reactors.

Author: Kawase, M., Pilgrim, A., Araki, T., Hashimoto, K.(2001) [61]

Name of the paper: Lactosucrose production using a simulated moving bed reactor

System investigated: Enzyme catalyzed reaction of lactose and sucrose to produce lactosucrose

Description of Work done: Design of SMBR for lactosucrose production was proposed and its performance was analyzed. A numerical simulation of the batch process showed improved reaction by product removal. A plug flow model without axial dispersion was used for simulation. Yield improved beyond the equilibrium due to effective removal of one of the reaction products; glucose. Higher yield couldn't be achieved due to strong product hydrolysis near the raffinate port.

Author: Pilgrim, A., Kawase, M., Matsuda, F., Miura, K.(2006) [62]

Name of the paper: Modeling of the simulated moving-bed reactor for the enzyme-catalyzed production of lactosucrose

System investigated: Enzyme catalyzed reaction of lactose and sucrose to produce lactosucrose

Description of Work done: Modeling and optimization of SMBR was done for enzyme catalyzed production of lactosucrose. A numerical model was derived and verified experimentally. Optimization was carried out based on the model. It was determined that along with the flow rate settings, substrate feed, enzyme concentration and thermal deactivation of enzyme strongly influenced the product yield. Simulation showed that despite of parallel and consecutive side reaction, the maximum lactosucrose yield can reach 69%, which represented a 36% increase compared to the equilibrium yield.

Author: Ziyang, Z., Hidajat, K., Ray, A.K.(2001) [31]

Name of the paper: Application of simulated countercurrent moving bed chromatographic reactor for MTBE synthesis

System investigated: Synthesis of Methyl Tertiary Butyl Ether (MTBE) from Tertiary Butyl Alcohol (TBA) and methanol

Description of Work done: SMBR was designed for direct synthesis of MTBE and its performance and sensitivity to various operating parameters were reported. A 4-section,

8-column SMBR was set up with Amberlyst 15 acting as both catalyst and adsorbent. Equilibrium dispersive model was used. Effects of switching time, solvent and raffinate flow rates and number of columns in a section on SMBR performance were studied. Above 95% conversion was achieved by selection of proper operating parameters, which acted in a conflicting manner on the SMBR.

Author: Ziyang, Z. Hidajat, K. Ray, A.K.(2002) [33]

Name of the paper: Multiobjective optimization of Simulated Countercurrent Moving Bed Chromatographic Reactor (SCMCR) for MTBE Synthesis

System investigated: Synthesis of Methyl Tertiary Butyl Ether (MTBE) from Tertiary Butyl Alcohol (TBA) and methanol

Description of Work done: An optimal design strategy was proposed for SMBR for MTBE synthesis using Genetic Algorithm. Multi objective optimization studies were performed. Objective functions were the purity and yield of MTBE, desorbent consumption, reactant conversion and volume of catalyst/adsorbent required. Pareto-optimal solutions for the optimization problems were determined. The effect of various operating parameters like, switching time, desorbent flow rate, length and number of columns on the Pareto optimal solutions was reported.

Author: Lode, F., Houmard, M., Migliorini, C., Mazzotti, M., Morbidelli, M.(2001) [15]

Name of the paper: Continuous reactive chromatography

System investigated: Esterification of acetic acid and methanol to produce methyl acetate

Description of Work done: Modeling, simulation and experiments were performed for an SMBR for methyl acetate esterification reaction. A 10-column SMBR set up was designed with Amberlyst 15 acting as both catalyst and adsorbent. Equilibrium dispersive model was used. Simulation and experimental results were compared. Effects of flow rate, feed composition and residence time on SMBR performance were analyzed. Triangle theory was used to map the region of complete conversion and separation. Guidelines for SMBR optimization based on numerical simulation were proposed.

Author: Yu, Weifang., Hidajat, K., Ray, A.K.(2003) [63]

Name of the paper: Modeling, simulation, and experimental Study of a simulated

moving bed reactor for the synthesis of methyl acetate ester

System investigated: Esterification of acetic acid and methanol to produce methyl acetate

Description of Work done: Performance of a SMBR for the synthesis of methyl acetate catalyzed by Amberlyst 15 ion-exchange resin was evaluated numerically and experimentally. A 4-column SMBR setup was used. A rigorous mathematical model was developed to describe the dynamic behavior of SMBR and validated experimentally at different operating conditions. The model could predict the experimental results quite well. A high yield and purity of methyl acetate and nearly complete conversion of the limiting reactant was achieved by selecting proper operating conditions. The effects of various process parameters such as switching time, feed, eluent flow rate, etc. on the behavior of the SMBR was also investigated.

Author: Yu, Weifang., Hidajat, K., Ray, A.K.(2003) [35]

Name of the paper: Application of multiobjective optimization in the design and operation of reactive SMB and its experimental verification

System investigated: Esterification of acetic acid and methanol to produce methyl acetate

Description of Work done: Performance of SMBR process was optimized for an experimentally verified mathematical model for the synthesis of methyl acetate ester. Multiobjective optimization was performed for an existing SMBR experimental setup, and optimum results obtained were subsequently verified experimentally. Thereafter, few other multiobjective optimization studies were performed for both existing setup and at the design stage. The effect of variable (distributed) feed flow rate on the optimum performance of SMBR was also investigated. The optimization was performed using AI-based nondominated sorting genetic algorithm (NSGA), which resulted in Pareto optimal solutions.

Author: Yu, Weifang., Hidajat, K., Ray, A.K.(2005) [36]

Name of the paper: Optimization of reactive simulated moving bed and Varicol systems for hydrolysis of methyl acetate

System investigated: Methyl acetate hydrolysis

Description of Work done: Multi-objective optimization technique was applied to improve the performance of SMBR and its modification, Varicol process for hydrolysis of methyl acetate. The optimization problems of interest considered were simultaneous maximization of purity and yield of acetic acid and methanol, respectively, in the

raffinate and extract streams. The effect of distributed feed flow rate on the performance of SMBR and the applicability of reactive Varicol systems were also investigated. The non-dominated sorting genetic algorithm (NSGA) was used in obtaining Pareto optimal solutions. It was observed that reactive Varicol performs better than SMBR due to non-synchronous switching and its increased flexibility in distributing columns in various sections.

Author: Mazzotti, M., Kruglov, A., Neri, B., Gelosa, D., Morbidelli, M.(1996) [64]

Name of the paper: A continuous chromatographic reactor: SMBR

System investigated: Esterification of acetic acid and ethanol

Description of Work done: Development, modeling and experimental verification was carried out for a SMBR unit for esterification of acetic acid and ethanol. A 13-column setup was used. Amberlyst 15 served as both catalyst and adsorbent. Multicomponent sorption equilibria and swelling of the resin, as well as esterification kinetics, were studied experimentally and described through appropriate models. Some experiments were done in a fixed-bed chromatographic reactor packed with the resin to demonstrate its capabilities. The thermodynamic and kinetic descriptions of the system were combined to develop a fully predictive mathematical model of the chromatographic reactor, able to predict its experimental behavior with reasonable accuracy. The model thus developed was an ideal plug flow SMBR model.

Author: Kawase, M., Suzuki, T. B., Inoue, K., Yoshimoto, K., Hashimoto, K.(1996) [65]

Name of the paper: Increased esterification conversion by application of the simulated moving-bed reactor

System investigated: Esterification of acetic acid and phenethyl alcohol to produce β -phenethyl acetate

Description of Work done: SMBR design for the said esterification reaction was proposed. 8-column SMBR setup was used with Amberlyst 15 as both catalyst and adsorbent. Dispersionless plug flow model was used. Experiments were carried out and compared with simulation results. The reaction conversion increased from equilibrium value of 63% to more than 99% in SMBR. It was proved that flow rates and temperature were the most important factors to achieve almost 100 % conversion.

Author: Dunnebier, G., Fricke, J., Klatt, K.U.(2000) [52]

Name of the paper: Optimal design and operation of simulated moving bed chromatographic reactors

System investigated: Esterification of acetic acid and phenethyl alcohol to produce β -phenethyl acetate

Description of Work done: A novel optimization design strategy for SMBR was developed. It was based on mathematical optimization, a rigorous dynamic process model, and a detailed cost function. The SMBR model accounted for axial dispersion and mass transfer resistances. The new approach used purity constraint to improve performance. Potential savings in operating cost of up to 20% and in desorbent consumption of up to 60% were identified.

Author: Kawase, M., Inoue, Y., Araki, T., Hashimoto, K.,(1999) [6]

Name of the paper: The simulated moving-bed reactor for production of bisphenol A

System investigated: Reaction of acetone and phenol to produce Bisphenol A

Description of Work done: Simulation studies were performed on SMBR. To determine the kinetic and adsorption parameters, batch experiments were performed on fixed bed, with Amberlyst 31 as catalyst and adsorbent. A dispersionless, plug-flow model for SMBR was used. Problems associated with water adsorption that were encountered in the conventional process were overcome by SMBR.

Author: Meissner, J.P., Carta, G.(2002) [66]

Name of the paper: Continuous regioselective enzymatic esterification in a simulated moving bed reactor

System investigated: Enzyme-catalyzed diol esterification in a hexane solvent

Description of Work done: SMBR was developed and tested experimentally to conduct a regioselective enzyme-catalyzed diol esterification in a hexane solvent. The reaction is equilibrium limited, and accumulation of water on the biocatalyst causes a reduction in biocatalytic activity. As a result simultaneous removal of water by adsorption on a catalytically inert ion-exchange resin in was used to improve conversion. A three-zone SMBR system was developed for integrating reaction, adsorption, and regeneration. The SMBR allowed continuous operation while reducing desorbent consumption and improving conversion relative to a conventional fixed-bed reactor. A mathematical model was developed to simulate the SMBR system based on independent analyses of adsorption and reaction phenomena. The model takes into account the interplay of these

phenomena and provided a useful tool to understand the effects of process variables and for the selection of optimum operating conditions.

Author: Kapil, A., Bhat, S.A., Sadhukhan, J.(2010) [67]

Name of the paper: Dynamic simulation of sorption enhanced reaction processes for biodiesel production

System investigated: Esterification of fatty acid and methanol to produce Fatty Acid Methyl Ester (FAME)

Description of Work done: Synthesis of FAME in SMBR was studied using rigorous dynamic simulation approaches. The simulation frameworks were developed to analyze the effect of various design and operating parameters such as length and velocity of the bed, feed ratio, and flow rate ratios in different zones in the case of the SMBR, on the feed conversion and outlet concentration/purity. The continuous production of pure FAME was designed by simulating the movement of solid catalyst and adsorbent bed through switching inlet and outlet fluid ports, in an SMBR process. The lower limit of the acceptable flow rates for the SMBR process was determined by a comparison with a true counter current system. The rigorous dynamic simulation of the SMBR process further helped to investigate the effect of various operating parameters such as switching time, length of the reactor adsorber unit, flow rate in desorption zone, solid regeneration, and reload zone on the purity of the raffinate and the conversion of fatty acid. The purity of FAME and conversion were the two main criteria to compare the performances among different sets of operating conditions.

Author: Meurer, M., Altenhöner, U., Strube, J., Schmidt-Traub, H.,(1997) [68]

Name of the paper: Dynamic simulation of simulated moving bed chromatographic reactors

System investigated: Simulation of both reversible and irreversible reaction in SMB

Description of Work done: Optimal design strategy was proposed for SMBR by rigorous modeling. Equilibrium dispersive model for mass transfer effects and adsorption isotherms for both adsorbent and catalyst were applied. Dynamic simulation studies were performed on SMBR and the results were compared with conventional chromatographic process. Effects of relative adsorptivities on conversion were studied. Optimization by rigorous modeling was done.

Author: Fricke, J., Meurer, M., Schmidt-Traub, H.(1999) [2]

Name of the paper: Design and layout of simulated-moving-bed chromatographic reactors

System investigated: Design and simulation of SMBR for a general ester hydrolysis reaction

Description of Work done: Dispersed plug flow model taking into account both axial dispersion and mass transfer effects and adsorption isotherms for both adsorbent and catalyst were used for model prediction. Effect of column packing; both homogenous and heterogeneous as well as the reactor length and column configuration were taken into account for dynamic simulation of the SMBR.

Author: Fricke, J., Meurer, M., Dreisörner, J., Schmidt-Traub, H.(1999) [4]

Name of the paper: Effect of process parameters on the performance of a simulated moving bed chromatographic reactor

System investigated: Study of process parameter effects on the performance of SMBR for a reversible decomposition reaction

Description of Work done: Equilibrium dispersive model taking into account the mass transfer effects was applied. Linear adsorption isotherms were used for model prediction. The effects of the adsorption and reaction constants on the SMBR performance based on feed and desorbent flow rates were studied. Guidelines were presented for enhanced SMBR performance.

Author: Migliorini, C., Fillinger, M., Mazzotti, M., Morbidelli, M.(1999) [69]

Name of the paper: Analysis of simulated moving-bed reactors

System investigated: Behavior and design strategy for SMBR based on non-reactive SMB theory

Description of Work done: Potential application of SMBR for a wide range of reactions, such as esterification, transesterification, etherification, acetylation, some isomerizations, hydrogenation, some enzyme reactions and others. Equilibrium dispersive model with linear adsorption isotherm were used for model prediction. Simulations of ethyl acetate synthesis from acetic acid and ethanol on Amberlyst 15 were performed. A triangular separation region similar to non-reactive SMB was observed. It was determined that feed concentration should be an optimization parameter.

Author: Huang, S. and Carr R.(2001) [70]

Name of the paper: A simple adsorber dynamics approach to simulated countercurrent moving bed reactor performance

System investigated: Investigation of high temperature reactions of both reversible and irreversible type in SMBR

Description of Work done: A novel but simple approach was followed for SMBR design. Algebraic material balance equations were used for model prediction. Simple algebraic expressions for dependence of reactor performance on per pass conversion, adsorption constants and reactant concentration were presented.

2.5 Design strategies proposed for Simulated Moving Bed systems

Various design strategies have been proposed to describe the behavior of SMB.

2.5.1 Theory proposed by research group at University of Minnesota

This theory states that the mass balance of any component i in a section of TMB in transient state is given by [71]:

$$\varepsilon \frac{\partial c_i}{\partial t} + (1 - \varepsilon) \frac{\partial q_i}{\partial t} + \varepsilon \cdot u_g \frac{\partial c_i}{\partial x} - (1 - \varepsilon) \cdot u_s \frac{\partial q_i}{\partial x} = 0 \quad (2.1)$$

Here,

u_s and u_g = solid phase velocity and mobile phase velocity respectively.

c_i and q_i = mobile phase concentration and solid phase concentration of the component i respectively.

The above mass balance equation assumes that there is one dimensional flow of solid and fluid, the adsorption equilibrium is instant, and there is axial dispersion & other mass transfer resistances are negligible. c_i is related to q_i by the following Langmuir isotherm equation:

$$q_i = \frac{N \cdot K_i \cdot c_i}{1 + K_i \cdot c_i} \quad (2.2)$$

Applying dimensionless parameters:

$$\gamma_i = K_i \cdot c_i ; \alpha_i = \frac{1-\varepsilon}{\varepsilon} N \cdot K_i ; \sigma_i = \alpha_i \frac{u_s}{u_g} \quad (2.3)$$

Equation (2.1) reduces to:

$$\left[1 + \frac{\alpha_i}{(1+\gamma_i)^2}\right] \frac{\partial \gamma_i}{\partial t} + \left[1 - \frac{\sigma_i}{(1+\gamma_i)^2}\right] = 0 \quad (2.4)$$

Rearranging the above equation:

$$-\frac{dx}{dt} = V_{i,s} = \frac{u_g \left[1 - \frac{\sigma_i}{(1+\gamma_i)^2}\right]}{\left[1 + \frac{\alpha_i}{(1+\gamma_i)^2}\right]} \quad (2.5)$$

Where $V_{i,s}$ is the velocity of a point of concentration γ ; it describes the location of a particular concentration with time. At low concentrations, $\gamma_i \ll 1$; hence $V_{i,x}$ reduces to:

$$V_{i,s} = \frac{u_g [1 - \sigma_i]}{[1 + \alpha_i]} \quad (2.6)$$

Equation (2.6) describes a system having linear isotherm. In such case, $V_{i,s}$ is independent of concentration, but dependent on σ_i . $V_{i,s}$ denotes the effective velocity with which a component i travels through the solid phase. The parameter σ_i , defined by Petroulas et al. , determines whether this velocity will be positive or negative. When $\sigma_i > 1$, $V_{i,s}$ is negative and the component i travels with the solid phase in the column,

irrespective of its concentration. If $\sigma_i < 1$, $V_{i,s}$ is positive and the component i travels with the mobile phase. This can be understood further by considering the True Moving Bed system as represented in Figure 2.3. Let us assume that a binary mixture of A and B is fed into the system. Then under ideal conditions, complete separation of A and B is possible by adjusting the fluid flow rates u_g in the four sections and the solid phase flow rates u_s , such that $\sigma_A > 1$ in section 1 and $\sigma_A < 1$ in sections 2, 3 and 4; and $\sigma_B > 1$ in section 4 and $\sigma_B < 1$ in sections 1, 2 and 3.

The above mentioned situation of ideal separation in a TMB system can also be achieved in an equivalent SMB setup. However the solid phase flow rate u_s is replaced by a hypothetical velocity ζ , where $\zeta = L/t_s$, which is the ratio between the switching distance and the switching time in SMB [32].

In case of reactive SMB where a reversible reaction $A \rightleftharpoons B$ is taking place, if the pseudo solid phase and mobile phase velocities are such adjusted that $\sigma_A > 1$ and $\sigma_B < 1$, countercurrent separation of the reactant and product is possible which also enhances the conversion of the reactant and product purity [71].

2.5.2 Theory proposed by research group at ETH, Zurich

This research group proposed what is known as Triangle theory to define the operating conditions of SMB [23, 72]. This theory is widely used for SMB design because it determines a complete separation region which is triangular in shape; which holds well with or without mass transfer resistance for both linear and nonlinear adsorption isotherms.

The triangle theory states that the TMB and SMB can be considered equivalent if the following conversions are satisfied:

$$V_\emptyset = N_\emptyset \cdot V_{col} \quad (2.7)$$

$$\frac{V_{col}}{t_s} = \frac{Q_s}{1 - \varepsilon}$$

(2.8)

$$Q_{\emptyset}^{SMB} = Q_{\emptyset}^{TMB} + \frac{Q_s \cdot \varepsilon}{1 - \varepsilon}$$

(2.9)

Here,

V_{\emptyset} = volume of section \emptyset of TMB

V_{col} = volume of single column of SMB

N_{\emptyset} = number of columns in section \emptyset of SMB

t_s = switch time

Q_s = volumetric solid flow rate in TMB

ε = bed void fraction

Q_{\emptyset}^{SMB} = volumetric flow rate of section \emptyset of SMB

Q_{\emptyset}^{TMB} = volumetric flow rate of section \emptyset of TMB

A mass balance equation was developed for an equilibrium TMB model for a two component system (A & B, A being the more strongly adsorbed species). Not taking into account the axial dispersion and mass transport resistances, in section \emptyset , the mass balance is given by:

$$\frac{\partial}{\partial \tau} [\varepsilon^* \cdot c_i + (1 - \varepsilon^*) q_i] + (1 - \varepsilon_p) \frac{\partial}{\partial \zeta} [m_{\emptyset} \cdot c_i - q_i] = 0 \quad (i = A, B) \quad (2.10)$$

Here,

τ, ζ = dimensionless time and space coordinates respectively

ε_p = intraparticle porosity of solid phase

$\varepsilon^* = \varepsilon + \varepsilon_p(1 - \varepsilon)$; Overall void fraction of bed

q_i = concentration of i in adsorbed phase

c_i = concentration of i in fluid phase

q_i is related to c_i by either linear or nonlinear adsorption isotherm.

$$m_\emptyset = \frac{Q_\emptyset^{TMB} - Q_s \cdot \varepsilon_p}{Q_s(1 - \varepsilon_p)} = \frac{\text{net fluid flow rate}}{\text{adsorbed phase flow rate}} \quad (2.11)$$

Equation (2.11) represents the ratio of the net fluid flow rate to the solid phase flow rate in a TMB unit. Selection of values of the m_\emptyset parameters is required for the design of a TMB unit for the given binary feed composition (A & B).

For an equivalent SMB unit, according to the conversion equations (2.7 – 2.9), m_\emptyset is defined as:

$$m_\emptyset = \frac{Q_\emptyset^{SMB} \cdot t_s - V_{col} \cdot \varepsilon^*}{V_{col}(1 - \varepsilon^*)} \quad (2.12)$$

The differential mass balance equation (2.10) was solved for both linear and nonlinear adsorption isotherms so that a complete, triangular separation region could be mapped [23, 73].

2.5.2.1 Linear isotherm

For linear adsorption isotherm, the triangle theory can be stated as:

$$q_i = H_i \cdot c_i \quad (i = A, B) \quad (2.13)$$

Where H_i is the Henry constant for component i . For complete separation of A and B, the following inequalities must be fulfilled [72] –

$$H_A < m_1 < \infty$$

(2.14a)

$$H_B < m_2 < H_A$$

(2.14b)

$$H_B < m_3 < H_A$$

(2.14c)

$$\frac{-\varepsilon_p}{(1 - \varepsilon_p)} < m_4 < H_B$$

(2.14d)

For a net positive feed flow rate, an additional inequality must be applied; $m_3 > m_2$. This results in combination of equations (2.14b) and (2.14c) into the following:

$$H_B < m_2 < m_3 < H_A$$

(1.14e)

Hence, if the constraints on m_1 (Eqn. 2.14a) and m_4 (Eqn. 2.14d) are fulfilled, a complete separation region can be mapped in the (m_2, m_3) plane, as is defined by equation (2.14e). This is shown in Figure 2.6. The triangle shaped region in the middle of the diagram shows the complete separation region where 100% product purity can be achieved for both raffinate and extract. In the upper portion of the diagram representing pure extract, the constraint $H_B < m_3 < H_A$ is not fulfilled. In this region, $m_3 > H_A$; hence although the extract is 100% pure, the strongly adsorbed component contaminates the raffinate stream. Similarly, in the pure raffinate region of the diagram, the constraint $H_B < m_2 < H_A$ is not satisfied. In this region $m_2 < H_B$; hence weakly adsorbed B contaminates the extract stream, only pure raffinate can be obtained. In the top left portion of the diagram, both $m_3 > H_A$ and $m_2 < H_B$, hence neither the raffinate nor the extract is 100% pure.

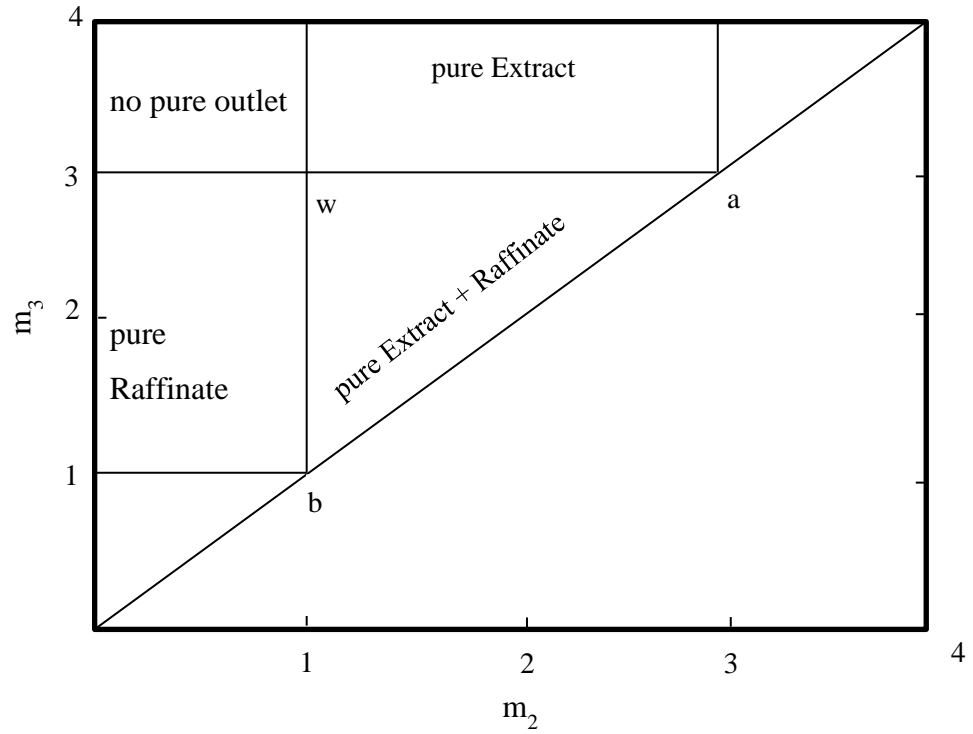


Figure 2.6 System described by a Linear Adsorption Isotherm [72]

2.5.2.2 Nonlinear isotherm

For nonlinear adsorption isotherm, the triangle theory can be stated as:

$$q_i = \frac{N_i \cdot K_i \cdot c_i}{1 + K_A \cdot c_A + K_B \cdot c_B} \quad (i = A, B) \quad (2.15)$$

The above equation represents a competitive non-stoichiometric Langmuir isotherm. The mass balance equation (2.10) is combined with equation (2.15) to derive the conditions for the flow rate ratio m_ϕ for complete separation of A and B. to achieve so, the following inequalities must be fulfilled [23, 73, 74]:

$$H_A = m_{1,min} < m_1 < \infty \quad (2.16a)$$

$$m_{2,min}(m_2, m_3) < m_2 < m_3 < m_{3,max}(m_2, m_3) \quad (2.16b)$$

$$\frac{-\varepsilon p}{(1-\varepsilon p)} < m_4 < m_{4,max}(m_2, m_3) = \frac{1}{2} \left\{ H_B + m_3 + K_B \cdot c_{B,f}(m_3 - m_2) - \sqrt{[H_B + m_3 + K_B \cdot c_{B,f}(m_3 - m_2)]^2 - 4 \cdot H_B \cdot m_3} \right\} \quad (2.16c)$$

Where, $H_i = N_i \cdot K_i$. The implicit constraints on m_2 and m_3 define the complete separation region in the (m_2, m_3) plane, which is triangle shaped as shown in Figure 2.7.

The lower constraint on $m_1(m_{1,min})$ and the upper constraint on $m_4(m_{4,max})$ are determined to be explicit; m_4 being dependent on the ratio between m_2 and m_3 .

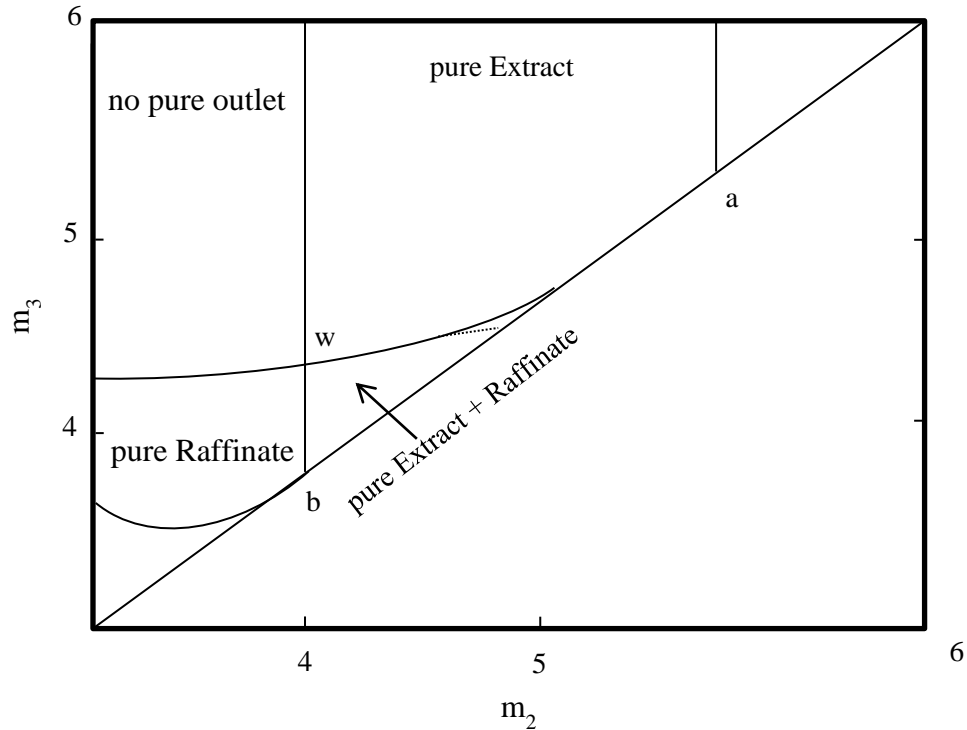


Figure 2.7 Triangle theory described by nonlinear adsorption isotherm [72]

It was also shown that the overall concentration of feed mixture, $c_{T,f} = c_{A,f} + c_{B,f}$, influences the region of complete separation in the (m_2, m_3) plane. The area of the separation region decreases with increasing total feed concentration. This is shown in Figure 2.8.

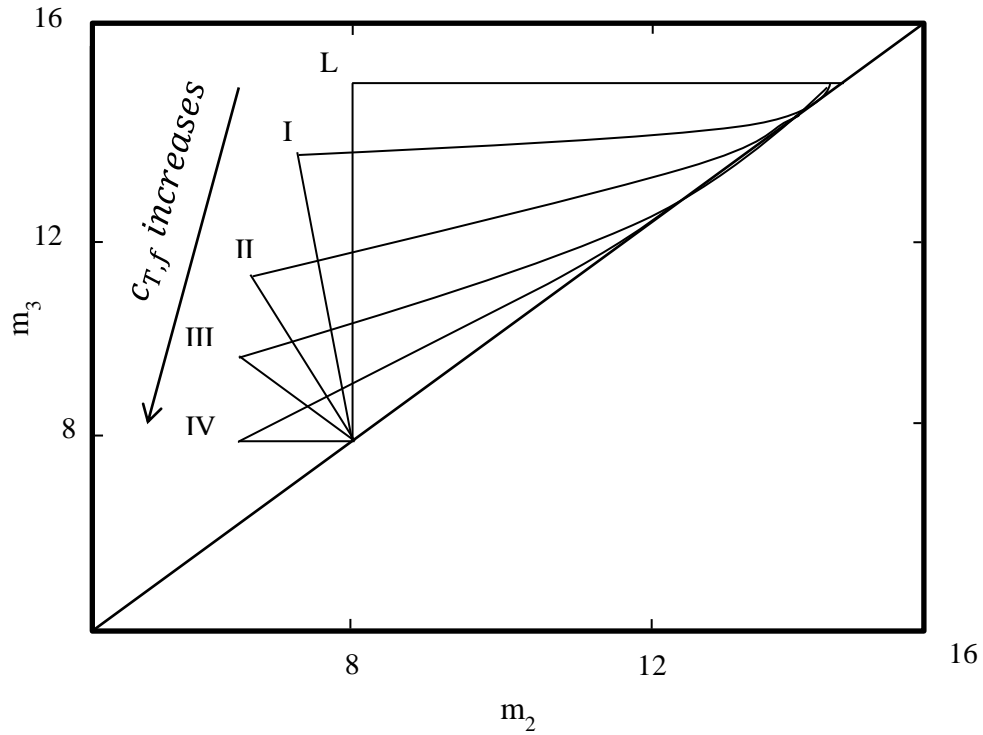


Figure 2.8 Effect of overall feed concentration on the region of complete separation in the (m_2, m_3) plane [72]

The triangle theory was also applied to other nonlinear isotherms, such as the modified Langmuir isotherm [72, 75] and bi-Langmuir isotherm [76]. In addition to binary systems, this theory was also applied to multi-component systems [5, 23, 73, 74]. Mazzotti et al. [72] defined certain parameters for the optimal operation of a SMB unit for separation of binary mixture of A and B. These parameters are:

$$\text{Desorbent Requirement} = DR = \frac{c_d}{c_{T,f}} \left(1 + \frac{m_1 - m_4}{m_3 - m_2} \right) \quad (2.17a)$$

$$\text{Enrichment: } E_A = \frac{c_{A,extract}}{c_{A,f}} = \frac{m_3 - m_2}{m_1 - m_2}, \quad E_B = \frac{c_{B,raffinate}}{c_{B,f}} = \frac{m_3 - m_2}{m_3 - m_4}$$

(2.17b)

$$\text{Productivity: } PR = \frac{Q_f \cdot c_{T,f}}{(1 - \varepsilon^*) \rho_s \cdot V_T} = \frac{c_{T,f} (m_3 - m_2)}{\rho_s \cdot t^* \sum_{\phi=1}^4 N_{\phi}} \quad (2.17c)$$

Here,

c_d = feed concentration of desorbent

Q_f = feed flow rate

ρ_s = density of adsorbent

V_T = total column volume

The operating conditions should be such selected so that minimization of DR as well as maximization of E_A , E_B and PR occurs in the region of complete separation. This design procedure is illustrated in Figure 2.9.

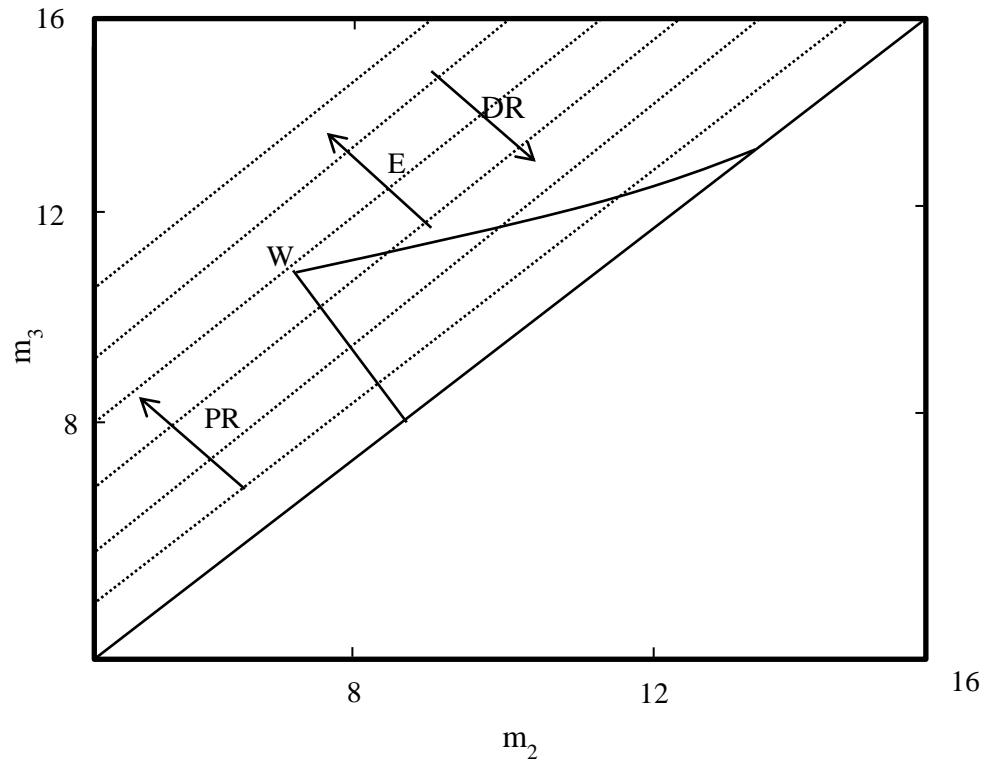


Figure 2.9 Application of triangle theory for optimal operating conditions in SMB [72]

The figure describes a Langmuir isotherm. The coordinates of the point W represent the optimal operating conditions in the (m_2, m_3) plane. This is because when the operating point is moved from the diagonal to the vertex W across the straight lines of unitary slope in the complete separation region, all the parameters improve; there is reduction of desorbent consumption as well as improvement of enrichment and productivity. This improvement occurs due to increased difference between m_2 and m_3 . The parameters are also improved when m_1 is small and m_4 is large. Hence optimum value of m_1 is its lower bound; whereas for m_4 it is its upper bound.

The triangle theory has also been extended to reactive SMB. The same criteria for non-reactive SMB can be applied here. It was reported that regeneration occurs in sections 1 and 4 of the SMB unit, where under conditions of complete conversion and separation, no reaction takes place [15, 69]. Hence flow rate ratio in section 1 (m_1) must be larger than its critical value for complete regeneration of adsorbent. Similarly flow rate ratio in section 4 (m_4) must be smaller than its critical value for complete regeneration of desorbent. Once these criteria are fulfilled, the values of m_1 and m_4 do not affect the conversion/purity of product.

The flow rates in sections 2 and 3 of the SMB unit determine the degree of separation. This is the reactive zone of SMB. The (m_2, m_3) plane represents the complete separation and conversion region. The vertex of this region represents the optimal operating conditions for maximum productivity in a reactive SMB, just as in the case of non-reactive SMB. The shape of this region depends on the feed composition and the residence time. There is a lower limit of the switch time, below which the residence time in the reactive zone is insufficient for the reaction to significantly proceed.

2.5.3 Standing Wave Theory proposed by research group at Purdue University

Another novel design procedure for SMB is the Standing Wave Concept. This theory states that each section of TMB has certain concentration waves. By making these waves stand, a particular section can fulfill its role to ensure proper performance of the unit. If the flow rates and the solid movement velocity in a TMB (port switching time in an equivalent SMB) are selected properly, separation of a binary mixture of A and B can be made possible.

The standing wave concept has been applied to study various systems, e.g. Separation of Raffinose and Fructose [77], Fructose and Glucose [78], separation of multiple sugars [79], Paclitaxel separation [80, 81], amino acid separation [82, 83], insulin separation [84], chiral and enantioseparation [85, 86] etc.

The standing wave concept is based on the idea that each section in a SMB system should perform a specific role in separation to ensure purity of the product; this is brought about by making the concentration waves stand in a particular section. By appropriately selecting the flow rates and solid phase movement velocity in TMB (port switching time in an equivalent SMB), the advancing front (or adsorption wave) of the less adsorbed component B can be made to stand in section IV and its desorption wave can stand in section II of the SMB system. The advancing front of the more strongly adsorbed component A is made to stand in section III and its desorption wave stands in section I. this is illustrated in Figure 2.10.

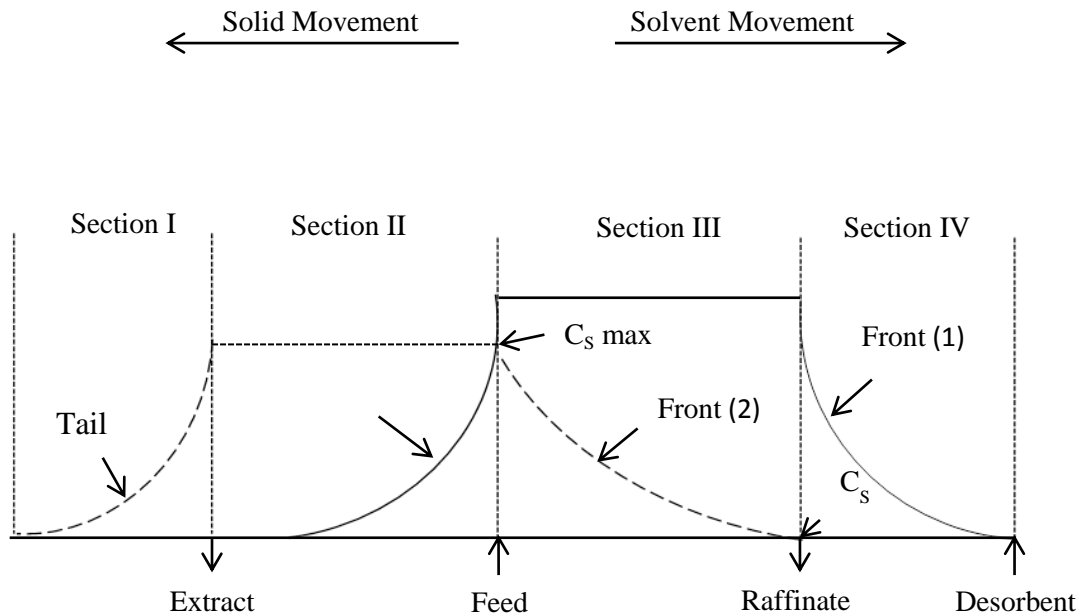


Figure 2.10 Standing wave theory for a linear TMB system [80]

A model was developed for a TMB to derive the standing wave equations. The mass balance equations for a component i in section 1 are:

$$\frac{\partial c_i}{\partial t} + E_i^1 \frac{\partial^2 c_i}{\partial x^2} + u_1^{TMB} \frac{\partial c_i}{\partial x} = P \cdot K_l^1 (c_i - c_i^*) \quad \text{for mobile phase} \quad (2.18)$$

$$\varepsilon_p \frac{\partial c_i^*}{\partial t} + (1 - \varepsilon_p) \frac{\partial q_i^*}{\partial t} = K_l^1 (c_i - c_i^*) + u_s \cdot \varepsilon_p \frac{\partial c_i^*}{\partial x} + (1 - \varepsilon_p) u_s \frac{\partial q_i^*}{\partial t} \quad \text{for solid phase} \quad (2.19)$$

Here,

c_i , c_i^* and q_i^* = mobile phase, average pore phase and solid phase concentration of i respectively

P = bed phase ratio; $(1 - \varepsilon) / \varepsilon$

$\varepsilon, \varepsilon_p$ = bed and intra-particle void fraction respectively

u_1^{TMB}, u_s = interstitial linear mobile phase velocity in section 1 and the solid phase velocity respectively

E_i^1, K_l^1 = axial dispersion coefficient and lumped mass transfer coefficient of i in section 1 respectively

For an equivalent SMB, the interstitial velocity u_1^{SMB} is related to u_1^{TMB} by:

$$u_1^{SMB} = u_1^{TMB} + u_s \quad (2.20)$$

The Standing Wave Concept was applied to systems having linear isotherm. It was explained taking into consideration the axial dispersion and mass transfer resistance.

2.5.3.1 Neglecting axial dispersion and mass transfer resistance

When axial dispersion and mass transfer resistances are negligible, the following equation holds true [77]:

$$(1 + P \cdot \delta_i) \frac{\partial c_i}{\partial t} + [u_1^{SMB} - u_s(1 + P \cdot \delta_i)] \frac{\partial c_i}{\partial t} = 0 \quad (2.21)$$

(derived from eqn. 2.18 and 2.19)

Here,

$\delta_i = \varepsilon_p + (1 - \varepsilon_p)K_i$; Where K_i is the linear adsorption isotherm constant of component i

The velocity of the concentration wave of component i relative to the feed entry point is:

$$u_{wi} = -\frac{dx}{dt} = \frac{u_1^{SMB}}{1 + P \cdot \delta_i} - u_s = u_{sol,i} - u_s \quad (2.22)$$

$u_{sol,i}$ is the migration velocity of the solute i .

Considering a binary mixture of A and B, where A is more strongly adsorbed in the solid phase, their separation would depend on u_s and $u_{sol,i}$. Some conditions have to be fulfilled. The solid phase velocity u_s should be greater than velocity of A ($u_{sol,A}$) in section 3 and less than velocity of B ($u_{sol,B}$) in section 4. In section 1, u_s should be less than desorption wave of A and in section 4, u_s should be less than desorption wave of solute B.

Hence, for complete separation of A and B to take place, the following inequalities must be satisfied:

$$\text{Section1: } u_{sol,A} - u_s > 0 \quad (2.23a)$$

$$\text{Section 2: } u_{sol,B} - u_s > 0 \quad (2.23b)$$

$$\text{Section3: } u_{sol,A} - u_s < 0 \quad (2.23c)$$

$$\text{Section 4: } u_{sol,B} - u_s < 0 \quad (2.23d)$$

The boundary values for the above equations can be defined as:

$$u_1^{SMB} = (1 + P \cdot \delta_A)u_s \quad (2.24a)$$

$$u_2^{SMB} = (1 + P \cdot \delta_B)u_s \quad (2.24b)$$

$$u_3^{SMB} = (1 + P \cdot \delta_A)u_s \quad (2.24c)$$

$$u_4^{SMB} = (1 + P \cdot \delta_B)u_s \quad (2.24d)$$

The above equations represent the optimum section flow rates, resulting in highest feed flow rate and lowest solvent flow rate for a given system.

When the inequalities (eqn. 2.23 a – d) alongwith their boundary conditions are fulfilled, a number of events take place in all the sections of SMB which facilitates separation. As A is more strongly adsorbed than B, the migration velocity of A is less than B. As a result, in section 3, the adsorption wave of B travels faster than that of A, moving past the raffinate port into section 4. Whereas the adsorption wave of A stands still in section 3. In section 2, the desorption wave of B stands still, whereas the desorption wave of A moves past the extract port and enters section 1. In section 1, the desorption wave of A stands still. Lastly the adsorption wave of B stands in section 4. Thus, the more strongly adsorbed A is obtained at the extract port and B is obtained at raffinate port.

Hence, this theory enables the determination of all the mobile and solid phase velocities from the equations 2.24 (a-d) if either feed flow rate or solvent flow rate is given:

$$\frac{F}{\varepsilon \cdot S} = u_3^{SMB} - u_2^{SMB} \quad (2.25a)$$

$$\frac{E}{\varepsilon \cdot S} = u_1^{SMB} - u_4^{SMB} \quad (2.25b)$$

Here,

F = feed flow rate

E = solvent flow rate

S = bed cross section

2.5.3.2 Linear system with axial dispersion and mass transfer resistance

Taking into account the dispersion and the mass transfer effects, a steady state model was used to derive the design equations. The time derivative term was removed from equations 2.21 and 2.22 and the following were obtained after derivation and rearrangement [77, 80] –

$$(1 + P \cdot \delta_A)u_s - u_1^{SMB} = -\beta_A^I \left(\frac{E_A^I}{L^I} + \frac{P \cdot u_s^2 \cdot \delta_A^2}{K_{fA}^I \cdot L^I} \right) \quad (2.26a)$$

$$(1 + P \cdot \delta_B)u_s - u_2^{SMB} = -\beta_A^{II} \left(\frac{E_B^{II}}{L^{II}} + \frac{P \cdot u_s^2 \cdot \delta_B^2}{K_{fB}^{II} \cdot L^{II}} \right) \quad (2.26b)$$

$$(1 + P \cdot \delta_A)u_s - u_3^{SMB} = -\beta_A^{III} \left(\frac{E_A^{III}}{L^{III}} + \frac{P \cdot u_s^2 \cdot \delta_A^2}{K_{fA}^{III} \cdot L^{III}} \right) \quad (2.26c)$$

$$(1 + P \cdot \delta_B)u_s - u_4^{SMB} = -\beta_B^{IV} \left(\frac{E_B^{IV}}{L^{IV}} + \frac{P \cdot u_s^2 \cdot \delta_A^2}{K_{fA}^{IV} \cdot L^{IV}} \right) \quad (2.26d)$$

Here,

β = ratio of the highest concentration to the lowest concentration of the standing wave in a particular section It defines the purity requirements; for example in section 1, $\beta_A^I = \ln \left(\frac{c_A|_{x=0}}{c_A|_{x=L^I}} \right)$, which represents the ratio of the concentration of the desorbent port to that of the extract port for solute A.

L = length of a particular section

K_f = mass transfer coefficient of A or B

Equations 2.26(a-d) are actually the modifications of equations 2.24(a-d). The linear velocities in equation 1.24 were modified taking into account the axial dispersion, the mass transfer coefficient, section length and product purity. For significant mass transfer resistance, equations 2.26(a-d) gave the highest throughput and lowest solvent consumption for a specified purity and feed flow rate in a system.

Although the triangle theory and the standing wave concept are based on a TMB model, the design principles are convenient for SMB systems with insignificant mass transfer resistances and simple adsorption isotherms. The same can be said for the sigma theory. For a simple reversible reaction system having linear adsorption isotherm and less number of columns in the SMB setup, the sigma theory is quite convenient. Hence, this theory has been used in the present study.

2.6 Biodiesel - A Brief Introduction

Biodiesel can be defined as monoalkyl (methyl, ethyl or propyl) ester derived from transesterification of vegetable oils/animal fats with alcohol. This transesterification reaction is reversible and hence requires the presence of catalysts (acid or base) to push the reaction in forward direction.

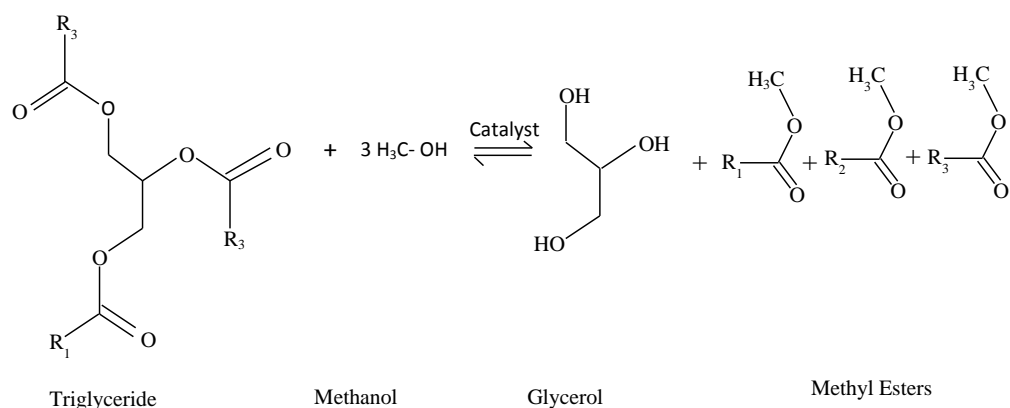


Figure 2.11 A general scheme for transesterification reaction

Thus, biodiesel is the fatty acid methyl ester (FAME) obtained as a product during the transesterification reaction. However, FAME, can also be produced by esterification of free fatty acid (FFA) with methanol in a reversible reaction to produce FAME and water. In general the transesterification reaction is base-catalyzed and the esterification reaction is catalyzed by acid [87].

The concept of biodiesel as an alternative diesel fuel has gained great importance worldwide owing to its renewable nature, biodegradability and good quality exhaust [88]. It has many favorable advantages compared to petroleum based diesel. It has a higher cetane number than conventional diesel [89]. Its use in diesel engines reduces the emissions of hydrocarbons, carbon monoxide, particulate matter and sulfur dioxide [90]. In a life cycle analysis the overall carbon dioxide emission was calculate to be decreased by 78% when biodiesel was used as fuel compared to mineral diesel [91]. Hence it does not contribute to the greenhouse gas levels. In the present world, when nonrenewable resources are rapidly depleting, biodiesel is the right alternative for use in the automobile industry. One of the greatest advantages of biodiesel is that that it can be used in any diesel engine with little or no modifications [89]. It can also be blended with petroleum diesel to create a biodiesel blend. Hence the use of biodiesel would greatly reduce the consumption of petroleum based diesel in automobile industry.

However, to use biodiesel as a fuel, it must be highly pure. It has to meet the standards set by American Standard for Testing Materials (ASTM) and European Union (EU). The fuel water content, free fatty acids, free and bound glycerin must be kept at a minimum level and purity must exceed 96.5% [88, 92]. Such high standards result in high production costs, which need to be lowered to encourage use of biodiesel.

2.6.1 Current processes for biodiesel production

At present most biodiesel manufacturing technologies apply homogenous catalysts in batch or continuous mode [87, 93]. There are several methods in use both at pilot or industrial scale:

- (1) Batch process – this employs either acid or basic catalysts. Although quite flexible, it has low productivity and high operating cost [94, 95].
- (2) Continuous process – this process mostly uses homogenous catalysts. It ensures higher productivity due to combination of the esterification and transesterification reactions. Recently heterogeneous solid catalysts [96-100] as well as reactive distillation [97, 101-108] have also been employed to continuous biodiesel production.
- (3) Supercritical process – this process does not require catalysts, but the operating conditions are quite severe; requiring temperature greater than 240 degree centigrade and pressured greater than 80 bar. At such extreme conditions, oil-alcohol miscibility does not hinder transesterification kinetics [87]. Several studies have been done in this field, all of them requiring extreme conditions and specialized equipment [109-117].
- (4) Enzymatic process – this process is carried out under mild conditions and hence has lower energy requirements as compared to other processes [118-124]. Product refining is simple and the reaction temperature is also low [125]. However, the reaction yield is low, enzymes are costly and reaction times are quite long. Due to

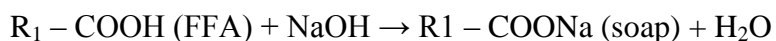
these major drawbacks, enzymatic catalysis fails to compete with other industrial processes [126, 127].

- (5) Hydro-pyrolysis – in this process, triglycerides are converted to fuel by hydrogenation followed by pyrolysis. Instead of conventional fatty acid ester, the fuel product is a mixture of long chain hydrocarbons [128]. This next generation biodiesel has advantages, but requires complex equipment and the availability of a low-cost hydrogen source [87].
- (6) Reactive separation – this involves carrying out the catalyzed transesterification reactions in a single integrated unit. Reactive distillation, reactive adsorption [67, 95] and membrane reactors [129] fall in this category.
- (7) Biodiesel from microalgae – recently, microalgae have been used to produce ethanol and biodiesel using biochemical processes. Due to its renewable nature, microalgae are being used as a feed stock for biodiesel production [130-133].

2.6.2 Choice of Catalyst: Homogenous vs. Heterogeneous

At present, production of biodiesel is still mostly done using homogenous basic catalysts (NaOH or KOH). They provide higher reaction rate than acid catalysts. Also they are cost effective and easily available. As far as the choice of raw material is concerned, edible vegetable oils like soyabean oil and rapeseed oil can be used. But recently their prices have gone up, and hence their use has become cost prohibitive. An alternative is the use of waste oils, such as frying oils, trap grease, soapstock etc. as feedstock for biodiesel production [134]. Thus, basic catalyst in conjunction with waste oil as raw material seems to be a promising option for lowering the production cost.

However, waste oil is high in free fatty acid (FFA) content. On transesterification in presence of alkaline catalyst, they form soap:



This makes the separation of biodiesel and alcohol difficult, while also decreasing the total biodiesel yield. This problem can be overcome if acid catalysts are used. FFAs react with alcohol in presence of an acid catalyst to form ester and water [135-137]; there is no soap formation:



However, use of homogeneous acid catalysts such as H_2SO_4 causes difficulties in recovery after reaction and produces toxic wastewater [134], which has to be removed by purification. Hence, the crude biodiesel produced by homogeneous catalyst has to go through several separation and purification techniques to produce high quality biodiesel.

A suitable alternative for this problem is the use of solid acid catalysts. In the recent years, there has been a tremendous interest in using solid acid heterogeneous catalysts instead of the conventional homogeneous ones for biodiesel production [87]. They have the advantage of being easy to recover and reuse, as well as being environmentally compatible [134, 138-142]. Because of their reusability, they are essential for development of technologies based on process intensification, such as reactive separation units. A solid acid catalyst can be easily packed in a rotating packed-bed continuous reactor, which has been reported to have a better performance than continuous stirred tank reactor [143]. The use of such catalysts for transesterification reactions to produce biodiesel have been widely studied; however they require high temperature conditions [87]. Various solid acid catalysts such as zeolites [90, 137, 144], metal oxides [144-147] (tungstated and sulfated zirconia, polyaniline sulfate, sulfated tin oxide) heteropoly acids, metal complexes, ion exchange resins [148-152] (Amberlyst, Nafeon, Relite CKS etc.) acidic ionic liquid, and others have been explored as potential heterogeneous catalysts.

2.6.3 Amberlyst 15 as catalyst

Amberlyst 15 is a cation exchange resin which has good esterification efficiency [134]. It has a cross linked three dimensional structure obtained by sulphonation of a copolymer of polystyrene and divinyl benzene.

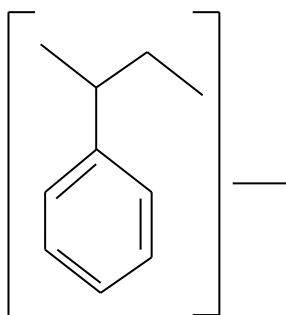


Figure 2.12 Amberlyst 15 polymer

It is a macroporous resin having a surface area of 42.5 m²/gm [153]. It is heat sensitive and loses activity above 393K. The macroreticular structure of Amberlyst 15 imparts unusual physical and chemical stability to the resins as well as unique properties when dry or when employed in nonpolar solvent systems, broadening the overall possibilities for ion exchange. This resin is suitable for applications in oxidizing atmospheres, nonpolar solvent systems, continuous fluidized systems where the physical stability of conventional resins is limiting [153]. Since it is macroporous, it does not swell appreciably in non-aqueous medium [154]. The swelling phenomenon is particularly important in case of such ion exchange resin because it controls the accessibility of the acid sites in the resin, therefore its reactivity [87].

However, reaction of free fatty acid with alcohol produces water, which poisons the catalytic sites on the resin. As a result, with the progress of esterification reaction, the catalytic activity of Amberlyst 15 decreases [136]. This problem can be overcome in a Simulated Moving Bed Reactor (SMBR), in which the resin would be periodically regenerated during a reaction cycle. Hence, this catalyst has been successfully used to carry out esterification reactions in a SMBR [15, 31, 63, 64, 65].

2.6.4 Production of biodiesel by simulated moving bed technology, a reactive – separation method

Reactive separation is a promising method as it involves carrying out reaction and separation in a single integrated unit. Doing so would definitely bring down the cost of biodiesel production, as it would eliminate the need of the traditional separation and purification techniques like gravitational settling, distillation, evaporation etc. which are required to produce high quality biodiesel [88]. Quite a few studies have been done involving reactive separation, some of which are tabulated below [87]:

Table 2.2 Biodiesel by reactive separation

Process	Reaction type and catalyst used
Reactive distillation	Transesterification using homogenous (NaOH, KOH) [101, 105] and heterogeneous catalyst (sodium ethoxide, tungstated zirconia, heteropolyacid) [155, 156]
	Esterification using homogenous (H ₂ SO ₄) [157-159] and heterogeneous (ion exchange resins, mixed metal oxides, sulfated zirconia) [97, 103, 104, 107, 117, 160-165] catalysts
Reactive absorption	Esterification using heterogeneous (mixed metal oxides, or sulfated zirconia) catalysts [95, 166, 167]
Reactive extraction	Transesterification using homogeneous (H ₂ SO ₄ , NaOH) catalysts [168-176]

Membrane reactor

Transesterification using homogenous catalyst and membrane (carbon, ceramic, zeolite) [177-183]

Esterification using homo/heterogeneous catalyst and membrane (PVA/PES) [184-187]

The processes tabulated above use extreme conditions of temperature and pressure to overcome biodiesel conversion and separation difficulties. Simulated moving bed technology shows a tremendous potential in this regard. Not only it eliminates the use extreme conditions of temperature and pressure, but can also improve conversion of the equilibrium limited esterification reaction by instantaneous removal of product as soon as it is formed. Furthermore, optimization of a reactive SMB system can improve purity and productivity of biodiesel.

In the following work, a simulated moving bed system has been investigated for the production of biodiesel from free fatty acid and methanol. The reaction is catalyzed by Amberlyst 15, which acts as both the adsorbent and catalyst. The entire process is carried out at room temperature, thus examining the feasibility of biodiesel production without the use of high temperature or pressure.

2.7 References

1. Lode F, Mazzotti M, Morbidelli M. A new reaction-separation unit: The simulated moving bed reactor. *Chimia (Aarau)*. 2001;55:883-886.
<http://www.scopus.com/inward/record.url?eid=2-s2.0-0035648308&partnerID=tZOtx3y1>.
2. Fricke J, Meurer M, Schmidt-Traub H. Design and Layout of Simulated-Moving-Bed Chromatographic Reactors. *Chem Eng Technol*. 1999;22(10):835-839.
doi:10.1002/(SICI)1521-4125(199910)22:10<835::AID-CEAT835>3.0.CO;2-0.
3. Gelosa D, Ramaioli M, Valente G, Morbidelli M. Chromatographic Reactors: Esterification of Glycerol with Acetic Acid Using Acidic Polymeric Resins. *Ind Eng Chem Res*. 2003;42(25):6536-6544. doi:10.1021/ie030292n.
4. Fricke J, Meurer M, Dreisörner J, Schmidt-Traub H. Effect of process parameters on the performance of a simulated moving bed chromatographic reactor. *Chem Eng Sci*. 1999;54(10):1487-1492. doi:10.1016/S0009-2509(99)00059-7.
5. Mazzotti M, Storti G, Morbidelli M. Robust design of countercurrent adsorption separation processes .4. Desorbent in the feed. *Aiche J*. 1997;43:64-72. <Go to ISI>://A1997WC25800008.
6. Kawase M, Inoue Y, Araki T, Hashimoto K. The simulated moving-bed reactor for production of bisphenol A. *Catal Today*. 1999;48:199-209. doi:10.1016/S0920-5861(98)00374-5.
7. Roginskii, S.Z., Yanovskii, M.I., Gaziev GA. Chemical reactions under chromatographic conditions. *Dokl Akad Nauk SSSR*. 1961;140:771-776.
8. Roginskii, S.Z., Yanovskii, M.I., Gaziev GA. Catalytic reaction and catalysis under chromatographic conditions. *Kinet Catal*. 1962;3:529-540.
9. Magee EM. The course of a reaction in a chromatographic column. *Ind Eng Chem Fundam*. 1963;2(1):32-36. doi:10.1021/i160005a007.

10. Gore FE. Performance of Chromatographic Reactors in Cyclic Operation. *Ind Eng Chem Process Des Dev.* 1967;6(1):10-16. doi:10.1021/i260021a003.
11. Chu C, Tsang LC. Behavior of a Chromatographic Reactor. *Ind Eng Chem Process Des Dev.* 1971;10(1):47-53. doi:10.1021/i260037a009.
12. Langer SH, Patton JE. Chemical Reactor applications of the Gas Chromatographic Column, "New Developments in Gas Chromatography." *Wiley, New York.* 1973;28:293-373.
13. Wetherold RG, Wissler EH, Bischoff KB. An experimental and computational study of the hydrolysis of methyl formate in a chromatographic reactor. *Adv Chem Ser.* 1974;133:181-190. doi:10.1021/ba-1974-0133.ch014.
14. Schweich D, Villermaux J. The Chromatographic Reactor. A New Theoretical Approach. *Ind Eng Chem Fundam.* 1978;17(1):1-7. doi:10.1021/i160065a001.
15. Lode F, Houmard M, Migliorini C, Mazzotti M, Morbidelli M. Continuous reactive chromatography. *Chem Eng Sci.* 2001;56(2):269-291. doi:10.1016/S0009-2509(00)00229-3.
16. Carr RW. Continuous Reaction chromatography. In: Ganetsos G, Barker PE, eds. *Preparative and Production Scale Chromatography.* Vol 790. New York: Marcel Dekker Inc.; 1993:421-447.
17. Cho BK., Carr RW, Aris R. A Continuous Chromatographic Reactor. *Chem Eng Sci.* 1980;35:74-81.
18. Sarmidi MR, Barker PE. Saccharification of Modified Starch to Maltose in a Continuous Rotating Annular Chromatograph (CACR). *J Chem Technol Biotechnol.* 1993;57(3):229-235. doi:10.1002/jctb.280570306.
19. Sarmidi MR, Barker PE. Simultaneous Biochemical Reaction and Separation in a Rotating Annular Chromatograph. *Chem Eng Sci.* 1993;48(14):2615-2623. doi:10.1016/0009-2509(93)80272-R.

20. Iberer G, Schwinn H, Josić D, Jungbauer A, Buchacher A. Improved performance of protein separation by continuous annular chromatography in the size-exclusion mode. In: *Journal of Chromatography A*. Vol 921.; 2001:15-24. doi:10.1016/S0021-9673(01)00832-9.
21. Uretschläger A, Jungbauer A. Scale-down of continuous protein purification by annular chromatography: Design parameters for the smallest unit. *J Chromatogr A*. 2000;890:53-59. doi:10.1016/S0021-9673(00)00395-2.
22. www.arifactal.com. What is simulated moving bed chromatography? *Amalgamated Res Inc.*:1-11.
23. Storti G, Inorganica C, Analitica M, et al. Robust Design of Binary Countercurrent Adsorption Separation Processes. *Aiche J*. 1993;39(3):471-492.
24. Shieh MT, Barker PE. Saccharification of modified starch to maltose in a semi-continuous counter-current chromatographic reactor-separator (SCCR-S). *J Chem Technol Biotechnol*. 1995;63:125-134. doi:10.1002/jctb.280630206.
25. Viswanathan S, Aris R. Countercurrent Moving Bed Chromatographic Reactors. *Adv Chem Ser*. 1974;(13):191-204.
26. Takeuchi K, Uraguchi Y. Separation Conditions of the Reactant and the Product with a Chromatographic Moving Bed Reactor. *Chem Eng Jap*. 1976;(9):164-166.
27. Takeuchi K, Uraguchi Y. Basic Design of Chromatographic Moving Bed Reactors for Product Refining. *Chem Eng Jap*. 1976;9:246-248.
28. Petroulas T, Aris R, Carr RW. Analysis and performance of a countercurrent moving-bed chromatographic reactor. *Chem Eng Sci*. 1985;40(12):2233-2240.
29. Fish B. The continuous countercurrent moving bed chromatographic reactor. *Chem Eng Sci*. 1986;41:661-668.

30. Takeuchi K, Uruguchi Y. Computational Studies of a Chromatographic Moving Bed Reactor for Consecutive and Reversible Reactions. *Chem Eng Jap.* 1978;11:216-220.
31. Zhang Z, Hidajat K, Ray AK. Application of Simulated Countercurrent Moving-Bed Chromatographic Reactor for MTBE Synthesis. *Ind Eng Chem Res.* 2001;40:5305-5316. doi:10.1021/ie001071+.
32. Ray AK, Carr RW, Aris R. The Simulated Countercurrent Moving-Bed Chromatographic Reactor - a Novel Reactor Separator. *Chem Eng Sci.* 1994;49:469-480. doi:Doi 10.1016/0009-2509(94)80048-0.
33. Ziyang Z, Hidajat K, Ray AK. Multiobjective Optimization of Simulated Countercurrent Moving Bed Chromatographic Reactor (SCMCR) for MTBE Synthesis. *Ind Eng Chem Res.* 2002;41(13):3213-3232. doi:10.1021/ie0106940.
34. Ray AK, Tonkovich AL, Aris R, Carr RW. The Simulated Countercurrent Moving Bed Chromatographic Reactor. *Chem Eng Sci.* 1990;45(8):2431-2437.
35. Yu W, Hidajat K, Ray AK. Application of Multiobjective Optimization in the Design and Operation of Reactive SMB and Its Experimental Verification. *Ind Eng Chem Res.* 2003;42:6823-6831. doi:10.1021/ie030387p.
36. Yu W, Hidajat K, Ray AK. Optimization of reactive simulated moving bed and Varicol systems for hydrolysis of methyl acetate. *Chem Eng J.* 2005;112(1-3):57-72. doi:10.1016/j.cej.2005.06.008.
37. Ray AK, Carr RW, Aris R. The Simulated Countercurrent Moving Bed Chromatographic Reactor: A Novel Reactor - Separator. *Chem Eng Sci.* 1994;49(4):469-480.
38. Ray AK, CRW. Experimental study of a laboratory scale simulated countercurrent moving bed chromatographic reactor. *Chem Eng Sci.* 1995;50:2195-2202. [http://www.eng.uwo.ca/people/aray/Ajay Publications PDF files/A5 SMB Minn Expt CES 1995.pdf](http://www.eng.uwo.ca/people/aray/Ajay%20Publications%20PDF%20files/A5%20SMB%20Minn%20Expt%20CES%201995.pdf).

39. Ray AK, Carr RW. Numerical simulation of a simulated countercurrent moving bed chromatographic reactor. *Chem Eng Sci.* 1995;50:3033-3041. doi:10.1016/0009-2509(95)00135-R.
40. Tonkovich ALY, Carr RW. A simulated countercurrent moving-bed chromatographic reactor for the oxidative coupling of methane: Experimental results. *Chem Eng Sci.* 1994;49:4647-4656. doi:10.1016/S0009-2509(05)80048-X.
41. Tonkovich ALY, Carr RW. Modeling of the simulated countercurrent moving-bed chromatographic reactor used for the oxidative coupling of methane. *Chem Eng Sci.* 1994;49:4657-4665. doi:10.1016/S0009-2509(05)80049-1.
42. Bjorklund MC, Carr RW. The simulated countercurrent moving bed chromatographic reactor: a catalytic and separative reactor. *Catal Today.* 1995;25:159-168. doi:10.1016/0920-5861(95)00105-O.
43. Kruglov A V., Bjorklund MC, Carr RW. Optimization of the simulated countercurrent moving-bed chromatographic reactor for the oxidative coupling of methane. *Chem Eng Sci.* 1996;51(11):2945-2950. doi:10.1016/0009-2509(96)00179-0.
44. Bjorklund MC, Kruglov A V., Carr RW. Further Studies of the Oxidative Coupling of Methane to Ethane and Ethylene in a Simulated Countercurrent Moving Bed Chromatographic Reactor. *Ind Eng Chem Res.* 2001;40:2236-2242. doi:10.1021/ie000775g.
45. Kundu PK, Zhang Y, Ray AK. Modeling and simulation of simulated countercurrent moving bed chromatographic reactor for oxidative coupling of methane. *Chem Eng Sci.* 2009;64:5143-5152. doi:10.1016/j.ces.2009.08.036.
46. Kundu PK, Ray AK, Elkamel A. Numerical simulation and optimisation of unconventional three-section simulated countercurrent moving bed chromatographic reactor for oxidative coupling of methane reaction. *Can J Chem Eng.* 2012;90:1502-1513. doi:10.1002/cjce.20663.

47. Bjorklund MC, Carr RW. Enhanced Methanol Yields from the Direct Partial Oxidation of Methane in a Simulated Countercurrent Moving Bed Chromatographic Reactor. *Ind Eng Chem Res.* 2002;41:6528-6536. doi:10.1021/ie0201617.
48. Kruglov A V. Methanol synthesis in a simulated countercurrent moving-bed adsorptive catalytic reactor. *Chem Eng Sci.* 1994;49:4699-4716. doi:10.1016/S0009-2509(05)80053-3.
49. Ganetsos G, Barker PE, Ajongwen JN. Batch and continuous chromatographic systems as combined bioreactor-separators. In: *Preparative and Production Scale Chromatography*. Vol 40.; 1993:375-394.
50. Meurer M, Altenhöner U, Strube J, Untiedt A, Schmidt-Traub H. Dynamic simulation of a simulated moving-bed chromatographic reactor for the inversion of sucrose. *Starch/Staerke.* 1996;48:452-457. doi:DOI 10.1002/star.19960481113.
51. Ching C, Lu Z. Simulated moving-bed reactor: application in bioreaction and separation. *Ind Eng Chem Res.* 1997;36:152-159. doi:Doi 10.1021/Ie9603171.
52. Dünnebier G, Fricke J, Klatt K-U. Optimal Design and Operation of Simulated Moving Bed Chromatographic Reactors. *Ind Eng Chem Res.* 2000;39(7):2290-2304. doi:10.1021/ie990820o.
53. Azevedo DCS, Rodrigues AE. Design methodology and operation of a simulated moving bed reactor for the inversion of sucrose and glucose-fructose separation. *Chem Eng J.* 2001;82:95-107. doi:10.1016/S1385-8947(00)00359-4.
54. Kurup AS, Subramani HJ, Hidajat K, Ray AK. Optimal design and operation of SMB bioreactor for sucrose inversion. *Chem Eng J.* 2005;108(1-2):19-33. doi:10.1016/j.cej.2004.12.034.
55. Borges da Silva EA, Souza DP, Ulson de Souza AA, Guelli U. Souza SMA, Rodrigues AE. Analysis of the Behavior of the Simulated Moving Bed Reactor in the Sucrose Inversion Process. *Sep Sci Technol.* 2005;40:2373-2389. doi:10.1080/01496390500267426.

56. Minceva M, Rodrigues AE. Simulated moving-bed reactor: Reactive-separation regions. *AIChE J.* 2005;51:2737-2751. doi:10.1002/aic.10532.
57. Hashimoto K, Adachi S, Noujima H, Ueda Y. A new process combining adsorption and enzyme reaction for producing higher-fructose syrup. *Biotechnol Bioeng.* 1983;25:2371-2393. doi:10.1002/bit.260251008.
58. Hashimoto K, Adachi S, Shirai Y. Development of new bioreactors of a simulated moving-bed type. In: Ganetsos G, Barker PE, eds. *Preparative and Production Scale Chromatography*. Vol 31. New York: Marcel Dekker Inc.; 1993.
59. Borges da Silva EA, Ulson de Souza AA, de Souza SGU, Rodrigues AE. Analysis of the high-fructose syrup production using reactive SMB technology. *Chem Eng J.* 2006;118:167-181. doi:10.1016/j.cej.2006.02.007.
60. Zhang Y, Hidajat K, Ray AK. Modified reactive SMB for production of high concentrated fructose syrup by isomerization of glucose to fructose. *Biochem Eng J.* 2007;35:341-351. doi:10.1016/j.bej.2007.01.026.
61. Kawase M, Pilgrim A, Araki T, Hashimoto K. Lactosucrose production using a simulated moving bed reactor. *Chem Eng Sci.* 2001;56:453-458. doi:10.1016/S0009-2509(00)00248-7.
62. Pilgrim A, Kawase M, Matsuda F, Miura K. Modeling of the simulated moving-bed reactor for the enzyme-catalyzed production of lactosucrose. *Chem Eng Sci.* 2006;61:353-362. doi:10.1016/j.ces.2005.07.012.
63. Yu W, Hidajat K, Ray AK. Modeling, Simulation, and Experimental Study of a Simulated Moving Bed Reactor for the Synthesis of Methyl Acetate Ester. *Ind Eng Chem Res.* 2003;42(26):6743-6754. doi:10.1021/ie0302241.
64. Mazzotti M, Kruglov A, Neri B, Gelosa D, Morbidelli M. A continuous chromatographic reactor: SMBR. *Chem Eng Sci.* 1996;51:1827-1836. doi:10.1016/0009-2509(96)00041-3.

65. Kawase M, Suzuki T Ben, Inoue K, Yoshimoto K, Hashimoto K. Increased esterification conversion by application of the simulated moving-bed reactor. *Chem Eng Sci.* 1996;51:2971-2976. doi:10.1016/0009-2509(96)00183-2.
66. Meissner JP, Carta G. Continuous Regioselective Enzymatic Esterification in a Simulated Moving Bed Reactor. *Ind Eng Chem Res.* 2002;41:4722-4732. doi:10.1021/ie0202625.
67. Kapil A, Bhat S a., Sadhukhan J. Dynamic Simulation of Sorption Enhanced Reaction Processes for Biodiesel Production. *Ind Eng Chem Res.* 2010;49(5):2326-2335. doi:10.1021/ie901225u.
68. Meurer M, Altenhöner U, Strube J, Schmidt-Traub H. Dynamic simulation of simulated moving bed chromatographic reactors. *J Chromatogr A.* 1997;769:71-79. doi:10.1016/S0021-9673(96)00980-6.
69. Migliorini C, Fillinger M, Mazzotti M, Morbidelli M. Analysis of simulated moving-bed reactors. *Chem Eng Sci.* 1999;54:2475-2480. doi:10.1016/S0009-2509(98)00487-4.
70. Huang S, Carr RW. A simple adsorber dynamics approach to simulated countercurrent moving bed reactor performance. *Chem Eng J.* 2001;82:87-94. doi:10.1016/S1385-8947(00)00356-9.
71. Ray AK. The Simulated Countercurrent Moving Bed Chromatographic Reactor: A Novel Reactor-Separator. PhD Dissertation. Univeristy of Minnesota. 1992.
72. Mazzotti M, Storti G, Morbidelli M. Optimal operation of simulated moving bed units for nonlinear chromatographic separations. *J Chromatogr A.* 1997;769(1):3-24. doi:10.1016/S0021-9673(97)00048-4.
73. Mazzotti M, Storti G, Morbidelli M. Robust Design of Countercurrent Adsorption Separation Processes .2. Multicomponent Systems. *Aiche J.* 1994;40:1825-1842. <Go to ISI>://A1994PP89700006.

74. Mazzotti M, Storti G, Morbidelli M. Robust design of countercurrent adsorption separation .3. Nonstoichiometric systems. *Aiche J.* 1996;42:2784-2796. <Go to ISI>://A1996VL16200009.
75. Charton F, Nicoud RM. Complete design of a simulated moving bed. In: *Journal of Chromatography A*. Vol 702.; 1995:97-112. doi:10.1016/0021-9673(94)01026-B.
76. Gentilini A, Migliorini C, Mazzotti M, Morbidelli M. Optimal operation of simulated moving-bed units for non-linear chromatographic separations. II. Bi-Langmuir isotherm. *J Chromatogr A.* 1998;805:37-44. doi:10.1016/S0021-9673(98)00006-5.
77. Ma Z, Wang N-HL. Standing wave analysis of SMB chromatography: Linear systems. *AICHE J.* 1997;43(10):2488-2508. doi:10.1002/aic.690431012.
78. Mallmann T, Burris BD, Ma Z, Wang NHL. Standing wave design of nonlinear SMB systems for fructose purification. *AICHE J.* 1998;44:2628-2646. doi:DOI 10.1002/aic.690441206.
79. Xie Y, Chin CY, Phelps DSC, et al. A five-zone simulated moving bed for the isolation of six sugars from biomass hydrolyzate. *Ind Eng Chem Res.* 2005;44:9904-9920. doi:10.1021/ie050403d.
80. Wu D-J, Ma Z, Wang N-HL. Optimization of throughput and desorbent consumption in simulated moving-bed chromatography for paclitaxel purification. *J Chromatogr A.* 1999;855(1):71-89. doi:10.1016/S0021-9673(99)00630-5.
81. Cremasco MA, Hritzko BJ, Linda Wang NH. Experimental purification of paclitaxel from a complex mixture of taxanes using a simulated moving bed. *Brazilian J Chem Eng.* 2009;26:207-218. doi:10.1590/S0104-66322009000100020.
82. Wu D, Xie Y, Ma Z, Wang N. Design of simulated moving bed chromatography for amino acid separations. *Ind Eng* 1998;5885:4023-4035. doi:Doi 10.1021/Ie9801711.

83. Xie Y, Wu D, Ma Z, Wang N-HL. Extended Standing Wave Design Method for Simulated Moving Bed Chromatography: Linear Systems. *Ind Eng Chem Res.* 2000;39:1993-2005. doi:10.1021/ie9905052.
84. Xie Y, Mun S, Kim J, Wang NHL. Standing wave design and experimental validation of a tandem simulated moving bed process for insulin purification. *Biotechnol Prog.* 2002;18:1332-1344. doi:10.1021/bp025547r.
85. Lee KB, Kasat RB, Cox GB, Wang NHL. Simulated Moving Bed Multiobjective Optimization Using Standing Wave Design and Genetic Algorithm. *AIChE J.* 2008;54:2852-2871. doi:Doi 10.1002/Aic.11604.
86. Lee KB, Chin CY, Xie Y, Cox GB, Wang NHL. Standing-wave design of a simulated moving bed under a pressure limit for enantioseparation of phenylpropanolamine. *Ind Eng Chem Res.* 2005;44:3249-3267. doi:10.1021/ie049413p.
87. Kiss A a., Bildea CS. A review of biodiesel production by integrated reactive separation technologies. *J Chem Technol Biotechnol.* 2012;87(7):861-879. doi:10.1002/jctb.3785.
88. Atadashi IM, Aroua MK, Aziz a. A. High quality biodiesel and its diesel engine application: A review. *Renew Sustain Energy Rev.* 2010;14(7):1999-2008. doi:10.1016/j.rser.2010.03.020.
89. Canakci M, Gerpen JH Van. The Performance and Emissions of a Diesel Engine Fueled with Biodiesel from Yellow Grease and Soybean Oil. 2001;0300(xx):1-17.
90. Ramos MJ, Casas A, Rodríguez L, Romero R, Pérez Á. Transesterification of sunflower oil over zeolites using different metal loading: A case of leaching and agglomeration studies. *Appl Catal A Gen.* 2008;346:79-85. doi:10.1016/j.apcata.2008.05.008.
91. Gunvachai K, Hassan MG, Shama G, Hellgardt K. A New Solubility Model to Describe Biodiesel Formation Kinetics. *Process Saf Environ Prot.* 2007;85:383-389. doi:10.1205/psep07033.

92. Karaosmanoglu F, Cigizoglu K, Tuter M, Ertekin S. Investigation of the refining step of biodiesel production. *Energy & Fuels*. 1996;10:890-895. doi:10.1021/ef9502214.
93. Vicente G, Martínez M, Aracil J. Integrated biodiesel production: A comparison of different homogeneous catalysts systems. *Bioresour Technol*. 2004;92:297-305. doi:10.1016/j.biortech.2003.08.014.
94. Hanna MA, Isom L, Campbell J. Biodiesel : Current perspectives and future. *Sci Ind reasearch*. 2005;64:854-857.
95. Kiss A a. Novel process for biodiesel by reactive absorption. *Sep Purif Technol*. 2009;69(3):280-287. doi:10.1016/j.seppur.2009.08.004.
96. Kiss AA, Dimian AC, Rothenberg G. Solid Acid Catalysts for Biodiesel Production --Towards Sustainable Energy. *Adv Synth Catal*. 2006;348(1-2):75-81. doi:10.1002/adsc.200505160.
97. Kiss AA, Omota F, Dimian AC, Rothenberg G. The heterogeneous advantage: Biodiesel by catalytic reactive distillation. In: *Topics in Catalysis*. Vol 40.; 2006:141-150. doi:10.1007/s11244-006-0116-4.
98. Sharma YC, Singh B, Korstad J. Advancements in solid acid catalysts for ecofriendly and economically viable synthesis of biodiesel. *Biofuels, Bioprod Biorefining*. 2011;5:69-92. doi:10.1002/bbb.253.
99. Sharma YC, Singh B, Korstad J. Latest developments on application of heterogenous basic catalysts for an efficient and eco friendly synthesis of biodiesel: A review. *Fuel*. 2011;90:1309-1324. doi:10.1016/j.fuel.2010.10.015.
100. Zhang J, Chen S, Yang R, Yan Y. Biodiesel production from vegetable oil using heterogenous acid and alkali catalyst. *Fuel*. 2010;89:2939-2944. doi:10.1016/j.fuel.2010.05.009.

101. He BB, Singh AP, Thompson JC. Experimental optimization of a continuous-flow reactive distillation reactor for biodiesel production. *Trans ASAE*. 2005;48:2237-2243. http://www.webpages.uidaho.edu/~bhe/pdfs/RD_2.pdf.
102. He BB, Singh AP, Thompson JC. A novel continuous-flow reactor using reactive distillation for biodiesel production. *Trans ASAE*. 2006;49:107-112.
103. Kiss AA, Dimian AC, Rothenberg G. Biodiesel by catalytic reactive distillation powered by metal oxides. *Energy and Fuels*. 2008;22:598-604. doi:10.1021/ef700265y.
104. Kiss AA, Dimian AC, Rothenberg G. Biodiesel production by heat-integrated reactive distillation. *Comput Aided Chem Eng*. 2008;25:775-780. doi:10.1016/S1570-7946(08)80135-6.
105. De Lima Da Silva N, Santander CMG, Batistella CB, Filho RM, MacIel MRW. Biodiesel production from integration between reaction and separation system: Reactive distillation process. *Appl Biochem Biotechnol*. 2010;161:245-254. doi:10.1007/s12010-009-8882-7.
106. Kiss AA. Heat-integrated reactive distillation process for synthesis of fatty esters. *Fuel Process Technol*. 2011;92:1288-1296. doi:10.1016/j.fuproc.2011.02.003.
107. Nguyen N, Demirel Y. Using thermally coupled reactive distillation columns in biodiesel production. *Energy*. 2011;36:4838-4847. doi:10.1016/j.energy.2011.05.020.
108. Phuenduang S, Chatsirisook P, Simasatitkul L, Paengjuntuek W, Arpornwichanop A. Heat-integrated reactive distillation for biodiesel production from Jatropha oil. *Comput Aided Chem Eng*. 2012;31:250-254. doi:10.1016/B978-0-444-59507-2.50042-1.
109. Saka S, Kusdiana D. Biodiesel fuel from rapeseed oil as prepared in supercritical methanol. *Fuel*. 2001;80:225-231. doi:10.1016/S0016-2361(00)00083-1.
110. Demirbaş A. Biodiesel from vegetable oils via transesterification in supercritical methanol. *Energy Convers Manag*. 2002;43:2349-2356. doi:10.1016/S0196-8904(01)00170-4.

111. Han H, Cao W, Zhang J. Preparation of biodiesel from soybean oil using supercritical methanol and CO₂ as co-solvent. *Process Biochem.* 2005;40:3148-3151. doi:10.1016/j.procbio.2005.03.014.
112. Demirbas A. Biodiesel from sunflower oil in supercritical methanol with calcium oxide. *Energy Convers Manag.* 2007;48:937-941. doi:10.1016/j.enconman.2006.08.004.
113. He H, Wang T, Zhu S. Continuous production of biodiesel fuel from vegetable oil using supercritical methanol process. *Fuel.* 2007;86:442-447. doi:10.1016/j.fuel.2006.07.035.
114. He H, Sun S, Wang T, Zhu S. Transesterification kinetics of soybean oil for production of biodiesel in supercritical methanol. *JAACS, J Am Oil Chem Soc.* 2007;84:399-404. doi:10.1007/s11746-007-1042-8.
115. Yin JZ, Xiao M, Song J Bin. Biodiesel from soybean oil in supercritical methanol with co-solvent. *Energy Convers Manag.* 2008;49:908-912. doi:10.1016/j.enconman.2007.10.018.
116. Kasim NS, Tsai T-H, Gunawan S, Ju Y-H. Biodiesel production from rice bran oil and supercritical methanol. *Bioresour Technol.* 2009;100:2399-2403. doi:10.1016/j.biortech.2008.11.041.
117. Gómez-Castro FI, Rico-Ramírez V, Segovia-Hernández JG, Hernández-Castro S. Esterification of fatty acids in a thermally coupled reactive distillation column by the two-step supercritical methanol method. *Chem Eng Res Des.* 2011;89:480-490. doi:10.1016/j.cherd.2010.08.009.
118. Habulin M, Krmelj V. Synthesis of Oleic Acid Esters Catalyzed by Immobilized Lipase. 1996;(lipozyme IM):338-342.
119. Nelson L a, Foglia T a, Marmer WN. Lipase-catalyzed production of biodiesel. *J Am Oil Chem Soc.* 1996;73:1191-1195. doi:10.1007/BF02523383.

120. Gao Y yu, Chen W wei, Lei H, Liu Y, Lin X, Ruan R. Optimization of transesterification conditions for the production of fatty acid methyl ester (FAME) from Chinese tallow kernel oil with surfactant-coated lipase. *Biomass and Bioenergy*. 2009;33:277-282. doi:10.1016/j.biombioe.2008.05.013.
121. Bajaj A, Lohan P, Jha PN, Mehrotra R. Biodiesel production through lipase catalyzed transesterification: An overview. *J Mol Catal B Enzym*. 2010;62:9-14. doi:10.1016/j.molcatb.2009.09.018.
122. Bisen PS, Sanodiya BS, Thakur GS, Baghel RK, Prasad GBKS. Biodiesel production with special emphasis on lipase-catalyzed transesterification. *Biotechnol Lett*. 2010;32:1019-1030. doi:10.1007/s10529-010-0275-z.
123. Hwang HT, Qi F, Yuan C, et al. Lipase-catalyzed process for biodiesel production: Protein engineering and lipase production. *Biotechnol Bioeng*. 2014;111:639-653. doi:10.1002/bit.25162.
124. Lai CC, Zullaikah S, Vali SR, Ju YH. Lipase-catalyzed production of biodiesel from rice bran oil. *J Chem Technol Biotechnol*. 2005;80:331-337. doi:10.1002/jctb.1208.
125. Harding KG, Dennis JS, von Blottnitz H, Harrison STL. A life-cycle comparison between inorganic and biological catalysis for the production of biodiesel. *J Clean Prod*. 2008;16:1368-1378. doi:10.1016/j.jclepro.2007.07.003.
126. Van Gerpen J. Biodiesel processing and production. *Fuel Process Technol*. 2005;86:1097-1107. doi:10.1016/j.fuproc.2004.11.005.
127. Demirbas A. Comparison of transesterification methods for production of biodiesel from vegetable oils and fats. *Energy Convers Manag*. 2008;49:125-130. doi:10.1016/j.enconman.2007.05.002.
128. Snåre M, Mäki-Arvela P, Simakova IL, Myllyoja J, Murzin DY. Overview of catalytic methods for production of next generation biodiesel from natural oils and fats. *Russ J Phys Chem B*. 2010;3(7):1035-1043. doi:10.1134/S1990793109070021.

129. Shi W, He B, Cao Y, et al. Continuous esterification to produce biodiesel by SPES/PES/NWF composite catalytic membrane in flow-through membrane reactor: experimental and kinetic studies. *Bioresour Technol.* 2013;129:100-107. doi:10.1016/j.biortech.2012.10.039.
130. Amin S. Review on biofuel oil and gas production processes from microalgae. *Energy Convers Manag.* 2009;50:1834-1840. doi:10.1016/j.enconman.2009.03.001.
131. Dragone G, Fernandes B, Vicente A, Teixeira J. Third generation biofuels from microalgae. In: *Current Research, Technology and Education Topics in Applied Microbiology and Microbial Biotechnology.*; 2010:1355-1366. <http://repositorium.sdum.uminho.pt/handle/1822/16807>.
132. Huang G, Chen F, Wei D, Zhang X, Chen G. Biodiesel production by microalgal biotechnology. *Appl Energy.* 2010;87:38-46. doi:10.1016/j.apenergy.2009.06.016.
133. Ahmad AL, Yasin NHM, Derek CJC, Lim JK. Microalgae as a sustainable energy source for biodiesel production: A review. *Renew Sustain Energy Rev.* 2011;15:584-593. doi:10.1016/j.rser.2010.09.018.
134. Park JY, Kim DK, Lee JS. Esterification of free fatty acids using water-tolerable Amberlyst as a heterogeneous catalyst. In: *Bioresource Technology.* Vol 101.; 2010. doi:10.1016/j.biortech.2009.03.035.
135. Lilja J, Murzin DY, Salmi T, Aumo J, Mäki-Arvela P, Sundell M. Esterification of different acids over heterogeneous and homogeneous catalysts and correlation with the taft equation. In: *Journal of Molecular Catalysis A: Chemical.* Vol 182-183.; 2002:555-563. doi:10.1016/S1381-1169(01)00495-2.
136. Liu Y, Lotero E, Goodwin JG. Effect of carbon chain length on esterification of carboxylic acids with methanol using acid catalysis. *J Catal.* 2006;243:221-228. doi:10.1016/j.jcat.2006.07.013.

137. De la Iglesia Ó, Mallada R, Menéndez M, Coronas J. Continuous zeolite membrane reactor for esterification of ethanol and acetic acid. *Chem Eng J.* 2007;131:35-39. doi:10.1016/j.cej.2006.12.015.
138. Collignon F, Loenders R, Martens JA, Jacobs PA, Poncelet G. Liquid Phase Synthesis of MTBE from Methanol and Isobutene over Acid Zeolites and Amberlyst-15. *J Catal.* 1999;182:302-312. doi:10.1006/jcat.1998.2366.
139. Kim HJ, Kang BS, Kim MJ, et al. Transesterification of vegetable oil to biodiesel using heterogeneous base catalyst. In: *Catalysis Today*. Vol 93-95.; 2004:315-320. doi:10.1016/j.cattod.2004.06.007.
140. López DE, Goodwin JG, Bruce DA, Lotero E. Transesterification of triacetin with methanol on solid acid and base catalysts. *Appl Catal A Gen.* 2005;295:97-105. doi:10.1016/j.apcata.2005.07.055.
141. Marchetti JM, Miguel VU, Errazu AF. Heterogeneous esterification of oil with high amount of free fatty acids. *Fuel.* 2007;86:906-910. doi:10.1016/j.fuel.2006.09.006.
142. Park YM, Lee DW, Kim DK, Lee JS, Lee KY. The heterogeneous catalyst system for the continuous conversion of free fatty acids in used vegetable oils for the production of biodiesel. *Catal Today.* 2008;131:238-243. doi:10.1016/j.cattod.2007.10.052.
143. Chen Y-H, Huang Y-H, Lin R-H, Shang N-C. A continuous-flow biodiesel production process using a rotating packed bed. *Bioresour Technol.* 2010;101:668-673. doi:10.1016/j.biortech.2009.08.081.
144. Suppes G. Transesterification of soybean oil with zeolite and metal catalysts. *Appl Catal A Gen.* 2004;257(2):213-223. doi:10.1016/j.apcata.2003.07.010.
145. Furuta S, Matsushashi H, Arata K. Biodiesel fuel production with solid superacid catalysis in fixed bed reactor under atmospheric pressure. *Catal Commun.* 2004;5(12):721-723. doi:10.1016/j.catcom.2004.09.001.

146. Abreu FR, Lima DG, Hamú EH, Einloft S, Rubim JC, Suarez P a. Z. New metal catalysts for soybean oil transesterification. *J Am Oil Chem Soc.* 2003;80(6):601-604. doi:10.1007/s11746-003-0745-6.
147. Refaat a. a. Biodiesel production using solid metal oxide catalysts. *Int J Environ Sci Technol.* 2010;8:203-221. doi:10.1007/BF03326210.
148. Tesser R, Di Serio M, Guida M, Nastasi M, Santacesaria E. Kinetics of Oleic Acid Esterification with Methanol in the Presence of Triglycerides. *Ind Eng Chem Res.* 2005;44(21):7978-7982. doi:10.1021/ie050588o.
149. Feng Y, Zhang A, Li J, He B. A continuous process for biodiesel production in a fixed bed reactor packed with cation-exchange resin as heterogeneous catalyst. *Bioresour Technol.* 2011;102(3):3607-3609. doi:10.1016/j.biortech.2010.10.115.
150. Shibasaki-Kitakawa N, Honda H, Kuribayashi H, Toda T, Fukumura T, Yonemoto T. Biodiesel production using anionic ion-exchange resin as heterogeneous catalyst. *Bioresour Technol.* 2007;98(2):416-421. doi:10.1016/j.biortech.2005.12.010.
151. Son SM, Kimura H, Kusakabe K. Esterification of oleic acid in a three-phase, fixed-bed reactor packed with a cation exchange resin catalyst. *Bioresour Technol.* 2011;102(2):2130-2132. doi:10.1016/j.biortech.2010.08.089.
152. Ni J, Meunier FC. Esterification of free fatty acids in sunflower oil over solid acid catalysts using batch and fixed bed-reactors. *Appl Catal A Gen.* 2007;333:122-130. doi:10.1016/j.apcata.2007.09.019.
153. Kunin R, Meitzner EF, Fisher SA, Frish N. CHARACTERIZATION OF AMBERLYST 15. *I EC Prod Res Dev.* 1962;1(2).
154. Yu W, Hidajat K, Ray AK. Determination of adsorption and kinetic parameters for methyl acetate esterification and hydrolysis reaction catalyzed by Amberlyst 15. *Appl Catal A Gen.* 2004;260(2):191-205. doi:10.1016/j.apcata.2003.10.017.

155. Suwannakarn K, Lotero E, Ngaosuwan K, Goodwin JG. Simultaneous free fatty acid esterification and triglyceride transesterification using a solid acid catalyst with in situ removal of water and unreacted methanol. *Ind Eng Chem Res.* 2009;48:2810-2818. doi:10.1021/ie800889w.
156. Noshadi I, Amin NAS, Parnas RS. Continuous production of biodiesel from waste cooking oil in a reactive distillation column catalyzed by solid heteropolyacid: Optimization using response surface methodology (RSM). *Fuel.* 2012;94:156-164. doi:10.1016/j.fuel.2011.10.018.
157. Omota F, Dimian AC, Bliet A. Fatty acid esterification by reactive distillation. Part 1: Equilibrium-based design. *Chem Eng Sci.* 2003;58:3159-3174. doi:10.1016/S0009-2509(03)00165-9.
158. Omota F, Dimian AC, Bliet A. Fatty acid esterification by reactive distillation: Part 2 - kinetics-based design for sulphated zirconia catalysts. *Chem Eng Sci.* 2003;58:3175-3185. doi:10.1016/S0009-2509(03)00154-4.
159. Cossio-Vargas E, Hernandez S, Segovia-Hernandez JG, Cano-Rodriguez MI. Simulation study of the production of biodiesel using feedstock mixtures of fatty acids in complex reactive distillation columns. *Energy.* 2011;36(11):6289-6297. doi:10.1016/j.energy.2011.10.005.
160. Dimian AC, Omota F, Bliet A. Entrainer-enhanced reactive distillation. *Chem Eng Process Process Intensif.* 2004;43:411-420. doi:10.1016/S0255-2701(03)00125-9.
161. Dimian AC, Bildea CS, Omota F, Kiss AA. Innovative process for fatty acid esters by dual reactive distillation. *Comput Chem Eng.* 2009;33:743-750. doi:10.1016/j.compchemeng.2008.09.020.
162. Kiss AA, Segovia-Hernández JG, Bildea CS, Miranda-Galindo EY, Hernández S. Towards FAME and fortune by reactive DWC. In: *Procedia Engineering.* Vol 42.; 2012:1908-1914. doi:10.1016/j.proeng.2012.07.587.

163. Gomez-Castro FI, Rico-Ramirez V, Segovia-Hernandez JG, Hernandez S. Feasibility study of a thermally coupled reactive distillation process for biodiesel production. *Chem Eng Process Process Intensif.* 2010;49:262-269. doi:10.1016/j.cep.2010.02.002.
164. Hernández S, Segovia-Hernández JG, Juárez-Trujillo L, Estrada-Pacheco JE, Maya-Yescas R. DESIGN STUDY OF THE CONTROL OF A REACTIVE THERMALLY COUPLED DISTILLATION SEQUENCE FOR THE ESTERIFICATION OF FATTY ORGANIC ACIDS. *Chem Eng Commun.* 2010;198(1):1-18. doi:10.1080/00986445.2010.493102.
165. Machado GD, Aranda DAG, Castier M, Cabral VF, Cardozo-Filho L. Computer Simulation of Fatty Acid Esterification in Reactive Distillation Columns. *Ind Eng Chem Res.* 2011;50(17):10176-10184. doi:10.1021/ie102327y.
166. Kiss AA, Bildea CS. Integrated reactive absorption process for synthesis of fatty esters. *Bioresour Technol.* 2011;102:490-498. doi:10.1016/j.biortech.2010.08.066.
167. Bildea CS, Kiss AA. Dynamics and control of a biodiesel process by reactive absorption. *Chem Eng Res Des.* 2011;89:187-196. doi:10.1016/j.cherd.2010.05.007.
168. Su EZ, Xu WQ, Gao KL, Zheng Y, Wei DZ. Lipase-catalyzed in situ reactive extraction of oilseeds with short-chained alkyl acetates for fatty acid esters production. *J Mol Catal B Enzym.* 2007;48:28-32. doi:10.1016/j.molcatb.2007.06.003.
169. Su EZ, You P, Wei D. In situ lipase-catalyzed reactive extraction of oilseeds with short-chained dialkyl carbonates for biodiesel production. *Bioresour Technol.* 2009;100:5813-5817. doi:10.1016/j.biortech.2009.06.077.
170. Kaul S, Porwal J, Garg MO. Parametric study of Jatropha seeds for biodiesel production by reactive extraction. *JAOCs, J Am Oil Chem Soc.* 2010;87:903-908. doi:10.1007/s11746-010-1566-1.

171. Lim S, Hoong SS, Teong LK, Bhatia S. Supercritical fluid reactive extraction of *Jatropha curcas* L. seeds with methanol: A novel biodiesel production method. *Bioresour Technol.* 2010;101:7169-7172. doi:10.1016/j.biortech.2010.03.134.
172. Shuit SH, Lee KT, Kamaruddin AH, Yusup S. Reactive extraction and in situ esterification of *Jatropha curcas* L. seeds for the production of biodiesel. *Fuel.* 2010;89:527-530. doi:10.1016/j.fuel.2009.07.011.
173. Shuit SH, Lee KT, Kamaruddin AH, Yusup S. Reactive extraction of *Jatropha curcas* L. seed for production of biodiesel: process optimization study. *Environ Sci Technol.* 2010;44:4361-4367. doi:10.1021/es902608v.
174. Dussan KJ, Cardona CA, Giraldo OH, Gutiérrez LF, Pérez VH. Analysis of a reactive extraction process for biodiesel production using a lipase immobilized on magnetic nanostructures. *Bioresour Technol.* 2010;101:9542-9549. doi:10.1016/j.biortech.2010.07.044.
175. Kasim FH, Harvey AP. Influence of various parameters on reactive extraction of *Jatropha curcas* L. for biodiesel production. *Chem Eng J.* 2011;171:1373-1378. doi:10.1016/j.cej.2011.05.050.
176. Gu H, Jiang Y, Zhou L, Gao J. Reactive extraction and in situ self-catalyzed methanolysis of germinated oilseed for biodiesel production. *Energy Environ Sci.* 2011;4:1337. doi:10.1039/c0ee00350f.
177. Dubé MA, Tremblay AY, Liu J. Biodiesel production using a membrane reactor. *Bioresour Technol.* 2007;98:639-647. doi:10.1016/j.biortech.2006.02.019.
178. Tremblay AY, Cao P, Dubé MA. Biodiesel production using ultralow catalyst concentrations. *Energy and Fuels.* 2008;22:2748-2755. doi:10.1021/ef700769v.
179. Cao P, Tremblay AY, Dubé MA, Morse K. Effect of Membrane Pore Size on the Performance of a Membrane Reactor for Biodiesel Production. *Ind Eng Chem Res.* 2007;46:52-58. doi:10.1021/ie060555o.

180. Cao P, Dubé MA, Tremblay AY. Methanol recycling in the production of biodiesel in a membrane reactor. *Fuel*. 2008;87:825-833. doi:10.1016/j.fuel.2007.05.048.
181. Cao P, Dubé MA, Tremblay AY. High-purity fatty acid methyl ester production from canola, soybean, palm, and yellow grease lipids by means of a membrane reactor. *Biomass and Bioenergy*. 2008;32:1028-1036. doi:10.1016/j.biombioe.2008.01.020.
182. Machsun AL, Gozan M, Nasikin M, Setyahadi S, Yoo YJ. Membrane microreactor in biocatalytic transesterification of triolein for biodiesel production. *Biotechnol Bioprocess Eng*. 2010;15:911-916. doi:10.1007/s12257-010-0151-7.
183. Baroutian S, Aroua MK, Raman AAA, Sulaiman NMN. A packed bed membrane reactor for production of biodiesel using activated carbon supported catalyst. *Bioresour Technol*. 2011;102:1095-1102. doi:10.1016/j.biortech.2010.08.076.
184. Inoue T, Nagase T, Hasegawa Y, et al. Stoichiometric ester condensation reaction processes by pervaporative water removal via acid-tolerant zeolite membranes. *Ind Eng Chem Res*. 2007;46:3743-3750. doi:10.1021/ie0615178.
185. Sarkar B, Sridhar S, Saravanan K, Kale V. Preparation of fatty acid methyl ester through temperature gradient driven pervaporation process. *Chem Eng J*. 2010;162:609-615. doi:10.1016/j.cej.2010.06.005.
186. Figueiredo KCS, Salim VMM, Borges CP. Ethyl oleate production by means of pervaporation-assisted esterification using heterogeneous catalysis. *Brazilian J Chem Eng*. 2010;27:609-617. doi:10.1590/S0104-66322010000400013.
187. Okamoto K, Yamamoto M, Noda S, et al. Vapor-Permeation-Aided Esterification of Oleic Acid. *Ind Eng Chem Res*. 1994;33(4):849-853. doi:10.1021/ie00028a010.

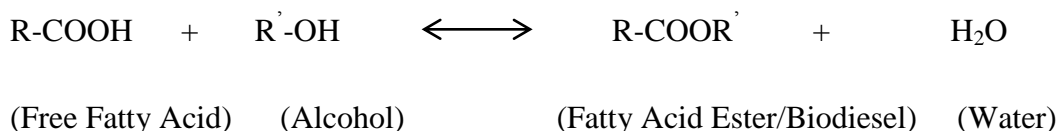
Chapter 3

3 Determination of Adsorption and Kinetic Parameters for Methyl Oleate Esterification Reaction in a Plug Flow Reactor Catalyzed by Amberlyst 15

3.1 Introduction

Fatty Acid Methyl Ester (biodiesel) is an environmentally friendly and renewable fuel which can be produced from waste such as used vegetable oils or animal fats, which have a high content of triglycerides and free fatty acids. In today's scenario, biodiesel is gaining its importance due to dwindling reserves of fossil fuels. In addition to being a renewable fuel, it reduces greenhouse gas emissions, tailpipe emissions; and is sulphur & benzene free. It can also be used in conventional diesel engines. It has a higher cetane number than regular diesel, resulting improved engine starting and reduced smoke emissions [1].

The formation of biodiesel from fatty acids is an equilibrium-limited reaction requiring the use of catalyst and high temperature.



Conventionally, biodiesel production can be done by use of basic, acid or enzymatic catalysts. But, these manufacturing technologies make use of homogenous catalysts, which causes bottlenecks during the reaction and separation steps [2]. The use of homogenous basic catalysts like NaOH and KOH presents the problem of saponification. This result in extra steps required to remove the catalysts during the industrial production of biodiesel, resulting in increase of production cost. Enzymatic catalysts like lipase have high reaction selectivity, but the enzyme is very costly and unstable [3]. Use of solid acid catalysts like Amberlyst has been shown to have a greater potential in biodiesel production from the viewpoint of cost saving. Unlike basic catalysts, saponification does

not occur in case of acid catalysts. Moreover, it is quite stable and can be regenerated. Such ion exchange resins have been used to produce biodiesel in various cases. For example, Shibasaki-Kitakawa et al. [3] used both cationic and anionic exchange resins to carry out continuous transesterification reaction between ethanol and triolein in an expanded bed reactor. The resin could be used repeatedly after regeneration without any loss of catalytic activity. Son et al. [4] carried out esterification of oleic acid with methanol in a fixed bed reactor filled with Amberlyst 15 at 80 to 120°C. They achieved a Fatty Acid Methyl Ester yield of above 90%. Feng et al. [5] achieved continuous esterification of Free Fatty Acid present in acidified oil with methanol in presence of NKC-9 cation exchange resin at 65°C in a fixed bed reactor. They achieved a conversion of over 98% during a 500 hour continuous esterification process. Kiss et al. [6] carried out esterification of dodecanoic acid with 2 ethyl hexanol at 130°C in presence of Amberlyst 15 and Nafeon NR-50 acid catalysts. They showed high initial activity, above 80% conversion within the first two hours.

However, the main drawback of solid acid catalysts is their low performance. Amberlyst 15 has been shown to produce a conversion of 0.7% of sunflower oil to FAME under the following circumstances: 60°C reaction temperature, 8 hour reaction time and 6:1 methanol to oil molar ratio [7, 8]. Sufficiently faster reaction rates can be obtained at 150-200°C reaction temperature. However Amberlyst 15 has low thermal stability and becomes unstable at temperature above 140°C [8, 9]. Thus, even in the presence of catalyst, conventional biodiesel production involves the use of extreme temperature. This is because this reaction is endothermic and conversion becomes severely limited at room temperature. Consequently, there is a need to develop a methodology which does not use high temperature for this process.

One of the promising approaches to this is use of chromatographic reactor. This involves reaction and separation in a single unit, ensuring high conversion by shifting the equilibrium towards forward direction [10]. This will bring down the production cost and simultaneously improve reaction efficiency. This also enables carrying out endothermic reactions at lower temperatures than normally applied due to low equilibrium constant [11]. In this regard, Simulated Moving Bed (SMB) technology has gained considerable

interest as it facilitates in-situ separation of products in the reactor thereby shifting of the equilibrium towards reaction completion, resulting in high purity product [12]. Hence, SMB technology shows considerable potential for production of biodiesel. Successful operation of SMB requires screening of operating parameters. In this regard, the adsorption equilibrium constants, dispersion coefficients and kinetic parameters of the model reaction stated above catalyzed by Amberlyst 15 packed in a single column need to be determined first. This article reports determination of the adsorption and the kinetic parameters.

3.2 Adsorbent and Catalyst

Amberlyst 15 is a cation exchange resin which has good esterification efficiency. It has a cross linked three dimensional structure obtained by sulphonation of a copolymer of polystyrene and divinyl benzene. It is a macroporous resin having a surface area of 42.5 m²/g [13]. Due to its macro reticular structure, it is better suited as catalyst than micro porous resin, as the latter does not swell appreciably in non-aqueous medium. It is also chemically stable, and has an operational stability over a wide temperature range. However, above 393 K, it loses its catalytic activity. In this study, the Amberlyst 15 acts both as an adsorbent and catalyst, and can be repeatedly used.

Table 1.1 Properties of Amberlyst 15 dry

Appearance	Hard, dry spherical particles
Particle size distribution	Retained on US standard screens (%)
16 mesh	2 – 5
16 – 20 mesh	20 – 30
20 – 30 mesh	45 – 55
30 – 40 mesh	15 – 25

40 – 50 mesh	5 – 10
Through 50 mesh	1
Bulk Density (kg/m³)	608
Moisture (by weight)	Less than 1%
Hydrogen ion concentration (meq/g dry)	4.7
Surface area (m²/g)	50
Porosity (ml pore/ml bead)	0.36
Average pore diameter (Å)	240

3.3 Reaction Kinetics

Several studies have been done regarding the kinetics of fatty acid esterification reaction with acid catalyst. Most reactions catalyzed by such resins can be classified as quasi homogenous or quasi heterogeneous. However, some other kinetic schemes have also been proposed. A kinetic equilibrium model was developed by Tesser et al. [14] for reaction of oleic acid with methanol in presence of Amberlyst 15 in a batch reactor. It took into account the partitioning equilibrium of the components between the liquid-phase adsorbed inside the resin and the external liquid-phase and also considered the swelling effect of the resin on internal volume. It also proposed the presence of ion exchange equilibrium between the protonated methanol and the surrounding molecules. Lastly, an Eley-Rideal surface reaction mechanism was proposed in which a protonated fatty acid reacts with methanol present in the liquid phase adsorbed in the resin. Berrios et al. [15] studied the esterification of free fatty acid present in sunflower oil with

methanol in presence of sulphuric acid catalyst. He proposed a pseudo-homogenous first-order model for the forward reaction. In another work, Tesser et al. [16] proposed a second-order pseudo homogenous model for oleic acid-methanol esterification using Relite cFs acid ion-exchange resin. Kapil et al. [10] proposed a Langmuir-Hinshelwood-Hougen-Watson model for oleic acid esterification in presence of Nafeon catalyst. The kinetic model was based on an experimental study of heterogeneously catalyzed esterification reaction of palmitic acid dissolved in sunflower oil over silica supported Nafion resin [17]. The quasi- homogenous model has also been used for describing esterification of acetic acid with methanol in presence of Amberlyst 15 catalyst [12, 18]. It has been shown to work well with binary systems.

In this work, oleic acid reacts with anhydrous methanol to produce methyl oleate (biodiesel) and water. This reaction was allowed to take place in an HPLC column, packed with Amberlyst 15 which acts as both catalyst for the reaction and stationary phase. A binary solution of oleic acid dissolved in methanol is injected into the column as a pulse input, after which methanol is passed through the column. Hence, methanol acts as both reactant and mobile phase and as a result is present in large excess. Thus, it is a continuous process. The resin is saturated initially with methanol, and hence it is assumed that it is completely swollen with polar solvent. The active sulfonic acid group in the resin is dissociated and the solvated protons are evenly distributed within the polymer phase. The chemical species participating in the reaction can penetrate the resin polymer and come in contact with the solvated protons. Hence, a quasi-homogenous kinetic model is proposed in this study. This kinetic model works only when methanol is present in large excess, because if its concentration decreases, the resin will deviate from ideal homogenous state, resulting in an adsorption based heterogeneous model.

3.4 Kinetic Model

In the quasi-homogenous kinetic model, the forward reaction rate is represented as:

$$R = k_f \left[q_{fa} - \frac{q_{me} \cdot q_w}{K_{eq}} \right] \quad (3.1)$$

where, R denotes the reaction rate, q_{fa} , q_{me} and q_w represent the concentrations of the fatty acid, methyl ester (biodiesel) and water respectively in the resin polymer. k_f is the forward reaction rate constant and K_{eq} is the reaction equilibrium constant. Since methanol is present in large excess, it is assumed that its concentration remains unchanged during the reaction. It is also assumed that the concentration of the adsorbed component i in the polymer phase is in equilibrium with its concentration in the mobile phase. Hence a linear adsorption isotherm can be used:

$$q_i = K_i \cdot C_i \quad (3.2)$$

where K_i is the adsorption equilibrium constant of the i^{th} component (fatty acid, methanol, methyl ester or water) for the esterification reaction, and C_i is the liquid-phase concentration of the i^{th} component. This isotherm is valid only if the concentrations of the reacting species are dilute in the mobile phase, which is ensured in this study. If the concentrations are not dilute enough, the adsorption behaviour may deviate from linear model. In such cases, a non-linear model such as the Langmuir model may be used to describe the adsorption.

3.5 Experimental details

3.5.1 Materials used

Oleic acid (purity > 99.9 wt%) and methyl oleate (purity > 99.9 wt%) was obtained from Sigma Aldrich. Anhydrous methanol (purity > 99.9 wt%) was obtained from Caledon. Amberlyst 15 catalyst was obtained from Sigma Aldrich.

3.5.2 Experimental set-up

An HPLC column of 0.25m length and 0.009m internal diameter was used as a packed bed reactor. It was filled with Amberlyst 15 saturated with solvent (methanol) and its porosity was checked by passing blue dextran through the packed column and

determining its elution time. The column was then connected to a JASCO PU 2080 Plus HPLC pump to provide a rectangular pulse input of the feed solution. The effluent was manually collected from the column exit at fixed time intervals.

3.5.3 Experimental procedure

Two types of experiments, reactive as well as non-reactive were carried out in the single column packed bed reactor with methanol as the mobile phase. The experiments were carried out at room temperature. The experiments were conducted at different flow rates, feed concentrations and pulse inputs. The column was washed for 30 minutes with anhydrous methanol to remove any water present in the resin. Pulse input of the reactants was introduced in the column. This was followed by passing anhydrous methanol which acted as both the mobile phase and a reactant. Effluent was collected manually from the column exit at regular intervals of 2 minutes. At the end of each experiment, methanol was passed for another 30 minutes to completely wash off the adsorbed species in the column.

3.5.4 Analysis

To determine the concentrations of methyl oleate and oleic acid, a Shimadzu GC with FID fitted with BPX5 column (30m x 0.25mm x 0.5 μ m) was used. The water concentration was measured using Mettler Toledo Karl Fisher DL31 volumetric titrator.

3.6 Mathematical model

In order to determine the adsorption parameters from the experimental study, a mathematical model has to be used. This model is based on the quasi homogenous kinetic model. As discussed before, this is an equilibrium-dispersive model, i.e., the concentration of a component adsorbed in the resin is assumed to be in equilibrium with

its concentration in the mobile phase. Hence, to determine the mass balance equation for any component for the reactive breakthrough system, it is assumed that all the non-equilibrium effects are lumped into a parameter defined as apparent dispersion coefficient, D , which is independent of the concentration of the component. The mass balance equation for a component i is thus:

$$\frac{\partial C_i}{\partial t} + \left(\frac{1-\varepsilon}{\varepsilon}\right) \frac{\partial q_i}{\partial t} + \frac{u}{\varepsilon} \frac{\partial C_i}{\partial z} - \left(\frac{1-\varepsilon}{\varepsilon}\right) v_i R = D_i \frac{\partial^2 C_i}{\partial z^2} \quad (3.3)$$

where C_i is the concentration of component i in the mobile phase, t is the time, q_i is the concentration of component i in the polymer phase, ε is the column void fraction, u is the superficial fluid phase flow velocity, z is the axial coordinate, v_i is the stoichiometric coefficient of the component i , R is the reaction rate, and D_i is the apparent axial dispersion coefficient of the component i . In the above partial differential equation, the first two terms denote the unsteady state for the component i in the mobile and polymer phase respectively. The third term is the convective term while the fourth term is the reaction term. For non-reactive breakthrough experiments, the fourth reaction term is zero. The right hand side of the equation has the diffusion term. It was assumed that the dispersion coefficient of oleic acid is equal to that of methyl oleate.

The initial and boundary conditions are given by

$$C_i [t = 0] = C_i^0 \quad (3.4)$$

$$C_i [0 < t < t_p]_{z=0} = C_{fi} \quad (3.5)$$

$$C_i [t > t_p]_{z=0} = 0 \quad (3.6)$$

$$\left[\frac{\partial C_i(t)}{\partial z} \right]_{z=0} = 0 \quad (3.7)$$

Here t_p is the time of the pulse input, C_i^0 is the initial concentration and C_{fi} is the feed concentration of the component i . The mass balance equation along with its boundary conditions, the rate equation, and the equation for the linear adsorption isotherm were solved together using Method of Lines approach. In this method, using Finite Difference

Method, the partial differential equation was discretized into a series of coupled Ordinary Differential Equations. Combining the Initial Value Problems of the Ordinary Differential Equations with the Boundary Value Problems, a set of stiff Ordinary Differential Equations was derived. This set was then solved using the DIVPAG subroutine (based on Gear's method) in the IMSL library. This entire operation was done using program in FORTRAN to determine the breakthrough curves of the reactants and products as predicted by the model.

To minimize the error between the experimental and model predicted values, an error function was introduced:

$$F(x) = \sum_{i=1}^n \sum_{j=1}^m [C_{ij,exp} - C_{ij,m}]^2 \quad (3.8)$$

where x is the vector of parameters tuned, $C_{ij,exp}$ is the experimental concentration of the component i for j^{th} data point and $C_{ij,m}$ is the model predicted concentration for the same. The adsorption and kinetic parameters were determined by tuning experimentally obtained elution profile with the model predicted profiles, thus minimising the error function (F). This was minimization was achieved using genetic algorithm (GA), which is a global optimization technique developed by John H. Holland on the basis of natural genetics [19]. This technique evolves in ways resembling natural selection. As a result, it is possible to explore a far greater range of potential solutions to a problem than traditional optimization algorithms [20].

3.7 Results and Discussion: Determination of Adsorption and Kinetic Parameters

3.7.1 Non-reactive breakthrough experiments

The adsorption equilibrium constants and the axial dispersion coefficients for methyl oleate and water were determined by the non-reactive breakthrough experiments. A binary pulse input of methyl oleate and water was fed into the column. Eluent was collected at regular time intervals from the column and the concentrations of methyl

oleate and water were determined for each of them. In this way an experimental concentration profile was obtained as shown in Figure 3.1a-3.1d. The breakthrough curves of Figure 3.1a were matched with the model predicted values with the sole objective of minimization of error function value F by tuning the four parameters, K_{MO} , K_W , D_{MO} , D_W , where, K and D represent the adsorption equilibrium constants and dispersion coefficients respectively, and the subscripts MO and W stand for methyl oleate and water respectively. The minimization of the error function was done using genetic algorithm in which a gene pool of 50 chromosomes was allowed to operate for 50 generations at which point they reached a global optimum value. Computation time was approximately 160 minutes using a computer equipped with Pentium core 2 duo processor. The parameters obtained are presented here in Table 3.2. Subsequent experiments as shown in Figure 3.1b-3.1d were carried out using different flow rates, pulse times and different feed concentrations to validate the predicted parameters obtained by fitting model with experimental results shown in Figure 3.1a. Figure 3.1b-3.1d shows that the model can predict the experimental results reasonably well.

Table 3.2 Adsorption equilibrium constants and apparent dispersion coefficients of methyl oleate (MO) and water (WA)

K_{MO}	K_W	$10^6 D_{MO}$ (m^2/s)	$10^6 D_W$ (m^2/s)	F (mol^2/lit^2)
0.760	4.081	0.853	7.877	0.002

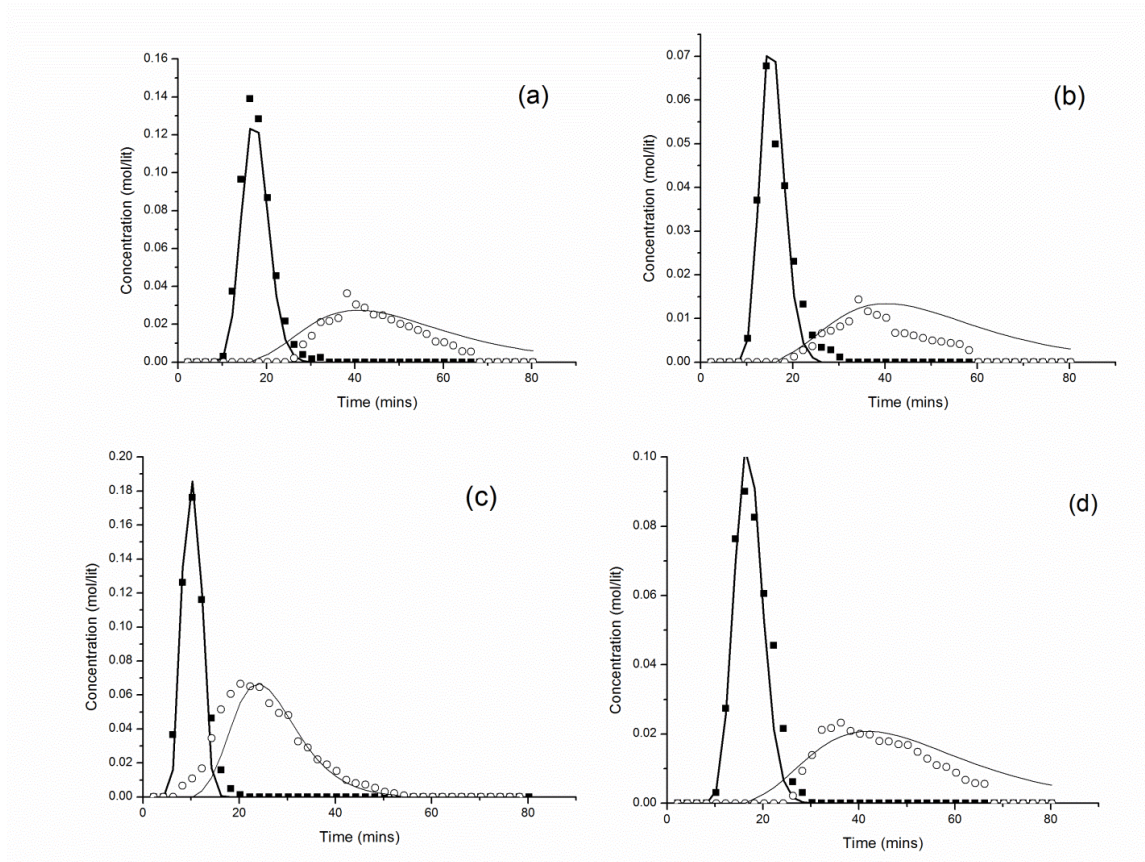


Figure 3.1 Non-reactive breakthrough of Methyl Oleate - Water system

Symbols : Experimental data (■ Methyl Oleate, ○ Water) ; Lines: Model Prediction.

Experimental conditions:

(a) 5 min pulse input, 1ml/min flow rate, 0.19 mol/lit methyl oleate, 0.23mol/lit water

(b) 2.5 min pulse input, 1ml/min flow rate, 0.19 mol/lit methyl oleate, 0.23mol/lit water

(c) 5 min pulse input, 2ml/min flow rate, 0.19 mol/lit methyl oleate, 0.23mol/lit water

(d) 5 min pulse input, 1ml/min flow rate, 0.15 mol/lit methyl oleate, 0.18 mol/lit water

Note: The symbols (■ Methyl Oleate) and (○ Water) represent average values from repetition of experiments

Figure 3.1 shows the experimental as well as model calculated elution profiles. Methyl oleate and water elute from the column at different times due to the difference in their adsorption affinities towards the adsorbent. From the figure it can be concluded that the experimental breakthrough curves agree with the model calculated results reasonably well. However, some band broadening is observed. This is mainly due to axial dispersion and mass-transfer resistance. These parameters are accounted for by the apparent dispersion coefficient values. It is also observed that while the model predicts the breakthrough curve of methyl oleate quite well, same cannot be said in case of water; there is some difference between experimental and model predicted curve. It is because water is much more strongly adsorbed by the resin. This fact is also reflected in the numerical values of adsorption equilibrium constants of methyl oleate and water, the value for water being much higher than that of methyl oleate.

3.7.2 Reactive breakthrough experiments

In order to determine the adsorption equilibrium constant of the reactant (K_A), the forward reaction rate constant (K_f) and the reaction equilibrium constant (K_{eq}), reactive breakthrough experiments were conducted. A pulse input of the reactant oleic acid dissolved in methanol was fed into the column. The oleic acid reacts with methanol as it passes through the column to form methyl oleate and water. Hence, the eluent consists of methyl oleate, water and unreacted oleic acid. The eluent was collected at regular time intervals and experimental concentration profiles for both the reactant and the products were obtained. Genetic algorithm was once again used to find out the parameters K_A , K_f and K_{eq} , that minimizes the error function between experimental results and model predicted results as shown in Figure 3.2a. In this part of the work, the parameters obtained earlier from non-reactive experiments were kept constant. The results are presented here in Table 3.3.

In order to establish the validity of the latest parameters, additional experiments were conducted under varying conditions as shown in Figures 3.2b-3.2d. Once again it can be seen that the model is able to predict the elution curves for methyl oleate and oleic acid

reasonably well, while the prediction slightly deviates in case of water as it is strongly adsorbed.

Table 3.3 Adsorption constant of Oleic Acid (K_{OA}), reaction rate constant (K_f) and equilibrium constant (K_{eq}) for synthesis of Methyl Oleate from Oleic Acid

K_A	$10^2 K_f$ (s^{-1})	K_{eq} (mol/lit)	F (mol^2/lit^2)	Yield (%)	Purity (%)
0.655	0.040	7.218	0.002	31%	22%

$$\text{Yield} = [MO]_{out}/[A]_0 ; \text{Purity} = [MO]_{out}/([A]_{out}+[MO]_{out} + [W]_{out})$$

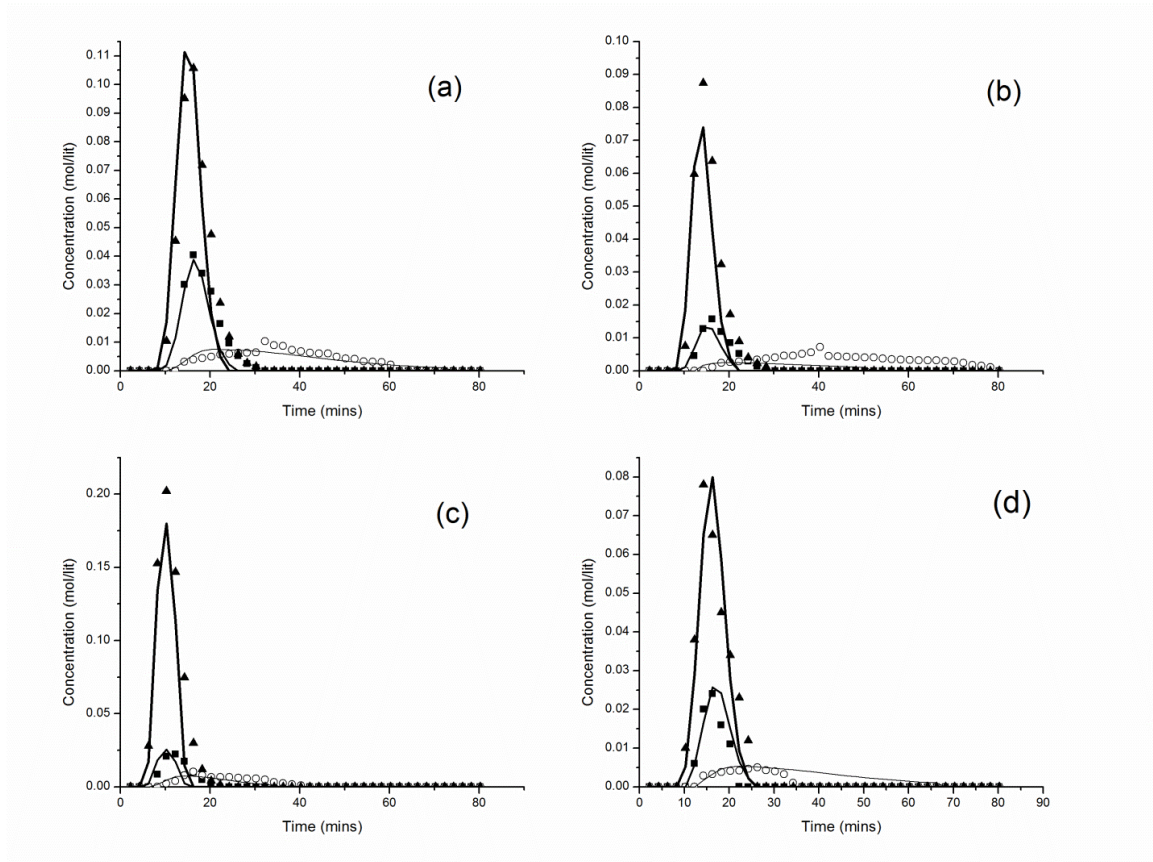


Figure 3.2 Reactive breakthrough of Oleic Acid – Methyl Oleate – Water system.

Symbols: Experimental data (▲ Oleic Acid, ■ Methyl Oleate, ○ Water); Lines: Model Prediction.

Experimental conditions:

- (a) 5 min pulse input, 1ml/min flow rate, 0.21mol/lit oleic acid
- (b) 2.5 min pulse input, 1ml/min flow rate, 0.21mol/lit oleic acid
- (c) 5 min pulse input, 2ml/min flow rate, 0.21mol/lit oleic acid
- (d) 5 min pulse input, 1ml/min flow rate, 0.15 mol/lit oleic acid

Note: The symbols (▲ Oleic Acid), (■ Methyl Oleate) and (○ Water) represent average values from repetition of experiments

3.7.3 Estimation of external and internal diffusion resistance

In order to further validate the kinetic parameters, it is necessary to have knowledge of the mass transfer taking place during the heterogeneous reaction sequence. The solid-phase used is Amberlyst 15, which is a porous particle. The mass transfer of reactants takes place from the mobile phase to the external surface of the Amberlyst 15 particles. From there the reactants diffuse through the pores into the particle interior where the reaction takes place. Hence, for the kinetic parameters to be valid, it is necessary to ensure that the external diffusion resistance and the internal pore diffusion resistance do not act as the rate-limiting step of the reaction. The external mass transfer resistance can be neglected if, according to Mear's Criterion [21]:

$$\frac{(-r'_A \rho_b) R n}{k_c C_A} < 0.15 \quad (3.9)$$

Where, $(-r'_A \rho_b)$ is the initial rate of the reaction ($\equiv 5.502 \times 10^{-2} \text{ mol/m}^3/\text{s}$), which was determined from Eqn. 3.1, R is the average radius of catalyst particles ($\equiv 3.75 \times 10^{-4} \text{ m}$), n is the order of the reaction, C_A is the bulk concentration of the reactant oleic acid ($\equiv 210 \text{ mol/m}^3$), and k_c is the mass-transfer coefficient which according to Dwidevi-Upadhyay mass-transfer correlation [22] comes to be $4.16 \times 10^{-5} \text{ m/sec}$. Taking these parameters into account, the Mear's criterion was calculated to be 2.36×10^{-3} , which is much smaller than 0.15. Hence the external diffusion resistance can be neglected, and it can be stated that it does not interfere with the calculation of the kinetic parameters.

The internal pore diffusion resistance can be measured by calculating the Weisz-Prater criterion [23], which states that this resistance is negligible if,

$$\frac{(-r'_A \rho_b)L^2}{D_e C_{As}} < 1 \quad (3.10)$$

where, C_{As} is the reactant concentration on resin surface, which is equal to ($C_A = 210 \text{ mol/m}^3$) since the external diffusion resistance is neglected, D_e is the effective diffusivity of oleic acid in methanol, which is given by $[\varepsilon/\tau]D_{OA}$, where ε is particle porosity (= 0.36), τ is the tortuosity factor taken as 1.3, and D_{OA} is taken as $0.85 \times 10^{-6} \text{ m}^2/\text{s}$; L is given by $R/3$, where R is the average radius of the spherical resin pellet ($= 3.75 \times 10^{-4} \text{ m}$). Based on the above parameters, the Weisz-Prater number for this system comes to be 0.174×10^{-4} , which is much less than 1. Hence, the internal diffusion resistance can be neglected, and it can be asserted that the effect of external and internal diffusion in calculation of the kinetic parameters is negligible.

3.8 Conclusions

Adsorption and kinetic parameters were determined for the esterification reaction of oleic acid with methanol to produce methyl oleate (biodiesel) and water. This was carried out in presence of Amberlyst 15 catalyst in an HPLC column, which served as a packed bed reactor. Since methanol was present in large excess, a quasi-homogenous kinetic model coupled with a linear adsorption isotherm was followed. The elution profiles of the reactant and products were experimentally determined. These were then compared with the elution profiles obtained by a mathematical model. The adsorption and kinetic parameters were determined by minimizing an error function so as to fit the experimentally obtained curves with the model predicted values using the genetic algorithm optimization technique. Experiments were conducted at room temperature under varying conditions to establish the validity of the parameters obtained. It was also determined that the internal and external mass-transfer resistances were negligible, further validating the kinetic parameters obtained. It was observed that the model predicted the experimental outcome reasonably well.

3.9 References

1. Canakci M, Gerpen JH Van. The Performance and Emissions of a Diesel Engine Fueled with Biodiesel from Yellow Grease and Soybean Oil. 2001;0300(xx):1-17.
2. Kiss A a., Bildea CS. A review of biodiesel production by integrated reactive separation technologies. *J Chem Technol Biotechnol*. 2012;87(7):861-879. doi:10.1002/jctb.3785.
3. Shibasaki-Kitakawa N, Honda H, Kuribayashi H, Toda T, Fukumura T, Yonemoto T. Biodiesel production using anionic ion-exchange resin as heterogeneous catalyst. *Bioresour Technol*. 2007;98(2):416-421. doi:10.1016/j.biortech.2005.12.010.
4. Son SM, Kimura H, Kusakabe K. Esterification of oleic acid in a three-phase, fixed-bed reactor packed with a cation exchange resin catalyst. *Bioresour Technol*. 2011;102(2):2130-2132. doi:10.1016/j.biortech.2010.08.089.
5. Feng Y, Zhang A, Li J, He B. A continuous process for biodiesel production in a fixed bed reactor packed with cation-exchange resin as heterogeneous catalyst. *Bioresour Technol*. 2011;102(3):3607-3609. doi:10.1016/j.biortech.2010.10.115.
6. Kiss AA, Dimian AC, Rothenberg G. Solid Acid Catalysts for Biodiesel Production --Towards Sustainable Energy. *Adv Synth Catal*. 2006;348(1-2):75-81. doi:10.1002/adsc.200505160.
7. Vicente G, Coteron A, Martinez, M., Aracil J. Application of the factorial design of experiments and response surface methodology to optimize biodiesel production. *Ind Crops Prod*. 1998;8:29-35. doi:10.1016/S0926-6690(97)10003-6.
8. Lam MK, Lee KT, Mohamed AR. Homogeneous, heterogeneous and enzymatic catalysis for transesterification of high free fatty acid oil (waste cooking oil) to biodiesel: a review. *Biotechnol Adv*. 2010;28(4):500-518. doi:10.1016/j.biotechadv.2010.03.002.

9. Lotero E, Liu Y, Lopez DE, Suwannakarn K, Bruce DA, Goodwin JG. Synthesis of biodiesel via acid catalysis. *Ind Eng Chem Res.* 2005;44:5353-5363. doi:10.1021/ie049157g.
10. Kapil A, Bhat S a., Sadhukhan J. Dynamic Simulation of Sorption Enhanced Reaction Processes for Biodiesel Production. *Ind Eng Chem Res.* 2010;49(5):2326-2335. doi:10.1021/ie901225u.
11. Ray AK, Carr RW, Aris R. The Simulated Countercurrent Moving Bed Chromatographic Reactor: A Novel Reactor - Separator. *Chem Eng Sci.* 1994;49(4):469-480.
12. Yu W, Hidajat K, Ray AK. Determination of adsorption and kinetic parameters for methyl acetate esterification and hydrolysis reaction catalyzed by Amberlyst 15. *Appl Catal A Gen.* 2004;260(2):191-205. doi:10.1016/j.apcata.2003.10.017.
13. Tesser R, Casale L, Verde D, Di Serio M, Santacesaria E. Kinetics and modeling of fatty acids esterification on acid exchange resins. *Chem Eng J.* 2010;157(2-3):539-550. doi:10.1016/j.cej.2009.12.050.
14. Berrios M, Siles J, Martin M, Martin a. A kinetic study of the esterification of free fatty acids (FFA) in sunflower oil. *Fuel.* 2007;86(15):2383-2388. doi:10.1016/j.fuel.2007.02.002.
15. Tesser R, Di Serio M, Guida M, Nastasi M, Santacesaria E. Kinetics of Oleic Acid Esterification with Methanol in the Presence of Triglycerides. *Ind Eng Chem Res.* 2005;44(21):7978-7982. doi:10.1021/ie050588o.
16. Ni J, Meunier FC. Esterification of free fatty acids in sunflower oil over solid acid catalysts using batch and fixed bed-reactors. *Appl Catal A Gen.* 2007;333:122-130. doi:10.1016/j.apcata.2007.09.019.
17. Mazzotti M, Neri B, Gelosa D, Kruglov A, Morbidelli M. Kinetics of liquid-phase esterification catalyzed by acidic resins. *Ind Eng Chem Res.* 1997;36:3-10. doi:10.1021/ie960450t.

18. Holland JH. *Adaptation in Natural and Artificial Systems: An Introductory Analysis with Applications to Biology, Control, and Artificial Intelligence.*; 1975:1-228. doi:10.1086/418447.
19. John H. Holland, *Adaptation in natural and artificial systems.* Ann Arbor MI Univ Michigan Press. 1992;Ann Arbor:1-200?
<http://www.citeulike.org/group/664/article/400721>\n<http://scholar.google.com/scholar?hl=en&btnG=Search&q=intitle:Adaptation+in+Natural+and+Artificial+Systems#1>.
20. Mears DE. Tests for Transport Limitations in Experimental Catalytic Reactors. *Ind Eng Chem Process Des Dev.* 1971;10(4):541-547. doi:10.1021/i260040a020.
21. Dwivedi P, Upadhyay S. Particle-fluid mass transfer in fixed and fluidized beds. *Ind Eng Chem* 1977;16:157-165. doi:10.1021/i260062a001.
22. Fogler HS. *Elements of Chemical Reaction Engineering.*; 2006:1080. doi:10.1016/0009-2509(87)80130-6.

Chapter 4

4 Modeling, Simulation and Experimental Study of a Simulated Moving Bed Reactor for the Synthesis of Biodiesel

4.1 Introduction

Chromatographic reaction-separation methods have gained considerable attention in recent years. It involves coupling of reaction and separation in a single unit, thereby bringing down production cost and improving process efficiency. They are competitive when the involved chemical species are thermally sensitive or when high purities are required that are better achieved by adsorptive separation such as chromatography. Though they are typically operated in the batch mode, better performances can be achieved through continuous mode operation [1]. Such a continuous process is the Simulated Moving Bed (SMB) technology, which has been used to carry out a number of applications of commercial importance [2-19]. These reported studies show that a substantial improvement in reactor performance can be achieved by Simulated Moving Bed Reactor (SMBR), particularly for equilibrium-limited reaction. An equilibrium-limited reaction can be forced to completion by in-situ separation and removal of the product as soon as it is formed such as esterification [2-8], hydrogenation [9, 10], oxidative coupling [11], and isomerisation of sugars [12, 13]. SMB technology also finds widespread applications for difficult separation such as chiral drug separation [14] and separation of sugars [15-19]. However, before its application to a particular process, a detailed understanding of the criteria for SMB performance and evaluation of process parameters needs to be done for successful operation of the SMB. In this work, the synthesis of methyl oleate (biodiesel) from free fatty acid (oleic acid) and methanol catalyzed by solid acid catalyst Amberlyst 15 was carried out in an SMB reactor-separator. Although this reaction has been previously investigated on SMB, the investigation was limited to simulation study only [20]. In our study, both experiments as well as numerical simulations based on first principle mathematical model were done. Experiments were carried out under different operating conditions to achieve a deeper

understanding of the behaviour and performance of SMB. The effect of various process parameters was investigated. The mathematical was validated with experimental studies and subsequently systematic sensitivity analysis was performed to determine the robustness of the mathematical model.

4.2 Synthesis of Biodiesel in SMBR

Figure 4.1 shows a schematic illustration of a SMBR and the principle of its operation. It comprises of a number of columns of uniform cross-section, each of length L and packed with ion-exchange resin (Amberlyst 15), which acts as both adsorbent and catalyst. The columns are connected in series in a circular array.

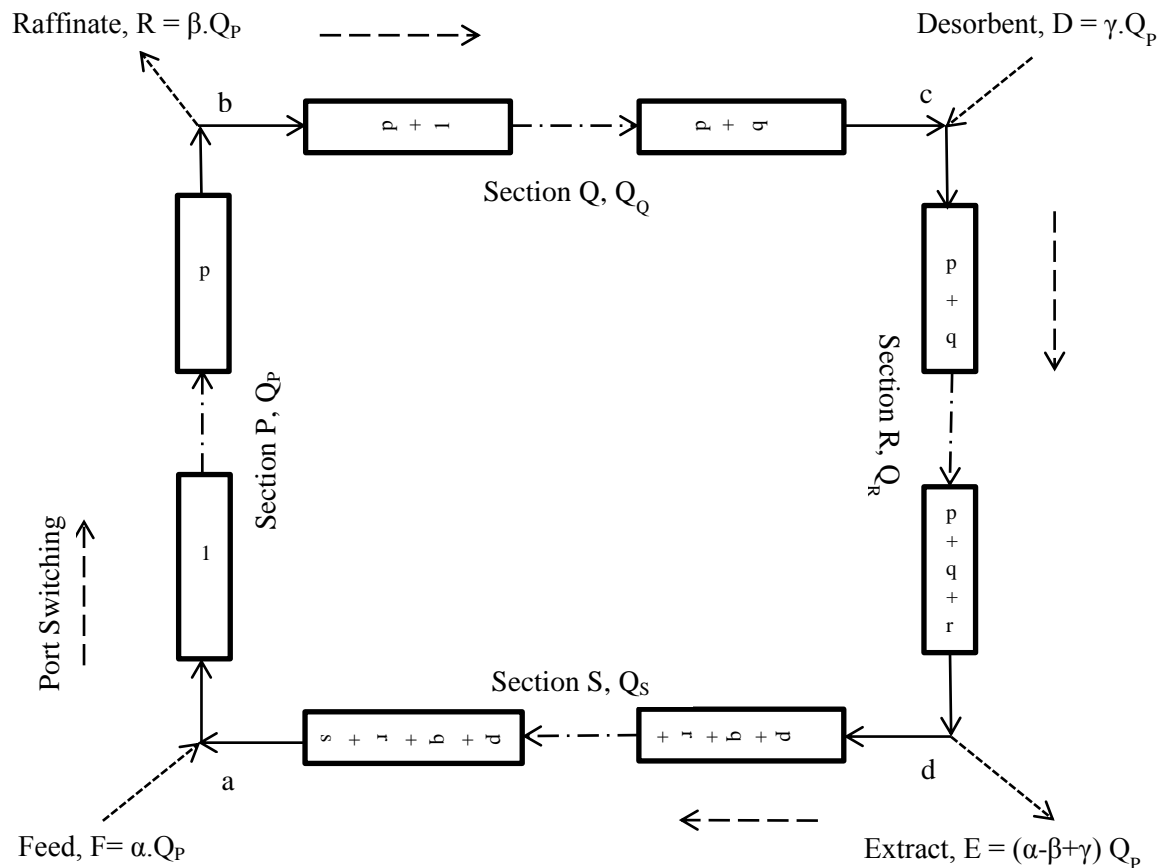


Figure 4.1 Schematic diagram of a SMBR system

There are two inlet ports for feed (F) and desorbent (D), and two outlet ports for raffinate (R) and extract (E) that divide the system into four sections (P, Q, R, and S), with p , q , r , and s representing the corresponding number of columns in each section, as shown in Figure 4.1. Q_P , the flow rate in section P, is regarded as the reference flow rate, based on which other flow rates are defined. Flow rates in each section are defined by: Section P: Q_P ; Section Q: $Q_Q = (1-\beta) Q_P$; Section R: $Q_R = (1-\beta+\gamma) Q_P$; Section S: $Q_S = (1-\alpha) Q_P$, where, $\alpha = F/Q_P$, $\beta = R/Q_P$ and $\gamma = D/Q_P$. A countercurrent movement with respect to the stationary phase is mimicked by port switching. During a port switch, these four ports move simultaneously by one column, in direction of the flow of mobile phase. This port switch takes place after a specific interval, defined as the switching time (t_s) – the hypothetical solid-phase velocity. By port switching, a countercurrent movement pertaining to the stationary phase is simulated, and hence the name Simulated Moving Bed. However, to achieve effective separation between the components, each of the four sections should fulfil their respective roles that are achieved by appropriate setting of internal flow rates and the switching time.

In order to mathematically describe the separation between two components, Petroulas et al. [21] introduced for a true countercurrent moving-bed system a parameter, σ , defined as relative carrying capacity of the solid-phase for any component i relative to the mobile fluid-phase:

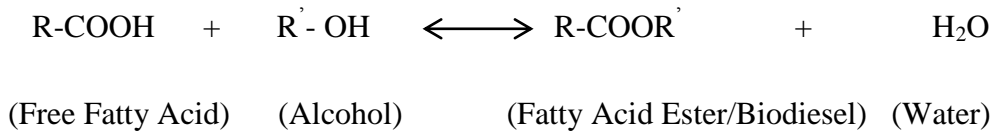
$$\sigma_i = \frac{1-\varepsilon}{\varepsilon} NK_i \frac{u_s}{u_g} = \delta_i \frac{u_s}{u_g} \quad (4.1)$$

where u_s and u_g represent the relative solid and fluid phase velocity respectively. They showed that, to achieve countercurrent separation between two components, one must set σ greater than 1 for one component and less than 1 for the other. A fixed-bed is represented by $\sigma = 0$. This was experimentally verified by Fish et al. [22] who also defined the net velocity V_i at which the component i travels (the concentration front moves) within the column as:

$$V_i = \frac{u_g [1-\sigma_i]}{[1+\delta_i]} \quad (4.2)$$

Hence, when $\sigma_i < 1$ ($V_i > 0$), the component i moves with the fluid-phase while for $\sigma_i > 1$ ($V_i < 0$), the species move with the solid-phase. Eqn. 4.2 is valid for a linear isotherm, which is the case in this study. Ray et al. [10, 23] re-defined σ_i for SMBR by replacing the true solid-phase velocity (u_s) by a hypothetical solid-phase velocity ζ , where $\zeta = L/t_s$. They observed that countercurrent movement between two components can be achieved if the re-defined σ values can be set in such a way that its value is greater than 1 for one component and less than 1 for the other. Hence, if σ is set properly, the less strongly adsorbed component will move with the fluid-phase and can be collected at raffinate port (which is ahead of the feed port) while the more strongly adsorbed component will relatively move with the solid-phase and can be collected at the extract port located behind the feed port.

The reaction investigated is given by:



The alcohol used also acts as the mobile phase for this study and hence its concentration is essentially unchanged. The goal of the study is to achieve high conversion of reaction of free fatty acid with alcohol via in-situ separation of biodiesel from water to reduce the rate of reverse reaction. In this study, methyl oleate (biodiesel) is synthesized by reaction of oleic acid with methanol. The primary objective of methyl oleate synthesis is obtaining high yield and purity of biodiesel. From the adsorption isotherm studies, it was found out that water is the more strongly adsorbed component. Hence, the product of interest (methyl oleate), which is faster moving component, is collected at the raffinate port while the more strongly adsorbed water is collected at the extract port. In order to achieve effectual operation of SMBR, the four sections must play pertinent roles. In Section P, Adsorption of water should takes place so that it does not break into the raffinate stream. The flow rate Q_P should not be high enough to enable water to desorb. The switching time is also important as it should be long enough to enable the esterification reaction to take place, but not too long so that water desorption occurs. Hence, in section P, σ for methyl oleate should be less than 1 ($V > 0$) and for water it

should be greater than 1 ($V < 0$) so that relative countercurrent movement of the two components take place. Moreover, axial dispersion is another factor which may adversely affects the yield and purity. In Section Q, which has a head start with the faster moving methyl oleate must be retained in order to prevent it from breaking into section R. Hence, the flow rate Q_Q should be low enough to prevent methyl oleate (as well as any water) from breaking into section R. This could be achieved by adjusting σ for both methyl oleate and water to be greater than 1 ($V < 0$) thereby establishing concurrent flow in Section Q. However, mobile phase methanol desorption should continue to take place in order to get mixed with the fresh methanol desorbent stream in section R. In Section R, desorption of water takes place so that columns are clean before port switching takes place. The switching time should be long enough as well as the flow rate Q_R in this section should be high ($\sigma < 1$, $V > 0$), to allow water to desorb completely. Hence, in this section, the objective is to establish co-current flow of both components. Axial dispersion also becomes a problem in this section along with tailing of the concentration front. In Section S, it is necessary to set flow rates such a way that relative countercurrent flow of the two components is established so that methyl oleate moves towards the feed port (recycle to section P) getting mixed with fresh feed while water travels towards extract port and collected in the extract stream. Hence the flow rate Q_S should be such that σ for methyl oleate is less than 1 ($V > 0$), while for water it is greater than 1 ($V < 0$). Hence, the critical factors affecting the performance of SMB are switching time and flow rates in each section. The dimensions of the column are also important as it influences axial dispersion. The main objectives of this study is to determine the optimal flow rates and switch time so as to obtain maximum conversion of the esterification reaction along with in-situ separation allowing recovery of pure biodiesel.

4.3 Mathematical Model

The mathematical model for SMBR is similar to that ascertained previously for a single-column fixed-bed reactor, aside from the fact that there are now multiple columns and switching scheme must be roped in to imitate the movement of solids. Hence, the SMB

unit resembles a fixed-bed chromatographic reactor except at the instant of column switching. In order to describe its dynamic behaviour, the mathematical model of a single reactive chromatographic column is used while incorporating the cyclic port switching. The modified material balance is:

$$\frac{\partial C_{ij}^{(N)}}{\partial t} + \left(\frac{1-\varepsilon}{\varepsilon}\right) \frac{\partial q_{ij}^{(N)}}{\partial t} + \frac{u_{\phi}}{\varepsilon} \frac{\partial C_{ij}^{(N)}}{\partial z} - \left(\frac{1-\varepsilon}{\varepsilon}\right) v_i R_j^{(N)} = D_i \frac{\partial^2 C_{ij}^{(N)}}{\partial z^2} \quad (4.3)$$

for the component i in the j^{th} column during the N^{th} switching period. u_{ϕ} signifies the superficial flow velocity in section ϕ (where $\phi = P, Q, R, S$) and the reaction rate expression and adsorption isotherm are given by:

$$R_j^{(N)} = k_f \left[q_{a,j}^{(N)} - \frac{q_{me,j}^{(N)} \cdot q_{w,j}^{(N)}}{K_e} \right] \quad (4.4)$$

Here, R denotes the reaction rate, q_a , q_{me} and q_w represent the concentrations of the fatty acid (oleic acid), methyl ester (biodiesel/methyl oleate) and water respectively in the resin polymer. k_f is the forward reaction rate constant and K_e is the reaction equilibrium constant.

Since methanol is present in large excess, it is assumed that its concentration remains unchanged during the reaction.

It is assumed that the concentration of the adsorbed component i in the polymer phase is in equilibrium with its concentration in the mobile phase:

$$q_{ij}^{(N)} = K_i \cdot C_{ij}^{(N)} \quad (4.5)$$

Here K_i is the adsorption equilibrium constant of the i^{th} component (fatty acid, methanol, methyl ester or water) for the esterification reaction. C_i is the liquid phase concentration of the i^{th} component.

The kinetic and adsorption constants for each component were determined by empirically fitting the breakthrough curves obtained by experiment with the model predicted values obtained by solving the non-reactive single-column mass balance equation. The forward

reaction rate constant and the equilibrium constant were also similarly determined using reactive single-column mass balance equation. The values are listed in Table 4.1.

Table 4.1 Adsorption equilibrium constants and dispersion coefficients of methyl oleate (MO), water (W) and oleic acid (A) along with forward reaction rate constant and equilibrium constant.

K_{MO}	K_W	K_A	$10^2 k_f$ (s^{-1})	K_e (mol/lit)	$10^6 D_{MO}$ (m^2/s)	$10^6 D_W$ (m^2/s)	Yield (%)	Purity (%)
0.760	4.081	0.655	0.040	7.218	0.853	7.877	31	22

Yield: $([MO]_{out}/[A]_0)$; Purity: $([MO]_{out}/([A]_{out}+[MO]_{out}+[W]_{out}))$

The initial and boundary conditions for equation (4.3) are:

Initial conditions

$$\text{When } N = 0, C_{ij}^{(0)} = C_{ij}^{Initial} = 0 \quad (4.6a)$$

When $N \geq 1$,

$$C_{ij}^{(N)} = C_{i,j+1}^{(N-1)} \quad \text{for } j = 1 \sim (N_{col} - 1) \quad (4.6b)$$

$$C_{ij}^{(N)} = C_{i,1}^{(N-1)} \quad \text{for } j = N_{col} \quad (4.6c)$$

Boundary conditions

Feed entry point (a in Figure 4.1)

$$C_{i1}^{(N)} \Big|_{z=0} = (1-\alpha) C_{i,N_{col}}^{(N)} \Big|_{z=L} + \alpha C_{i,f} \quad (4.7a)$$

Raffinate take-off point (b in Figure 4.1)

$$C_{i,p+1}^{(N)} \Big|_{z=0} = C_{i,p}^{(N)} \Big|_{z=L} \quad (4.7b)$$

Eluent inlet point (c in Figure 4.1)

$$C_{i,p+q+1}^{(N)} \Big|_{z=0} = \left[\frac{1-\beta}{1-\beta+\gamma} \right] C_{i,p+q}^{(N)} \Big|_{z=L} \quad (4.7c)$$

Extract take off point (d in Figure 4.1)

$$C_{i,p+q+r+1}^{(N)} \Big|_{z=0} = C_{i,p+q+r}^{(N)} \Big|_{z=L} \quad (4.7d)$$

The mass balance equation (Eq. 4.3), initial and boundary conditions (Eq. 4.6 & Eq. 4.8 respectively), kinetic rate equation (Eq. 4.4) and adsorption isotherm (Eq. 4.5) completely define the SMBR system. The partial differential equations (PDEs) were solved using Method of Lines. They were first discretized using Finite Difference Method (FDM) to convert it into a set of several coupled Ordinary Differential Equation of Initial Value Problems (ODE-IVP) and the resultant stiff ODEs were solved using the DIVPAG subroutine (based on Gear's method) in the IMSL library. Due to the presence of periodic switching in the system, whenever a switching is performed, a new IVP must be solved. Eventually, a periodic steady state with a period equal to the switching time is eventually attained. After each switching, the column numbering is redefined as follows

–

<i>Before switching</i>	<i>After switching</i>
Column 1	Column N_{col}
Column j	Column $j-1$ $j = 1, 2, 3, \dots, N_{col}$ (4.8)

The concentration profiles of the different components were obtained from the solution of above equations (Eq. 4.3 – 4.8). The objective of this study is to obtain higher yield and product purity for biodiesel in SMBR due to in-situ separation of products at the site of reaction compared to single column fixed-bed reactor where at the exit products leaves

at equilibrium. For this purpose, the design of the SMBR configuration and operating parameters must be adjusted such that yield and conversion at the desired exit port is much higher than the thermodynamic equilibrium value. The two quantities, yield and purity, are defined as follows:

Yield of methyl ester (Y_{me})

$$Y_{me} = \frac{\text{methyl oleate collected in raffinate}}{\text{oleic acid fed}} = \frac{\beta \cdot \left[\int_0^{t_s} C_{me, P}^{(N)} \Big|_{z=L_{col}} dt \right]}{\alpha C_{af} t_s} \quad (4.9)$$

Purity of methyl ester (P_{me})

$$P_{ME} = \frac{\text{methyl oleate collected in raffinate}}{(\text{oleic acid} + \text{water} + \text{methyl oleate}) \text{ collected in raffinate}}$$

$$= \frac{\int_0^{t_s} C_{me, P}^{(N)} \Big|_{z=L_{col}} dt}{\int_0^{t_s} (C_{me}^{(N)} + C_W^{(N)} + C_a^{(N)})_P \Big|_{z=L_{col}} dt} \quad (4.10)$$

Hence, the operating conditions of the SMBR must be set such that the yield and purity of methyl oleate are maximized at the raffinate port. The switching time and the internal flow rates of the mobile phase within the four sections P, Q, R and S accordingly have to be set appropriately.

4.4 Experimental Details

In order to analyse and test the validity and robustness of the SMBR model predictions, methodical experiments need to be carried out. Ray et al. [9] have shown that in case of an equilibrium-limited reaction, it is possible to break the thermodynamic barrier and push the reaction towards completion under certain operating conditions. This allows for a higher conversion and product purity than can be achieved in a traditional fixed-bed

reactor. Hence, experimental investigation of SMBR is required to achieve the flowing objectives:

1. To determine if SMBR can achieve a higher yield and purity of biodiesel than the single column fixed-bed reactor for a given reactor length, switching time and eluent flow rate.
2. To predict the SMBR performance using the model and comparing the model predicted results with experimental results. This will ascertain the validity and robustness of the mathematical model.
3. To characterize the effect of changing variables on the overall performance of SMBR. This also determines how good are the adsorption and kinetic parameters obtained from single-column experiments as well as sensitivity of each parameter on SMBR performance.

4.4.1 Materials Used

Oleic acid (purity > 99.9 wt%) and methyl oleate (purity > 99.9 wt%) was obtained from Sigma Aldrich. Anhydrous methanol (purity > 99.9 wt%) was obtained from Caledon. Amberlyst 15 catalyst was obtained from Sigma Aldrich.

4.4.2 Experimental Set-up

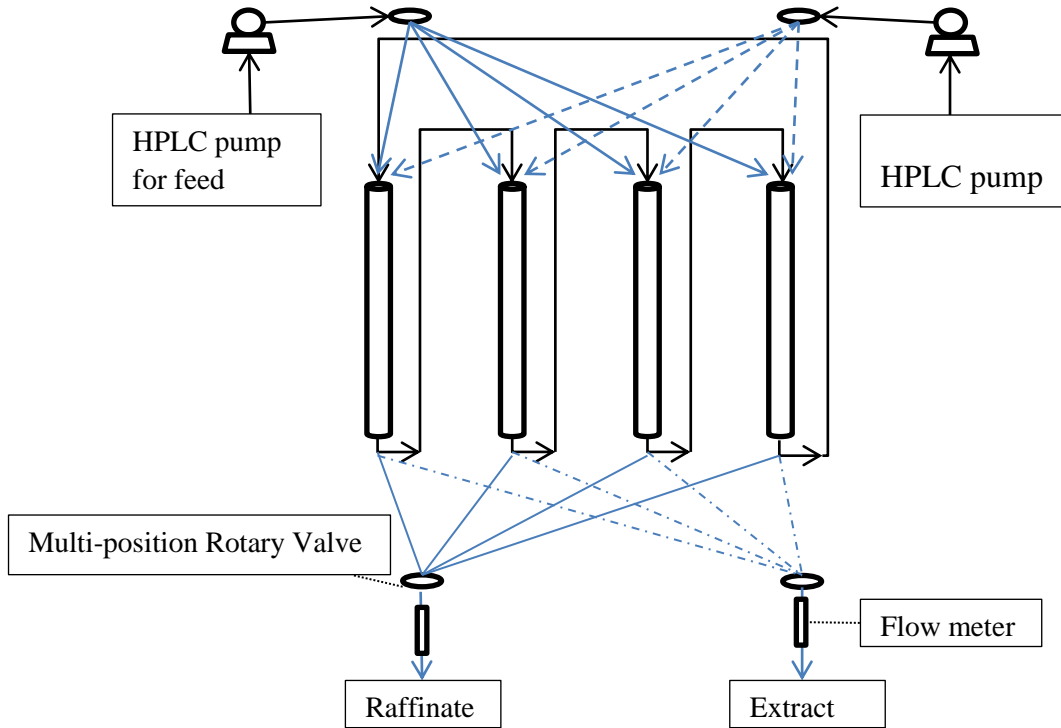


Figure 4.2 Experimental setup of a 4-column SMBR system

The experimental setup consists of four HPLC columns ($0.25\text{m} \times 0.009\text{m}$ I.D.) corresponding to the four sections P, Q, R and S (see Figure 4.2). The columns were packed with Amberlyst 15 ion-exchange resin. The average porosity of the columns was determined to be 0.4. Each column is connected to four rotary valves controlled by the actuator system. These valves correspond to positions of feed, raffinate, extract and desorbent; allowing the delivery of feed/desorbent or withdrawal of raffinate/extract from the column, as required. At the end of a pre-set time interval (switch time), all the valve positions are switched simultaneously by one column in the direction of the flow of the mobile phase; thus simulating the movement (co- or counter- current) of the fluid and solid phase. The columns were arranged in a bank with the last column connected to the

first one so that the switching of various streams can take place continuously. Two JASCO PU 2080 Plus HPLC pumps were connected to the SMBR unit for the feed and desorbent streams. The raffinate and extract streams were controlled by QUANTIM mass flow controllers. Samples were collected from raffinate and extract ports during a particular switch time and the concentrations of methyl oleate and oleic acid were determined by a Shimadzu GC with FID fitted with BPX5 column (30m x 0.25mm x 0.5 μ m). The water concentration was measured using Mettler Toledo Karl Fisher DL31 volumetric titrator. All the experiments were carried out at room temperature.

4.5 Results and Discussion

Experiments were conducted at different switching times, raffinate flow rates and feed flow rates to investigate their influence on the performance of SMBR. Based on equations 4.1 & 4.2, the solid-phase pseudo velocities of methyl oleate and water in various sections of SMBR under all the experimental conditions were evaluated. The values are listed in Table 4.2.

The yield and purity of raffinate obtained from experimental results were then compared with model predicted results (Eqs.4.9 – 4.10). To evaluate the SMBR performance, the concentration profiles of the reactant (oleic acid) as well as products (methyl oleate and water) were also obtained (Eq. 4.3). It was found out that the model always over predicted the purity. This is because of the non-linear adsorption behaviour of the strongly adsorbed component, water. Due to this the adsorbent requires more time to be regenerated and eventually water appears in higher concentration in the raffinate stream. The effects of various parameters are discussed as follows.

Table 4.2 Comparison of σ and V (cm/min) values of methyl oleate and water in various sections of SMBR under different experimental conditions

Effect of	Experimental variation	Section P				Section R				Section S			
		σ_{MO}	σ_W	V_{MO}	V_W	σ_{MO}	σ_W	V_{MO}	V_W	σ_{MO}	σ_W	V_{MO}	V_W
Switching time ^a	8 min	0.566	3.039	0.724	-1.466	0.235	1.261	3.076	-0.452	0.602	3.234	0.624	-1.570
	12 min	0.377	2.026	1.040	-0.737	0.156	0.841	3.394	0.275	0.401	2.156	0.939	-0.781
	17 min	0.266	1.430	1.225	-0.309	0.110	0.593	3.579	0.705	0.283	1.522	1.125	-0.353
Raffinate flow rate ^b , βQ_P	1 ml/min	0.627	3.365	0.375	-1.023	0.156	0.841	3.394	0.275	0.696	3.736	0.275	-1.067
	1.66 ml/min	0.377	2.026	1.040	-0.737	0.156	0.841	3.394	0.275	0.401	2.156	0.939	-0.781
	2 ml/min	0.313	1.683	1.381	-0.591	0.156	0.841	3.394	0.275	0.330	1.770	1.280	-0.634
Feed flow rate ^c , αQ_P	0.05 ml/min	0.377	2.026	1.040	-0.737	0.156	0.841	3.394	0.275	0.389	2.088	0.989	-0.760
	0.1 ml/min	0.377	2.026	1.040	-0.737	0.156	0.841	3.394	0.275	0.401	2.156	0.939	-0.781
	0.2 ml/min	0.377	2.026	1.040	-0.737	0.156	0.841	3.394	0.275	0.429	2.303	0.838	-0.824
	Desired Effect	< 1	> 1	> 0	< 0	< 1	< 1	> 0	> 0	< 1	> 1	> 0	< 0
		Retention of water				Desorption of water				Desorption of Methyl Oleate			

a Experimental conditions: Feed flow rate = 0.1 ml/min, Raffinate flow rate = 1.66 ml/min, Desorbent flow rate = 4 ml/min.

b Experimental conditions: Switching time = 12 min, Feed flow rate = 0.1 ml/min, Desorbent flow rate = 4 ml/min.

c Experimental conditions: Switching time = 12 min, Raffinate flow rate = 1.66 ml/min, Desorbent flow rate = 4 ml/min.

4.5.1 Effect of Switching Time

Switching time is a critical factor for viable operation and satisfactory performance of SMB. Figure 4.3 shows the effect of three different values of switching time on the yield and purity of methyl oleate. The experimental values are shown as filled square symbol while the simulation results are shown as filled diamond symbol. The model predicts quite adequately the yield for switch time of 12 and 17 minutes while the simulation slightly over-predicts the purity value. It is clear that at low switching time (8 minutes) both the yield and purity is low. When the switch time is increased to 12 minutes, yield and purity increase significantly but both decrease once again when the switch time is increased to 17 minutes. This can be explained as follows. At 8 minutes switch time, $\sigma_w > 1$ (desired is < 1) in section R (see Table 4.2), which means that there is insufficient time for desorption of water in this section, as a result this section is poorly regenerated (inaptly purged) before the next switch. At low switching time, the pseudo solid-phase velocity is high ($\zeta = L/t_s$) implying all components travel at a much faster rate with the solid-phase, which in turn reduces the residence time of the reactant and product in each section. There is insufficient time for adsorption of water in section P and desorption of methyl oleate in section S. This means at the end of a switch time, water will appear in raffinate and methyl oleate appears in extract, which is the exact opposite of what is desired. Consequently both the yield and purity are low at low switch time. Experimentally, the yield and purity are even lower than the predicted values. This is because according to single column experiments, the breakthrough of the product of interest (methyl oleate) does not occur before 10 minutes. This means that if the switching time is less than 10 minutes, reaction will not proceed to adequate value. This will severely affect both yield and purity, as is clear from the figure. The experimental yield and purity are only 3.2% and 3.9% respectively, as compared to simulation result of 40% and 17% respectively.

When the switch time is increased to 12 minutes, both yield and purity increase drastically. The σ value for both the components decreases and the V value increases. This means that the methyl oleate is moving faster in the fluid phase as well as low solid-

phase velocity improving residence time and yield. Thus, there is sufficient time for desorption of water in section R, adsorption of water in section P and desorption of methyl oleate in section S. Moreover, countercurrent separation sets in for the two components ($\sigma_{MO} < 1$, $\sigma_W > 1$) in sections P and S. Also as the switch time is more than 10 minutes, the simulation predicts the experiment much better than the previous case. The experimental yield and purity are 56% and 32% respectively, while the simulation result predicts quite well the values respectively as 51% and 42.9%. On further increasing the switch time to 17 minutes, yield decreases from 56% to 37% and the purity drops from 32% to 25%. This can be explained from the σ values as well as using the effective velocity values or the separation factor, which is the difference in velocity values of the two components, ΔV . It is clear from the table that at a higher switch time, the σ value decreases for both methyl oleate and water, implying that all the components are now moving faster in the fluid-phase than the solid-phase. In this situation, the adsorption and desorption of methyl oleate and water takes place sufficiently in their respective sections. It is no longer a factor affecting yield due to insufficient residence time. However, ΔV decreases for both methyl oleate and water in all the three sections. In section P, ΔV decreases from 1.777 cm/min to 1.534 cm/min when switch time increases from 12 minutes to 17 minutes. In section R, ΔV decreases from 3.119 cm/min to 2.874 cm/min while in section S, ΔV decreases from 1.72 cm/min to 1.478 cm/min. Thus, in all the sections, the decrease in ΔV value deteriorates the net separation of the concentration fronts of methyl oleate and water. This is also evident from their concentration profiles as shown in Figure 4.4.

To summarize, at 8 minutes switch time yield and purity are poor due to insufficient residence time in SMBR. The residence time increases at 12 minutes switch time resulting in better yield and purity. On further increasing the switch time to 17 minutes, reduced separation between the two components decreases yield and purity as separation factor dictates overall performance over increase of residence time.

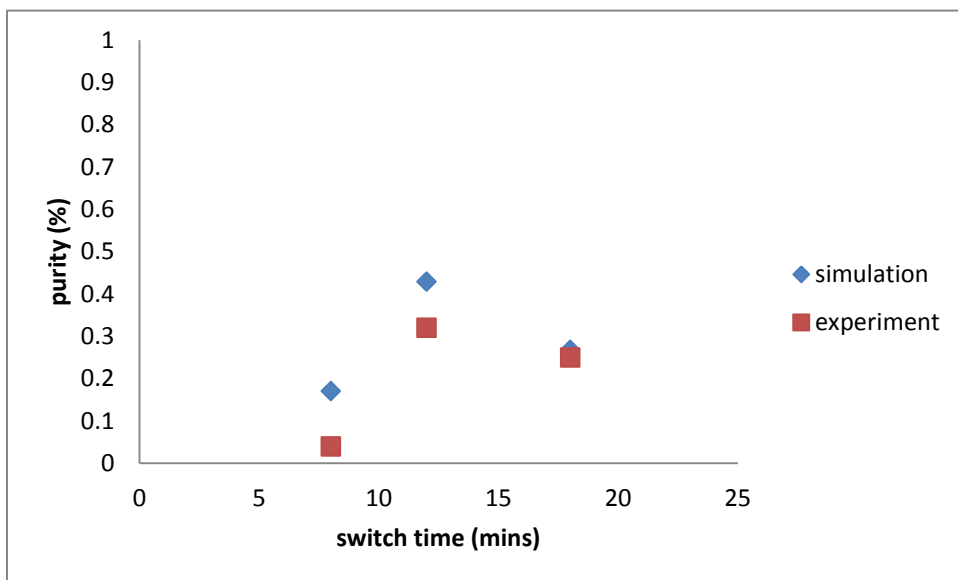
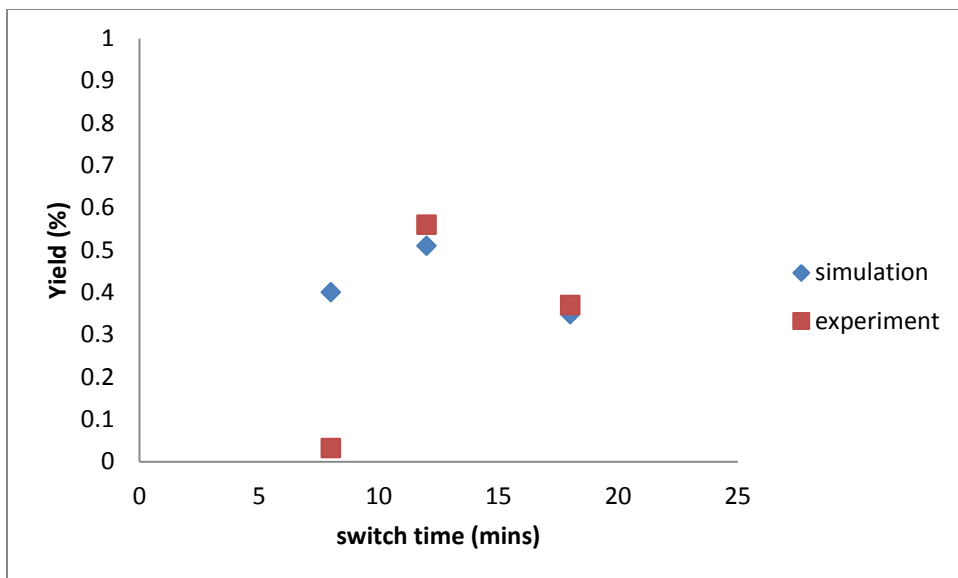


Figure 4.3 Effect of switching time on SMBR performance

Experimental conditions: $Q_P = 1.66$ ml/min, $\alpha = 0.06$, $\beta = 1$, $\gamma = 2.41$

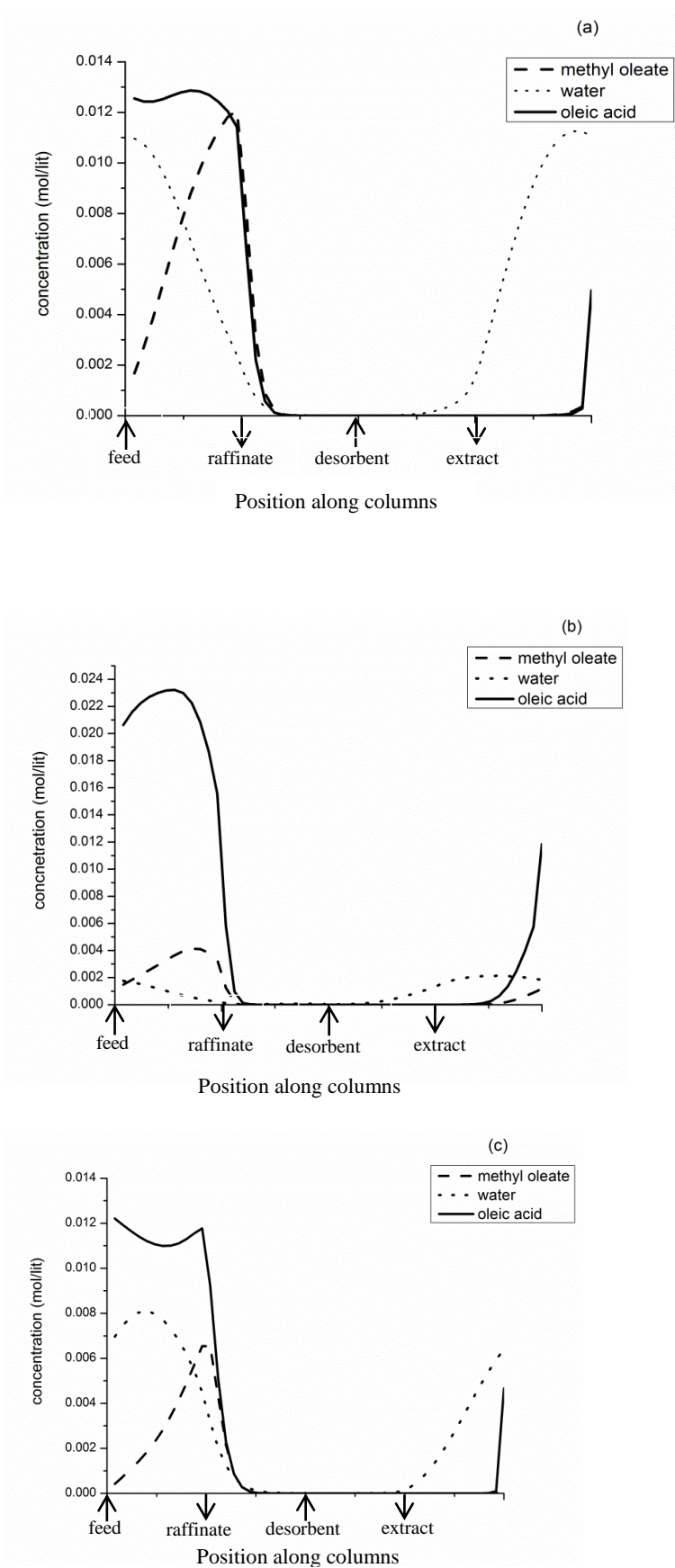


Figure 4.4 Effect of switching time on cyclic steady state concentration profiles of methyl oleate-water-oleic acid. (a) 12min, (b) 8min, (c) 17min . Experimental Conditions: $\alpha = 0.06$, $\beta = 1$, $\gamma = 2.41$

4.5.2 Effect of Raffinate Flow Rate

The effect of raffinate flow rate on behaviour of SMBR is shown in Figure 4.5. Experiments were carried out at three different raffinate flow rates (βQ_P): 1 ml/min, 1.66 ml/min and 2 ml/min. The feed flow rate, desorbent flow rate and switch time was kept constant at 0.1 ml/min, 4 ml/min and 12 minutes respectively. It was observed that both yield and purity decrease when the raffinate flow rate is decreased from 1.66 ml/min to 1 ml/min; or increased to 2 ml/min. This can be explained as follows.

When the raffinate flow rate is decreased from 1.66 ml/min to 1 ml/min, ΔV decreases from 1.777 ml/min to 1.398 ml/min in section P. In section S, ΔV decreases from 1.72 ml/min to 1.342 ml/min. This deteriorates the separation of concentration fronts of both methyl oleate and water in sections P and S where countercurrent separation of the two components must be as high as possible, decreasing both yield and purity. Simulation shows that yield decreases from 51.8% to 29.7% and purity drops from 43% to 28.9%. Experimental results however show that the drop in yield and purity is much more drastic. The yield drops from 56% to a mere 3.1%; purity drops from 32% to 2.8%. This is because when the raffinate flow rate is decreased but the high desorbent flow rate remains unchanged, the pressure drop inside the column rises. This pressure drop causes a backflow and some of the desorbent flows through sections Q and P, thus opposing the direction of the mobile phase movement. This severely hampers the forward reaction in section P. This section plays a central role in reaction and in-situ separation. As a result the reactant is mostly not consumed, and unreacted oleic acid appears in the raffinate stream. This is also evident from the column concentration profiles as shown in Figure 4.6. Due to tailing of the water concentration front from the column, if the desorbent flow rate is increased, the model predicted value will match much better the experimental value.

When the raffinate flow rate was increased from 1.66 ml/min to 2 ml/min, the yield dropped by about 16% while the purity dropped by about 9%. This was true for both experimental and model predicted results. This is because higher raffinate flow rate reduces the residence time of the reactant in section P. As a result the conversion of oleic

acid decreases and more of it appears in the raffinate stream, thus decreasing both yield and purity. Hence, even though the ΔV value increases for both sections P and S, it does not improve the performance of SMB. The detrimental effect caused by the decrease in residence time overcomes the positive effect caused by increased separation of concentration fronts.

To summarise, the increase or decrease of raffinate flow rate predominantly affects section P, which is important for reaction-separation. A lower flow rate reduces the forward reaction in section P, whereas a higher flow rate reduces the residence time thus deteriorating the SMBR performance. The forward reaction is more hampered at raffinate flow rate of 1 ml/min, resulting in a sharper drop in yield and purity than at higher raffinate flow rate of 2 ml/min. The optimum raffinate flow rate was observed to be 1.66 ml/min. It is to be noted that since the adsorbent flow rate is unchanged, the σ and V values do not change in section R. Hence performance of section R is not affected at different raffinate flow rates.

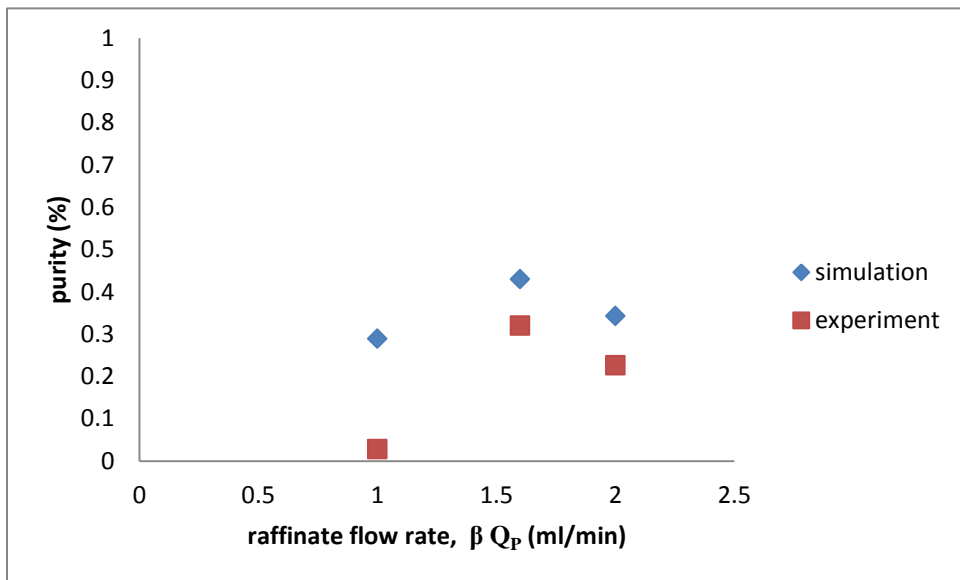
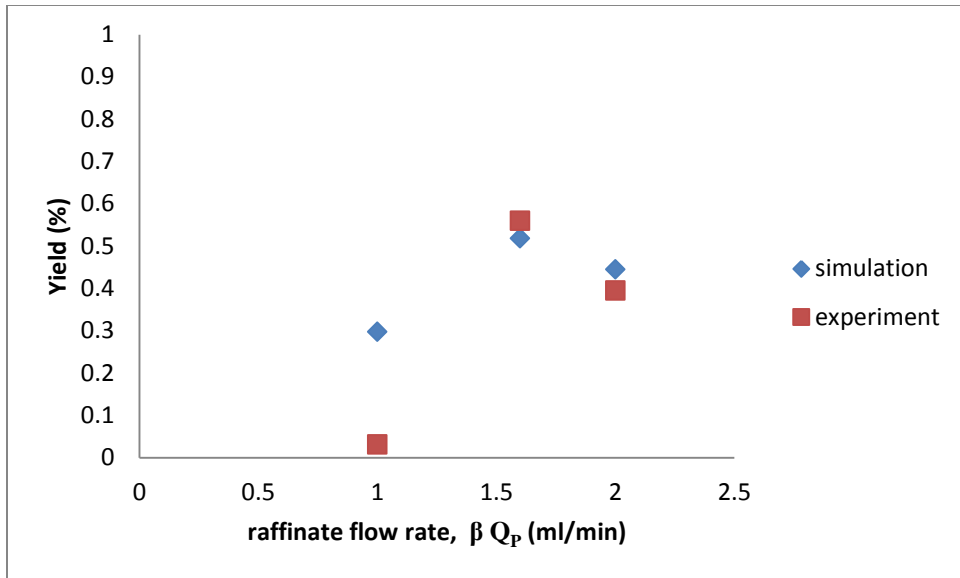


Figure 4.5 Effect of raffinate flow rate on SMBR performance

Experimental conditions: $\alpha Q_p = 0.1$ ml/min, $\gamma Q_p = 4$ ml/min, $t_s = 12$ min

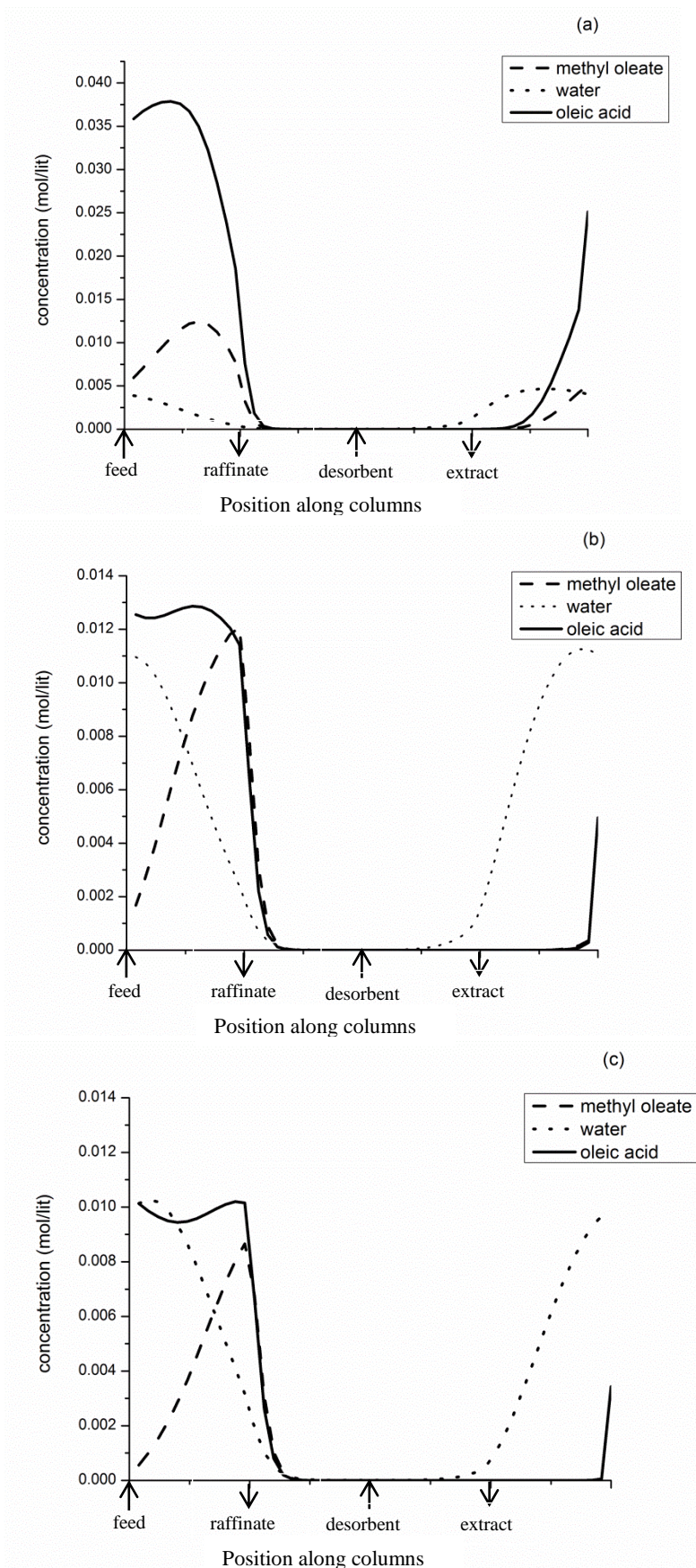


Figure 4.6 Effect of raffinate flow rate on cyclic steady state concentration profiles of methyl oleate-water-oleic acid. (a) $\beta Q_P = 1 \text{ ml/min}$, (b) $\beta Q_P = 1.66 \text{ ml/min}$, (c) $\beta Q_P = 2 \text{ ml/min}$

Experimental conditions: $\alpha Q_P = 0.1 \text{ ml/min}$, $\gamma Q_P = 4 \text{ ml/min}$, $t_s = 12 \text{ mins}$

4.5.3 Effect of Feed Flow Rate

Experiments were carried out at three different feed flow rates: 0.05 ml/min, 0.1 ml/min and 0.2 ml/min. The raffinate flow rate, desorbent flow rate and switch time was kept constant at 1.66 ml/min, 4 ml/min and 12 minutes respectively. The SMB performance at different feed flow rates are shown in the Figure 4.7. When the feed flow rate was reduced from 0.1 ml/min to 0.05 ml/min, there was no appreciable change in yield and purity. However, on increasing the feed flow rate to 0.2 ml/min, the yield dropped from 56.3% to 34.7%; purity dropped from 32% to 25%. Hence, the observed trend was that increasing feed flow rate decreased both yield and purity. This can be explained from the calculated values of effective velocity shown in Table 4.2. It is clear that at different feed flow rates, the σ and V values of methyl oleate and water remain unchanged in sections P and R. Hence, their performances are not affected by changing feed flow rate. Whereas in section S, the increase in feed flow rate causes decrease in fluid flow velocity. The σ_{MO} value increases from 0.389 to 0.429, deteriorating desorption of methyl oleate in section S. More and more methyl oleate is retained in this section which ultimately appears in the extract at the end of a switch, when section S becomes section R. Also at higher feed flow rate, more water is produced. Due to this adsorbent regeneration becomes more difficult unless desorbent flow rate is increased. Moreover, with increase in feed flow rate, ΔV value in section S decreases from 1.749 to 1.662, resulting in deterioration of the separation of concentration front. All these factors reduce yield and purity. This is reflected in the steady state column concentration profiles given in Figure 4.8.

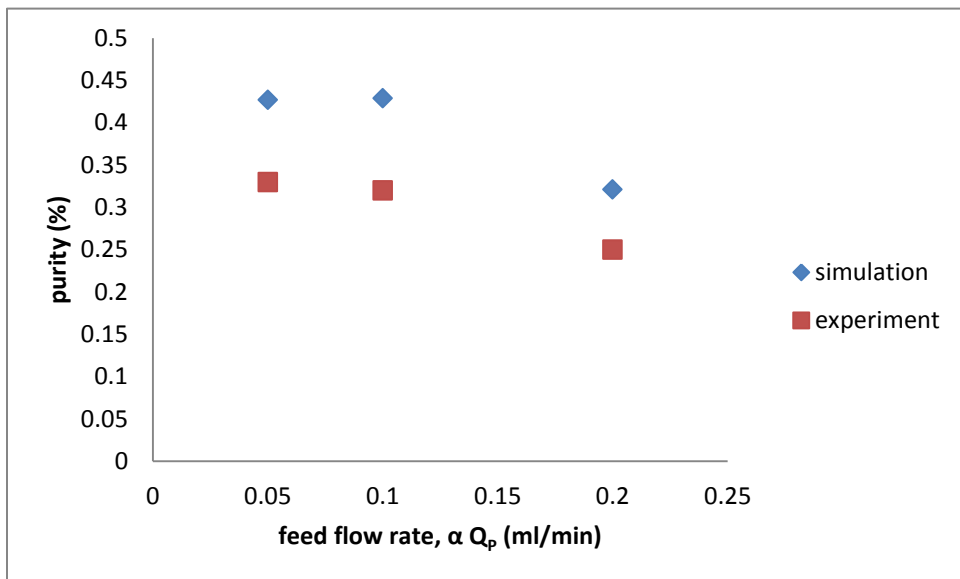
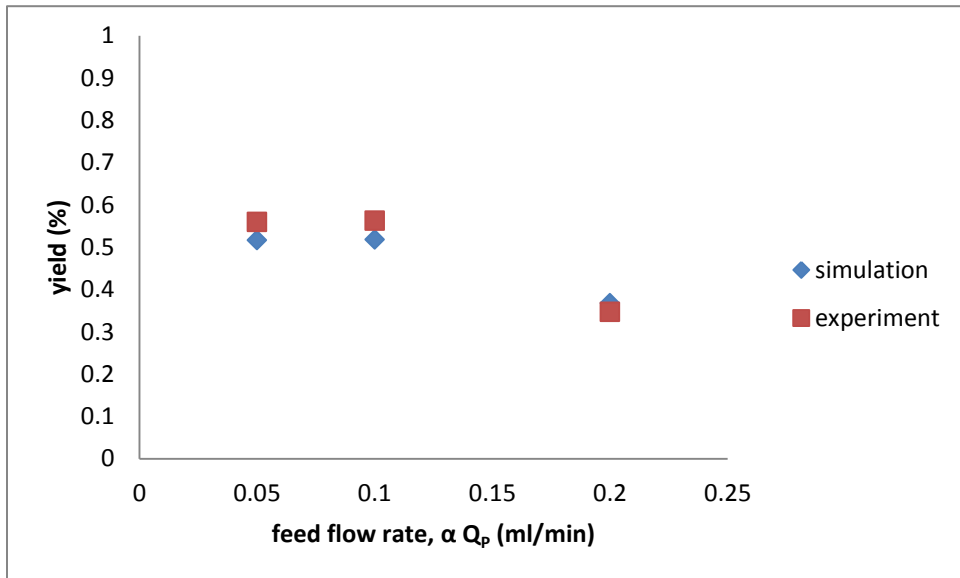


Figure 4.7 Effect of feed flow rate on SMBR performance

Experimental conditions: $\beta Q_P = 1.66\text{ml/min}$, $\gamma Q_P = 4\text{ml/min}$, $t_s = 12\text{min}$

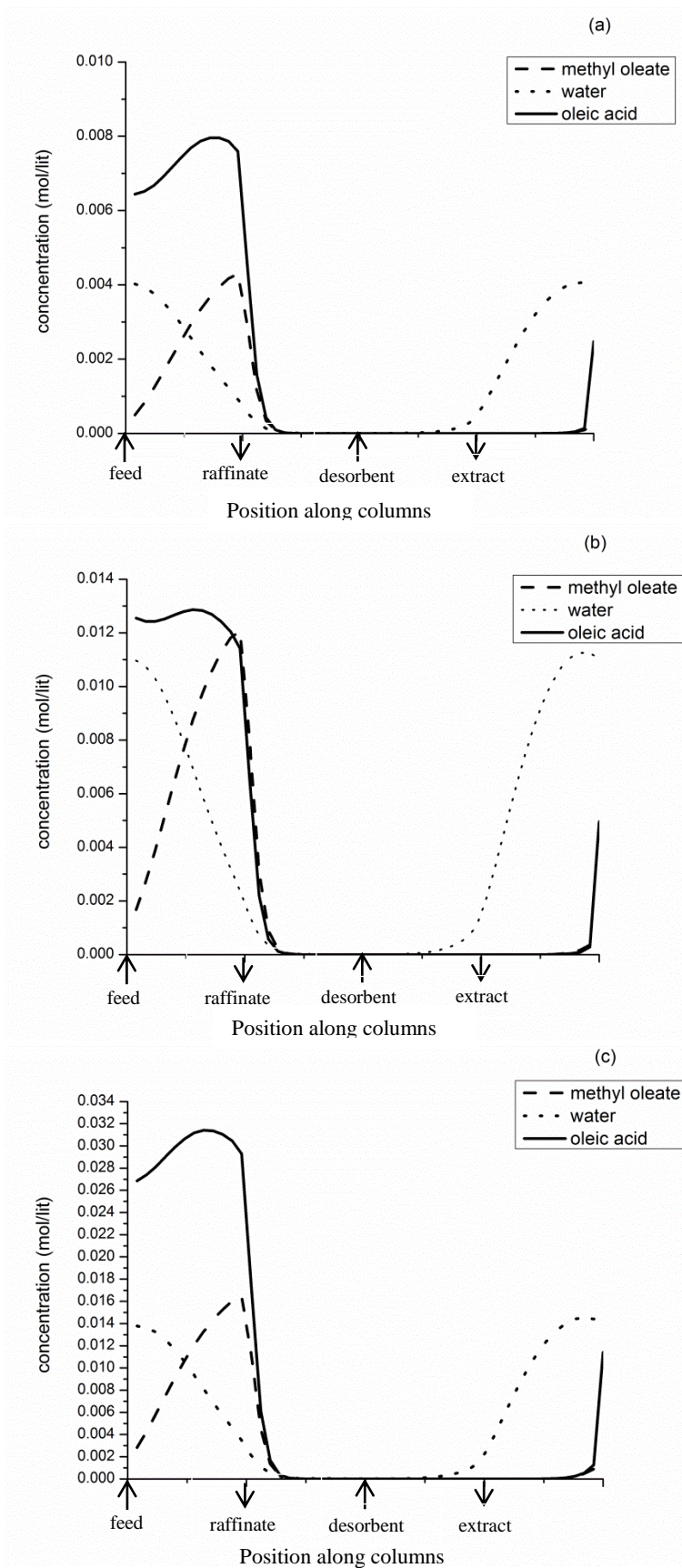


Figure 4.8 Effect of feed flow rate cyclic steady state concentration profiles of methyl oleate-water-oleic acid. (a) $\alpha Q_P = 0.05\text{ml/min}$, (b) $\alpha Q_P = 0.1\text{ml/min}$, (c) $\alpha Q_P = 0.2\text{ml/min}$

Experimental conditions: $\beta Q_P = 1.66\text{ml/min}$, $\gamma Q_P = 4\text{ml/min}$, $t_s = 12\text{min}$

4.6 Sensitivity Studies

To have a better understanding of the functioning of SMBR, sensitivity studies need to be done. This involves analysing the effect of various process parameters on the yield and purity of methyl oleate synthesis. From the experiments as well as the model, it was demonstrated that it is possible to obtain improved yield and purity for methyl oleate synthesis using an SMBR. There is a complex interaction between various operating parameters in the SMBR and collectively they impact the synthesis reaction in conflicting way. Hence, to understand these interactions and interplay of the various parameters, a sensitivity analysis was carried out by changing only one process parameter at a time while fixing the other operating parameters at a reference set of values. This will also allow us to know which parameters are sensitive (or insensitive) to SMBR performance and which parameters effects in conflicting manner.

Figure 4.9 shows the results of the sensitivity study. The effect of operating parameters such as switch time (t_s), feed (α), desorbent (γ) and raffinate (β) flow rate were studied on the yield and purity of methyl oleate. The first row of graphs shows the effect of switch time. Subsequent graphs show the effect of α , β and γ at three different switch times: 8 minutes, 12 minutes and 17 minutes.

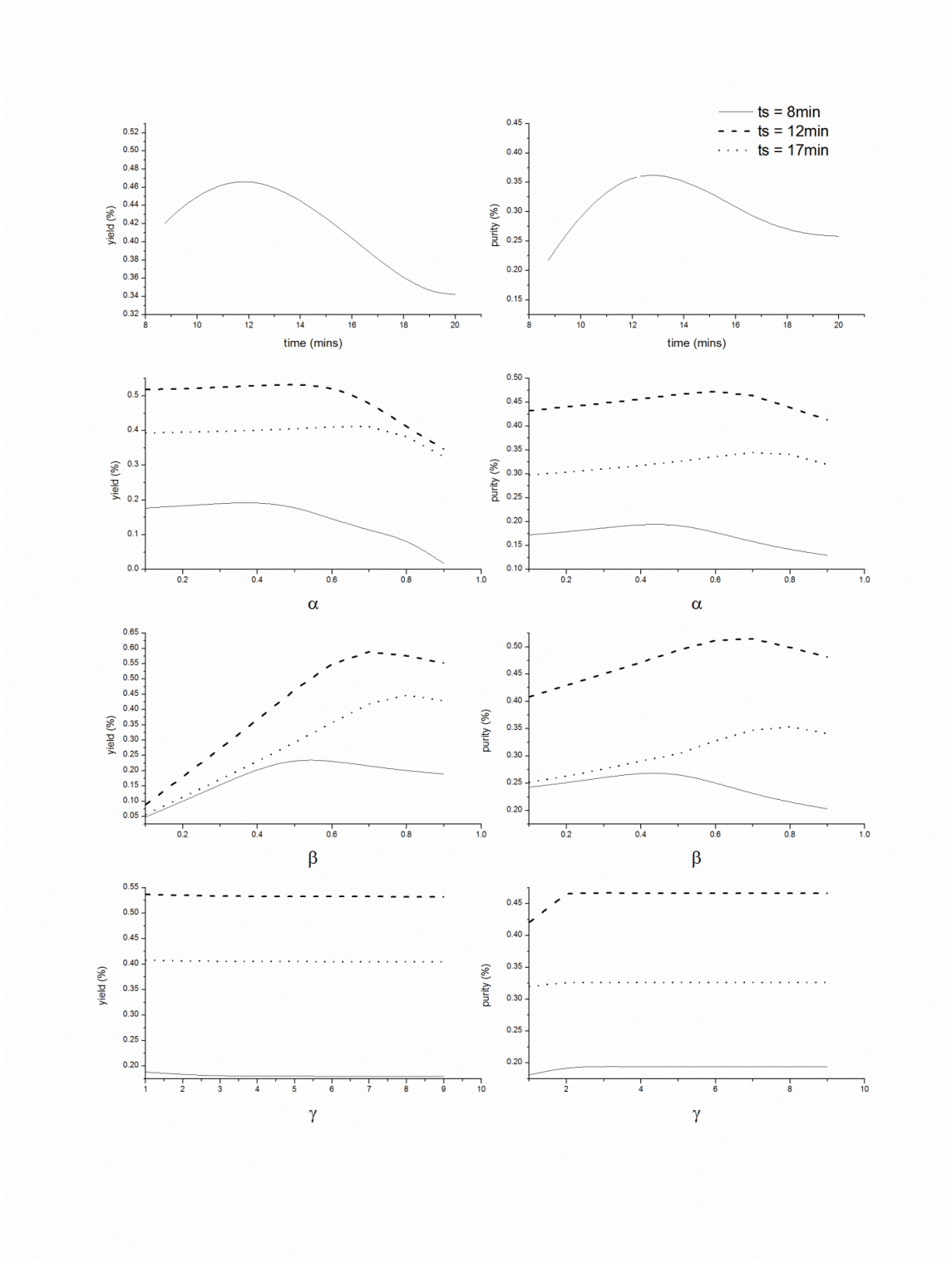


Figure 4.9 Sensitivity analysis of various process parameters on synthesis of methyl oleate

Reference values: $p = 1$, $q = 1$, $r = 1$, $s = 1$, $L_{col.} = 25\text{cm}$, $\varepsilon = 0.4$, oleic acid feed concentration = 0.21mol/lit , $Q_P = 1.66\text{ml/min}$, $\alpha = 0.5$, $\beta = 1$, $\gamma = 4$

Effect of α : Initially both yield and purity show a very slight increase with α . But on further increasing α both of them deteriorate. Hence increasing α has a detrimental effect on both yield and purity. This is also reflected in the experimental studies where it was found out that increasing feed flow rate reduces SMBR performance.

Effect of β : Both yield and purity shows a strong linear increase with β . The rate of increase is more pronounced at 12 minutes switch time and least at 8 minutes switch time. Hence β has a significant effect on SMBR performance for the present reactive system.

Effect of γ : The studies show that when γ is high enough, increasing its value does not affect yield or purity, as is evident from figure 9. Hence, a minimum γ is required for purging the column and a value greater than the minimum has no further effect. During the experiments the high desorbent flow rate was maintained and likewise kept constant. This ensured that the column in section R was fully purged before switching occurred.

In the above studies, the yield and purity were highest when switch time was 12 minutes, and lowest at 8 minutes switch time. This is also reflected in the experimental studies done. Hence, from these studies it can be concluded that in this system, the two most critical factors affecting SMBR performance are raffinate flow rate (β) and switch time (t_s). It is possible to further optimize the various process parameters to get even higher values of yield and purity through systematic optimization of the process. Further improvement of performance is possible by multi-objective optimization. This is necessary to successfully design and implement the SMBR on an industrial scale.

4.7 Conclusions

The synthesis of biodiesel (methyl oleate) from the transesterification reaction of free fatty acid (oleic acid) and alcohol (methanol) was investigated in a Simulated Moving Bed Reactor (SMBR). A four column SMBR experimental setup was used; one column for each section. Experiments were carried out at different switch times, feed and raffinate flow rates. A rigorous mathematical model was used to predict the dynamic

behaviour of the system. The adsorption and kinetic parameters obtained from single column experiments were used by the model to predict the experimental outcome of the SMBR. It was observed that the model predicted the experimental results reasonably well. For this experimental setup, the highest yield and purity obtained were 56% and 32% respectively; corresponding to 12 minutes switch time, 0.1 ml/min feed flow rate, 1.66 ml/min raffinate flow rate and 4 ml/min desorbent flow rate. To further investigate the influence of operating conditions on the performance of SMBR, a parametric sensitivity analysis was carried out on the experimentally verified model. From the sensitivity analysis, it was observed that switch time and raffinate flow rate significantly affected SMBR performance for the current system. To further improve the performance and successfully implement the SMBR on an industrial scale, a multi-objective optimization must be carried out.

4.8 References

1. Gelosa D, Ramaioli M, Valente G, Morbidelli M. Chromatographic Reactors: Esterification of Glycerol with Acetic Acid Using Acidic Polymeric Resins. *Ind. Eng. Chem. Res.* 2003;42(25):6536-6544. doi:10.1021/ie030292n.
2. Mazzotti M, Kruglov A, Neri B, Gelosa D, Morbidelli M. A continuous chromatographic reactor: SMBR. *Chem. Eng. Sci.* 1996;51:1827-1836. doi:10.1016/0009-2509(96)00041-3.
3. Kawase M, Suzuki T Ben, Inoue K, Yoshimoto K, Hashimoto K. Increased esterification conversion by application of the simulated moving-bed reactor. *Chem. Eng. Sci.* 1996;51:2971-2976. doi:10.1016/0009-2509(96)00183-2.
4. Migliorini C, Fillinger M, Mazzotti M, Morbidelli M. Analysis of simulated moving-bed reactors. *Chem. Eng. Sci.* 1999;54:2475-2480. doi:10.1016/S0009-2509(98)00487-4.

5. Dunnebier G, Fricke J, Klatt KU. Optimal design and operation of simulated moving bed chromatographic reactors. *Ind. Eng. Chem. Res.* 2000;39:2290-2304. doi:Doi 10.1021/Ie990820o.
6. Lode F, Houmard M, Migliorini C, Mazzotti M, Morbidelli M. Continuous reactive chromatography. *Chem. Eng. Sci.* 2001;56(2):269-291. doi:10.1016/S0009-2509(00)00229-3.
7. Zhang Z, Hidajat K, Ray AK. Application of Simulated Countercurrent Moving-Bed Chromatographic Reactor for MTBE Synthesis. *Ind. Eng. Chem. Res.* 2001;40:5305-5316. doi:10.1021/ie001071+.
8. Yu W, Hidajat K, Ray AK. Modeling, Simulation, and Experimental Study of a Simulated Moving Bed Reactor for the Synthesis of Methyl Acetate Ester. *Ind. Eng. Chem. Res.* 2003;42(26):6743-6754. doi:10.1021/ie0302241.
9. Ray AK, Carr RW, Aris R. The Simulated Countercurrent Moving-Bed Chromatographic Reactor - a Novel Reactor Separator. *Chem. Eng. Sci.* 1994;49:469-480. doi:Doi 10.1016/0009-2509(94)80048-0.
10. Ray AK, CRW. Experimental study of a laboratory scale simulated countercurrent moving bed chromatographic reactor. *Chem. Eng. Sci.* 1995;50:2195 -2202. Available at: [http://www.eng.uwo.ca/people/aray/Ajay Publications PDF files/A5 SMB Minn Expt CES 1995.pdf](http://www.eng.uwo.ca/people/aray/Ajay%20Publications%20PDF%20files/A5%20SMB%20Minn%20Expt%20CES%201995.pdf).
11. Kundu PK, Zhang Y, Ray AK. Modeling and simulation of simulated countercurrent moving bed chromatographic reactor for oxidative coupling of methane. *Chem. Eng. Sci.* 2009;64:5143-5152. doi:10.1016/j.ces.2009.08.036.
12. Zhang Y, Hidajat K, Ray AK. Modified reactive SMB for production of high concentrated fructose syrup by isomerization of glucose to fructose. *Biochem. Eng. J.* 2007;35:341-351. doi:10.1016/j.bej.2007.01.026.

13. Meurer M, Altenhöner U, Strube J, Untiedt A, Schmidt-Traub H. Dynamic simulation of a simulated moving-bed chromatographic reactor for the inversion of sucrose. *Starch/Staerke* 1996;48:452-457. doi:DOI 10.1002/star.19960481113.
14. Zhang Y, Hidajat K, Ray AK. Enantio-separation of racemic pindolol on alpha1-acid glycoprotein chiral stationary phase by SMB and Varicol. *Chem. Eng. Sci.* 2007;62:1364-1375. doi:10.1016/j.ces.2006.11.028.
15. Azevedo DCS, Rodrigues AE. Separation of Fructose and Glucose from Cashew Apple Juice by SMB Chromatography. *Sep. Sci. Technol.* 2005;40:1761-1780. doi:10.1081/SS-200064559.
16. Coelho MS, Azevedo DCS, Teixeira JA, Rodrigues A. Dextran and fructose separation on an SMB continuous chromatographic unit. *Biochem. Eng. J.* 2002;12:215-221. doi:10.1016/S1369-703X(02)00071-2.
17. Azevedo DCS, Rodrigues AE. Fructose-glucose separation in a SMB pilot unit: Modeling, simulation, design, and operation. *AIChE J.* 2001;47:2042-2051. doi:10.1002/aic.690470915.
18. Azevedo DCS, Rodrigues AE. Design methodology and operation of a simulated moving bed reactor for the inversion of sucrose and glucose-fructose separation. *Chem. Eng. J.* 2001;82:95-107. doi:10.1016/S1385-8947(00)00359-4.
19. Hashimoto K, Adachi S, Noujima H, Ueda Y. A new process combining adsorption and enzyme reaction for producing higher-fructose syrup. *Biotechnol. Bioeng.* 1983;25:2371-2393. doi:10.1002/bit.260251008.
20. Kapil A, Bhat S a., Sadhukhan J. Dynamic Simulation of Sorption Enhanced Reaction Processes for Biodiesel Production. *Ind. Eng. Chem. Res.* 2010;49(5):2326-2335. doi:10.1021/ie901225u.
21. Petroulas T, Aris R, Carr RW. Analysis and performance of a countercurrent moving-bed chromatographic reactor. *Chem. Eng. Sci.* 1985;40:2233-2240.

22. Fish B. The continuous countercurrent moving bed chromatographic reactor. *Chem. Eng. Sci.* 1986;41:661-668.
23. Ray AK, Carr RW. Numerical simulation of a simulated countercurrent moving bed chromatographic reactor. *Chem. Eng. Sci.* 1995;50:3033-3041. doi:10.1016/0009-2509(95)00135-R.

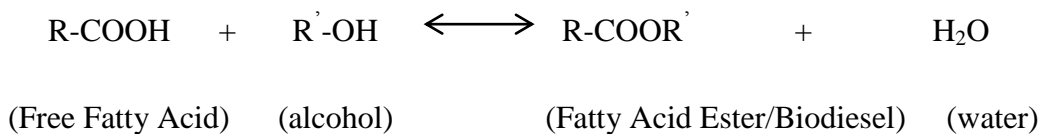
Chapter 5

5 Multi-objective Optimization of Biodiesel Synthesis in Simulated Moving Bed Reactor

5.1 Introduction

The Simulated Moving Bed (SMB) Technology has recently gained considerable interest for a wide variety of applications. It is an adsorption-based chromatographic separation process in which the countercurrent movement of the mobile phase with respect to stationary phase is simulated by periodic switching of the introduction and withdrawal ports along a series of columns. This technology has been successfully used to achieve higher yield in case of equilibrium-limited reversible reactions. In case of equilibrium-limited reversible reactions, it helps to push the equilibrium forward by in-situ separation of the products as soon they are formed. However, the SMB process is complex to implement. Various operating parameters such as switch time, flow rates in each section, length of columns, etc. have to be optimally selected for successful and efficient operation. Hence, systematic optimization of SMB is necessary for its industrial implementation and to make it economically viable.

The modeling, simulation and experimental study of SMBR for biodiesel synthesis have been carried out and reported in earlier chapters. The reaction investigated in this study is given by:



The free fatty acid used in this work was oleic acid, alcohol used was methanol and fatty acid ester obtained was methyl oleate, which is biodiesel. A mathematical model was used to describe the dynamic behaviour of SMBR. It was validated by carrying out

experiments and comparing the experimental results with the model predicted values. It was observed that the model predicted the experiments reasonably well. Thereafter, a parametric sensitivity study was carried out to determine the effect of various operating parameters on the functioning of SMBR. It was found out that there is a complex interplay between the various operating parameters such as switch time, the feed, desorbent and raffinate flow rates. Together, they collectively influence the yield and purity of biodiesel in SMBR. Sensitivity studies show that although some parameters influence yield and purity in conflicting manner, it is possible to further improve the yield and purity in a SMBR, if systematic optimization is performed to determine an optimal set of the operating parameters. In order to determine these best (optimal) set of values, an optimization study of the SMBR needs to be done. In this study, optimization of the SMBR for biodiesel synthesis was carried out for different set of objective functions.

5.2 Multi-objective Optimization

The optimization of a chemical process has been an interesting field of study for quite some time. Most researchers solve optimization problems that involve single objective function. Usually, this single-objective accounted for only cost and/or economic efficiency of the process, which is a scalar quantity. But, real world chemical engineering problems often involve a variety of factors that requires multiple objectives to fulfill simultaneously. For example, yield, purity, selectivity, solvent consumption as well as variables such as reliability, safety, quality control, etc. which cannot be easily compared to each other. Hence, very often they cannot be scalarized into a single, meaningful objective function. Until a few years ago, this scalarization was done by assigning some weightage to all the factors involved. But, this was not a practical approach, as in real world the various factors do not equally affect a process. As a result, the solution obtained from such optimization was largely dependent on the weightage assigned to the various factors. Moreover, if the objective function is non-convex, it gave rise to a duality gap as a result of which optimization algorithm misses some optimal solutions which can never be found regardless of the weighting factors chosen [1, 2]. Furthermore, a single

objective function defined as cost or profit results in solution that is time-specific and site-specific. The optimal value based on cost of raw material or revenue generated from products differed from region-to-region and year-to-year. One can calculate cost or profit at any location and at any time if the optimization study is done using real variables such as conversion, yield, selectivity, etc.

Optimization of multiple criteria simultaneously takes into account several objectives together, even when they are conflicting in nature. In case of conflicting effect, instead of finding the best possible single global solution, a set of equally-good non-dominated solutions are obtained. These are known as Pareto optimal solutions. In such a set, no one solution can be considered superior to other with respect to all objective functions. As one moves from one optimal solution to another, it results in improvement of at least one objective function and deterioration of at least one another objective function. Hence, an operator has to select, one solution according to priority. In recent years multi-objective optimization has gained popularity for solving problems in various aspects of chemical engineering [3-10]. It has also been used for both reactive and separative SMB process [2, 11].

5.3 Optimization Methodology - Genetic Algorithm

In this work, Genetic Algorithm (GA), a non-traditional search and optimization method that has become quite popular in engineering optimization has been used. GA mimics the principles of genetics and the Darwinian principle of natural selection (i.e., survival of the fittest). A simple genetic algorithm (SGA) is suitable for optimizing problems with a single-objective function. In single-objective function optimization, one attempts to find the best solution, which is usually the global minimum (or maximum). However, most real-world problems involve the simultaneous optimization of multiple objective functions (a vector). Such problems are conceptually different from single-objective-function problems. In multiple objective-function optimizations, a solution that is the best (global optimum) with respect to all objectives might not exist. Instead, an entire set of optimal solutions may exist that might be equally good. These solutions are known as

Pareto-optimal (or non-dominated) solutions. A Pareto set, for example, for a two-objective-function problem is described by a set of points such that, when one moves from one point to any other, one objective function improves while the other worsens. Thus, one cannot say that any one of these points is superior (or dominant) to any other. Because none of the non-dominated solutions in the Pareto set is superior to any other, any one of them is an acceptable solution. The choice of one solution over another requires additional knowledge of the problem, and often, this knowledge is intuitive and non-quantifiable. There are various approaches available for solving a multi-objective optimization problem: The goal attainment method, the ϵ -constraint method, and the Non-Dominated Sorting Genetic Algorithm (NSGA) method [1]. In this work, the NSGA method has been used to carry out the optimization process to obtain the Pareto optimal set.

The Genetic Algorithm method is a search technique developed by Holland [12, 13] in 1975. It imitates the process of natural selection and natural genetics. In this technique, the decision variables are coded into a set of binary strings or numbers, known as chromosomes, thereby creating a “population (gene pool)” of such binary strings. These chromosomes are generated using random number generators. Each chromosome is then mapped into a set of real values of the decision variables using an upper and lower bounds for each of these decision variables. When all the chromosomes are allocated, the process model is used to assign a value of the objective function that reflects its “fitness” value. In this way, a ‘gene pool’ of chromosomes is created, with the value of the objective function of each chromosome representing its ‘fitness’ value. The Darwinian principle of “survival of the fittest” is then used to create a new and improved gene pool (new generation). This is done by preparing a “mating pool” that comprises copies of chromosomes, the number of copies of any chromosome being proportional to its fitness based on Darwin’s principle of ‘survival of the fittest’. After this, pairs of chromosomes are randomly selected and ‘mated’ using operations similar to those in genetic reproduction so that information exchange takes place between them, giving rise to daughter chromosomes. This gives rise to a new and improved gene pool with ‘fitness’ value better than the previous one. This process is repeated over a number of generations

so as to get a more improved gene pool. The process goes on until the chromosomes match the criteria assigned by the objective functions [1, 14].

Three common operators are used in simple GA (SGA), to distinguish it from its various adaptations, to obtain a superior (next) generation of chromosomes. These are referred to as reproduction, crossover, and mutation. Reproduction is the generation of the mating pool, where the chromosomes are copied probabilistically, based on their fitness values. However, no new strings are formed in the reproduction phase. *New* strings are formed using the crossover operator by trading information among pairs of strings in the mating pool. A pair of daughter chromosomes is produced by selecting a crossover site (selected randomly) and trading the two parts of the pair of parent chromosomes (selected randomly from the mating pool). The effect of crossover can be harmful or favourable. It is hoped that the daughter strings are superior. If they are worse than the parent chromosomes, they will slowly die a natural death over the next few generations. In order to preserve some of the good strings that are already present in the mating pool, not all strings in the pool are used in crossover. A crossover probability, p_c , is used, where only $100p_c$ % of the strings in the mating pool are engaged in crossover, while the rest continue untouched to the next generation. After a crossover is performed, mutation takes place. The mutation operator changes a binary number at *any* location (selected randomly) in a chromosome from a 1 to a 0 and vice versa to create a location in the neighbourhood of the current point, thereby achieving a local search around the existing solution and to preserve diversity in the population. The entire process is replicated until some stopping criterion is met (the specified maximum number of generations is attained, or the improvements in the values of the objective functions become lower than a specified tolerance).

The optimal solutions to a multi-objective function optimization problem are non-dominated (or equally good optimal Pareto) solutions. In order to handle multiple objective functions and find optimal Pareto solutions, the SGA has to be amended. The new algorithm, non-dominated sorting genetic algorithm (NSGA), varies from the SGA only in the way the selection operator works. The NSGA uses a grading (ranking) selection method to accentuate the good points and a niche method to create miscellany

in the population without squandering a stable sub-population of good solutions. In the new procedure, several groups of non-dominated chromosomes from among all the members of the population at any generation are identified and classified into “fronts.” Each of the members in a particular front is assigned a large, common, front fitness value (a dummy value) arbitrarily. To evenly distribute the points in this (or any other) front evenly in the variable decision domain, the dummy fitness value is then modified according to a sharing procedure by dividing it by the niche count of the chromosome.

The niche count is a quantity that represents the number of neighbours around it, with distant neighbours contributing less than those nearby. The niche count, thus, gives an idea of how crowded the chromosomes are in the variable decision space. Using the shared fitness value for reproduction, thus, helps spread the chromosomes in the front, since crowded chromosomes are assigned lower fitness values. This procedure is repeated for all members of the first front. Once this is done, these chromosomes are temporarily removed from consideration, and all the *remaining* ones are tested for non-dominance. The non-dominated chromosomes in *this* round are classified into the next front. These are all assigned a dummy fitness value that is a bit lower than the *lowest* shared fitness value of the previous front. Sharing is performed thereafter. The sorting and sharing is continued until all the chromosomes in the gene pool are assigned shared fitness values. The usual operations of reproduction, crossover, and mutation are now performed once again. It is clear that the non-dominated members of the first front with fewer neighbours will get the highest representation in the mating pool. Members of later fronts, which are dominated, will get lower representations (they are still assigned some low fitness values, rather than “killed,” in order to maintain the diversity of the gene pool). Sharing forces the chromosomes to be spread out in the variable decision space. The population usually is found to converge very rapidly to the Pareto set. It should also be noted that any number of objectives (both minimization and maximization problems) can be solved using this procedure.

The genetic algorithm is robust and superior to traditional optimization algorithms. It has a number of advantages [1, 14]:

- a) Efficient handling of uncertainty problems, stochasticities and discrete search spaces,
- b) Its efficiency has little effect on the shape and ‘spread’ of the Pareto optimal front, unlike other techniques where efficiency of the technique determines the spread of the solution obtained,
- c) An entire Pareto set can be obtained in a single application, unlike other techniques like the ϵ -constraint method where the technique has to be applied over and over again to generate a Pareto front.

Several versions of the genetic algorithm [15] have been used to solve problems in chemical and reaction engineering [1, 14]. In this work, the NSGA II has been used to optimize the synthesis of biodiesel in the SMBR.

5.4 Mathematical model of SMBR

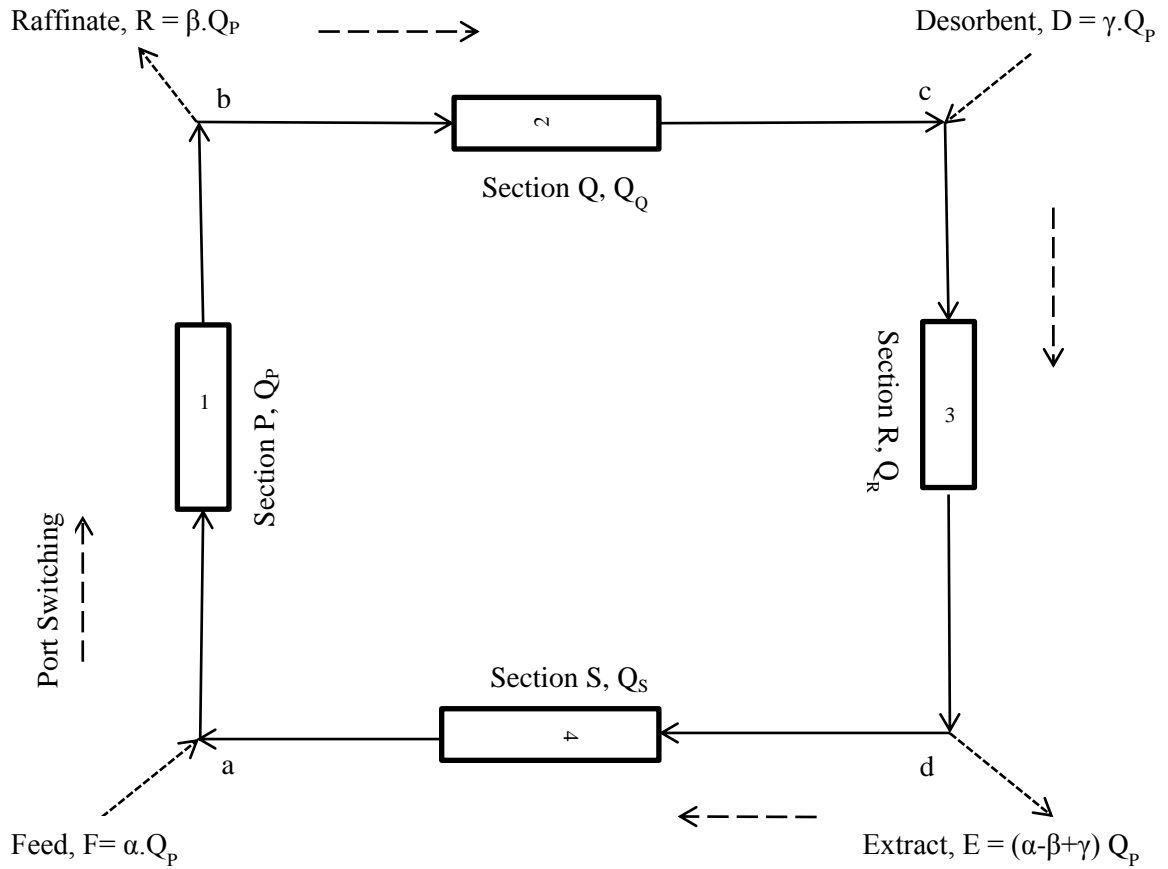


Figure 5.1 Schematic diagram of a 4-column SMBR

Figure 5.1 show the schematic diagram of a 4 column SMBR system, with one column in each of the sections P, Q, R and S. Flow rates in each section are given by:

Section P: Q_P

Section Q: $Q_Q = (1-\beta) \cdot Q_P$

Section R: $Q_R = (1-\beta+\gamma) \cdot Q_P$

Section S: $Q_S = (1-\alpha) \cdot Q_P$

Where, $\alpha = F/Q_P$, $\beta = R/Q_P$ and $\gamma = D/Q_P$

There are two inlet ports for feed and desorbent, and two outlet ports for raffinate and extract. During a switch, these ports move simultaneously by one column, in direction of the flow of mobile phase. This achieves a countercurrent movement of the solid phase with respect to the fluid phase. This switch takes place after a specific interval, known as the switching time. The switching time and column configuration are firstly decided and then kept constant throughout the process. The material balance of the SMBR is based on the equilibrium dispersive model which is as follows:

$$\frac{\partial C_{ij}^{(N)}}{\partial t} + \left(\frac{1-\varepsilon}{\varepsilon}\right) \frac{\partial q_{ij}^{(N)}}{\partial t} + \frac{u_0}{\varepsilon} \frac{\partial C_{ij}^{(N)}}{\partial z} - \left(\frac{1-\varepsilon}{\varepsilon}\right) v_i R_j^{(N)} = D_{iK} \frac{\partial^2 C_{ij}^{(N)}}{\partial z^2} \quad (5.1)$$

Where,

C_i is the concentration of component i in the mobile phase

t is the time

q_i is the concentration of component i in the polymer phase

ε is the column void fraction

u is the superficial fluid phase flow velocity

z is the axial coordinate

v_i is the stoichiometric coefficient of the component i

r is the reaction rate

D_i is the apparent dispersion coefficient of the component i

For the component i in the j^{th} column during the N^{th} switching period, u_ϕ denotes superficial flow velocity in section ϕ (where $\phi = P, Q, R, S$) and the reaction rate expressions and adsorption isotherms are given by –

$$R_j^{(N)} = k_f [q_{a,j}^{(N)} - \frac{q_{me,j}^{(N)} \cdot q_{w,j}^{(N)}}{k_{es}}] \quad (5.2)$$

$$q_{ij}^{(N)} = K_i \cdot C_{ij}^{(N)} \quad (5.3)$$

The initial and boundary conditions are:

Initial conditions-

$$\text{When } N = 0, C_{ij}^{(0)} = C_{ij}^{\text{Initial}} = 0 \quad (5.4a)$$

When $N \geq 1$,

$$C_{ij}^{(N)} = C_{i,j+1}^{(N-1)} \quad \text{for } j = 1 \sim (N_{col} - 1) \quad (5.4b)$$

$$C_{ij}^{(N)} = C_{i,1}^{(N-1)} \quad \text{for } j = N_{col} \quad (5.4c)$$

Boundary conditions-

Feed entry point (a in Figure 5.1) –

$$C_{i1}^{(N)} \Big|_{z=0} = (1-\alpha) C_{i,N_{col}}^{(N)} \Big|_{z=L} + \alpha C_{i,f} \quad (5.5a)$$

Raffinate take-off point (b in Figure 5.1) –

$$C_{i,p+1}^{(N)} \Big|_{z=0} = C_{i,p}^{(N)} \Big|_{z=L} \quad (5.5b)$$

Eluent inlet point (c in Figure 5.1) –

$$C_{i,p+q+1}^{(N)} \Big|_{z=0} = \left[\frac{1-\beta}{1-\beta+\gamma} \right] C_{i,p+q}^{(N)} \Big|_{z=L} \quad (5.5c)$$

Extract take off point (d in Figure 5.1) –

$$C_{i,p+q+r+1}^{(N)} \Big|_{z=0} = C_{i,p+q+r}^{(N)} \Big|_{z=L} \quad (5.5d)$$

The mass balance equation (Eqn. 5.1), initial and boundary conditions (Eqs. 5.4 & 5.5 respectively), reaction kinetic equation (Eqn. 5.2) and adsorption isotherm (Eqn. 5.3) completely define the SMBR system. The partial differential equations were solved using Method of Lines. They were first discretized using Finite Difference Method to convert it into a set of several coupled Ordinary Differential Equation of Initial Value Problems (ODE-IVP) and the resultant stiff ODEs were solved using the DIVPAG subroutine (which is based on Gear's method) in the IMSL library. Due to the presence of periodic switching in the system, whenever a switching is performed, a new IVP must be solved. Eventually, a periodic steady state with a period equal to the switching time is attained. After each switching, the column numbering is redefined as follows –

<i>Before switching</i>	<i>After switching</i>	
Column 1	Column N_{col}	
Column j	Column $j-1$	$j=1,2,3,\dots\dots N_{col}$ (5.6)

The model can also predict the concentration profiles of the reactant and products. It was observed that the SMBR reached the pseudo-steady state after about 20 switching operations. Improved yield and purity of biodiesel was achieved due to reaction and in-situ separation of products in the system. The time taken for one simulation run to achieve the cyclic steady state for SMB was about 4 seconds in a computer equipped with Intel Pentium Core 2 Duo CPU.

The design of the SMBR and the operating conditions to be used therein is set such that the yield and purity of biodiesel are maximized. The yield and purity are defined in this work as follows:

(a) Yield of methyl ester (Y_{ME}) :

$$Y_{ME} = \frac{\text{methyl oleate collected in raffinate}}{\text{oleic acid fed}} = \frac{\beta \cdot \left[\int_0^{t_s} C_{me, P}^{(N)} \Big|_{z=L_{col}} dt \right]}{\alpha C_{af} t_s} \quad (5.7)$$

(b) Purity of methyl ester (P_{ME}) :

$$P_{ME} = \frac{\text{methyl oleate collected in raffinate}}{(\text{oleic acid} + \text{water} + \text{methyl oleate}) \text{ collected in raffinate}}$$

$$= \frac{\int_0^{t_s} C_{me, P}^{(N)} \Big|_{z=L_{col}} dt}{\int_0^{t_s} (C_{me}^{(N)} + C_W^{(N)} + C_a^{(N)})_P \Big|_{z=L_{col}} dt} \quad (5.8)$$

As described earlier, the mathematical model was validated with experimental results. The model was subsequently checked for robustness through a parametric sensitivity study. It was determined that improved yield and purity were possible if the various operating parameters were optimized. Moreover, some decision variables found to be influencing the yield and purity value in conflicting manner. Hence, a multi-objective optimization of the SMBR is carried out which is expected to result in non-dominated equally-good Pareto optimal solutions.

5.5 Optimization of biodiesel production in SMB

In the open literature, many investigations of SMBRs can be found, but there are still no reported industrial application of this technology, probably because of the complexity of the process and the absence of any general guidelines for the design of the process. Most of the design approaches are not based on systematic and rigorous mathematical optimization methods. In recent years, an extremely robust technique, the genetic algorithm (GA) as well as its adaptations for more useful but complex multi-objective optimization problems, has become popular. GA-based approaches do not require any initial guesses and converge to the global optimum even when several local optima are

present. GA uses a population of several points simultaneously and also works with probabilistic (rather than deterministic) operators. In addition, GA uses information on the objective function and not its derivatives.

In the chapter, we report work on the multi-objective optimization of the complex chemical processes involved in a simulated moving-bed reactor (SMBR) for biodiesel synthesis. For the proper design of a SMBR, and more importantly, for an understanding of the principles of operation of a SMBR, a multi-objective optimization study is much more meaningful. To the best of our knowledge, this is the first attempt at a multi-objective optimization study of simulated moving-bed reactor systems for biodiesel production.

Different objectives can be used for optimization of reactive SMB. In this case, the optimization can be categorized into two approaches:

- (1) Existing stage optimization – This involves optimization of the existing set-up in which one does not have the freedom to select length, diameter or number of columns in the system. The process variables that can be used as decision variables are switch time and flow rates in different sections. Objectives which can be considered for this problem are maximization of yield and purity, which are related to increasing quality of the product, or minimization of desorbent flow rate, which is related to the operating cost of the system.
- (2) Design stage optimization – This involves performance enhancement by altering the design parameters of the unit such as length, diameter as well as number of columns as decision variables in addition to the other operating variables. The objective functions can be same as that of the existing-stage optimization.

For biodiesel production in reactive SMB, the product of interest is methyl ester which is obtained at the raffinate port. Hence, one can consider objective functions such as maximization of the product quality (yield and/or purity of the product at the raffinate port) or conversion of the limiting reactant. One can also consider minimization of desorbent consumption as an objective functions. All these objective functions can be

considered together, but that gives rise to complexity in analyzing the optimum solutions. For example, if we want to simultaneously improve three objectives, Pareto optimal solutions will include deterioration of two objective functions and improvement of the third, or vice versa. It will give rise to multi-dimensional solutions, which are difficult to analyse as optimal solutions lie on 3-dimensional surfaces. Hence, in this work, only two objective functions are considered at a time. Production of high quality biodiesel is of paramount importance for their use in engines [16, 17]. Hence maximization of purity is considered in all the optimization problems considered.

For this work, a four column SMBR setup was used, with one column in each section. Both existing stage and design stage optimization problems were considered. The various decision variables involved were:

- (1) Switching time t_s (process parameter)
- (2) Feed flow rate α and raffinate flow rate β (throughput parameter)
- (3) Eluent flow rate γ and flow rate in section P i.e. Q_P , which is related to the pressure drop in the system (operating cost parameter)
- (4) Length of the column L_{col} (fixed cost parameter) – only for design-stage optimization

The objective functions considered were:

- (1) Maximization of purity (P_{ME})
- (2) Maximization of yield (Y_{ME})
- (3) Minimization of desorbent consumption (γ)

Table 5.1 represents the optimization problems studied in this work.

Table 5.1 Optimization problems along with their objective functions, constraints, decision variables and fixed parameters

Case	Objective function	Constraint	Decision Variables	Fixed parameters
1.1 Existing setup	Maximum Y_{ME} Maximum P_{ME}	$Y_{ME} \geq 50\%$ $P_{ME} \geq 50\%$	$1 \leq t_s \leq 17$ (min); $0.1 \leq \beta \leq 1$; $1 \leq \gamma \leq 5$	$Q_p=1.66$ ml/min, $\alpha = 0.1$, Feed concentration = 0.21mol/lit, L_{col} = 25cm, $N_{col} = 4$ (1 column in each section)
1.2 Existing setup	Maximum P_{ME} Minimum γ	$Y_{ME} \geq 50\%$ $P_{ME} \geq 50\%$	$1 \leq t_s \leq 17$ (min); $0.1 \leq \beta \leq 1$; $1 \leq \gamma \leq 5$	Same as Case 1.1
2.1 Design stage	Maximum Y_{ME} Maximum P_{ME}	$Y_{ME} \geq 50\%$ $P_{ME} \geq 50\%$	$1 \leq t_s \leq 17$ (min); $0.1 \leq \beta \leq 1$; $1 \leq \gamma \leq 5$; $0.2 \leq L_{col} \leq 0.5$ (m)	$Q_p=1.66$ ml/min, $\alpha = 0.1$, Feed concentration = 0.21mol/lit, N_{col} = 4 (1 column in each section)
2.2 Design stage	Maximum P_{ME} Minimum γ	$Y_{ME} \geq 50\%$ $P_{ME} \geq 50\%$	$1 \leq t_s \leq 17$ (min); $0.1 \leq \beta \leq 1$; $1 \leq \gamma \leq 5$; $0.2 \leq L_{col} \leq 0.5$ (m)	Same as Case 2.1

The Pareto optimal solutions were generated using NSGA. 50 chromosomes (solutions) along with 50 generations (iterations) were considered for obtaining converged Pareto set. Table 5.2 represents the numerical parameter values used in NSGA for all the optimization runs. The time taken for one optimization run (50 solutions for 50 generations – 2500 simulation runs) was about 7 hours in a computer equipped with Intel Pentium Core 2 Duo CPU.

Table 5.2 Numerical parameter values used in NSGA optimization

Number of generations, N_{gen}	50
Population size, P_{pop}	50
Probability of crossover, P_{cross}	0.65
Probability of mutation, P_{mute}	0.002
Spreading parameter, σ	0.075
Sharing function exponent, α	2.0
Random number generator seed, S_r	0.455

5.6 Optimization of Existing Setup

The first two multi-objective optimization problems solved are for an existing set-up and is described below:

Case 1.1 Simultaneous maximization of yield and purity:

The optimization problem is mathematically described as:

$$\text{Maximize } I_1 = P_{ME} \quad (5.9)$$

$$\text{Maximize } I_2 = Y_{ME} \quad (5.10)$$

Subject to constraints:

$$P_{ME} \geq 50\% ; Y_{ME} \geq 50\% \quad (5.11)$$

Decision variables:

$$1(\text{min}) \leq t_s \leq 17(\text{min}); 0.1 \leq \beta \leq 1; 1 \leq \gamma \leq 5 \quad (5.12)$$

Fixed variables:

$Q_P = 1.66$ ml/min, $\alpha = 0.1$, Feed concentration = 0.21 mol/lit, Column length (L_{col}) = 25 cm, Number of columns (N_{col}) = 4 (1 column in each section)

The objective of this problem is to achieve simultaneous maximization of yield and purity.

Figure 5.2 represents the Pareto optimal solutions for this optimization problem and the influence of the decision variables on the Pareto set. It is clear that some of the decision variables act on yield and purity in a conflicting manner. A yield of about 79% can be obtained but the maximum purity possible is reduced to 76% (point 1 in Figure 5.2a); whereas increasing the purity to 87% reduces the maximum possible yield to about 72% (point 2 in Figure 5.2a). The purity level is also very sensitive to raffinate flow rate (β), as is clear from Figure 5.2c; decreasing β below 0.26 results in an increase in purity, with about 87% purity being achieved at $\beta \approx 0.22$. This happens because increasing the raffinate flow rate decreases the residence time within the column, thus reducing the conversion of the reactant (oleic acid) to biodiesel. Hence, lower raffinate flow rate is required to increase residence time and purity. As far as optimum switching time is concerned, it seems to remain constant at around 5 minutes (Figure 5.2b), indicating it is not affected for achieving high or low purity value. In case of desorbent flow rate, the purity seems to linearly increase when γ increases from 1 to 2, but further increasing γ does not significantly affect purity. Hence, at high desorbent flow rates, purity is not

affected. This is because when the desorbent flow rate is achieved above a minimum threshold, complete regeneration of column occurs before a switch; its further increase doesn't matter thereafter.

Figure 5.3 illustrates the steady state concentration profiles of the reactant and products in the column. Figure 5.3a corresponds to point 1 and Figure 3b corresponds to point 2 of Figure 5.2a. It is evident that at point 1, water which is more strongly adsorbed breaks through the raffinate stream, thereby contaminating the product. Hence, purity of product decreases. On the other hand, a high β and low γ results in presence of unreacted oleic acid, which gets recycled to section P at the end of a switch, resulting in higher yield. Point 2 corresponds to low raffinate flow rate and increased desorbent flow rate. As this condition, the residence time of the reactant in section P increases, resulting in higher conversion and increased product purity. Water is retained in section P and doesn't breakthrough in the raffinate stream. Also complete regeneration of column occurs at high desorbent flow rate. However, this also means that unreacted oleic acid is washed out in the extract stream, and hence is not available for recycle after the next switch. Hence yield of the product decreases.

It is clear that according to this optimization problem, the product purity is most significantly affected by β . Increasing γ above a certain point does not affect the SMBR performance

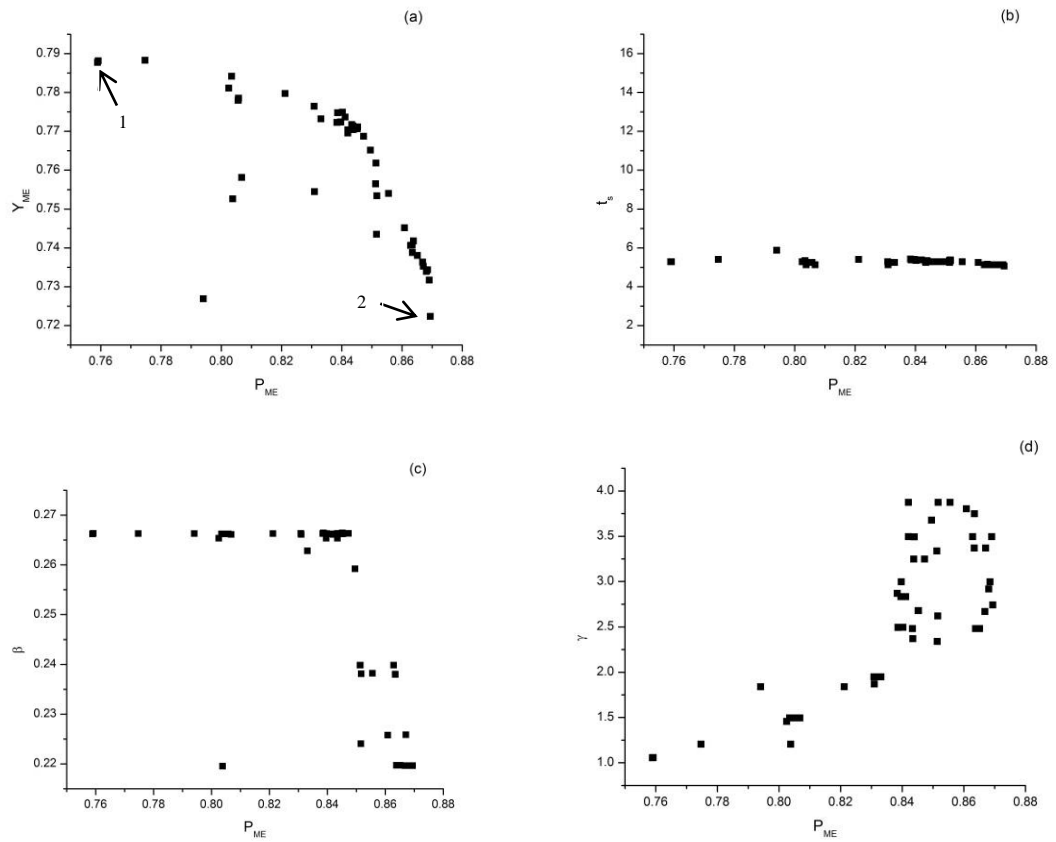


Figure 5.2 Pareto optimal solutions and corresponding operating variables for maximizing yield and purity of biodiesel

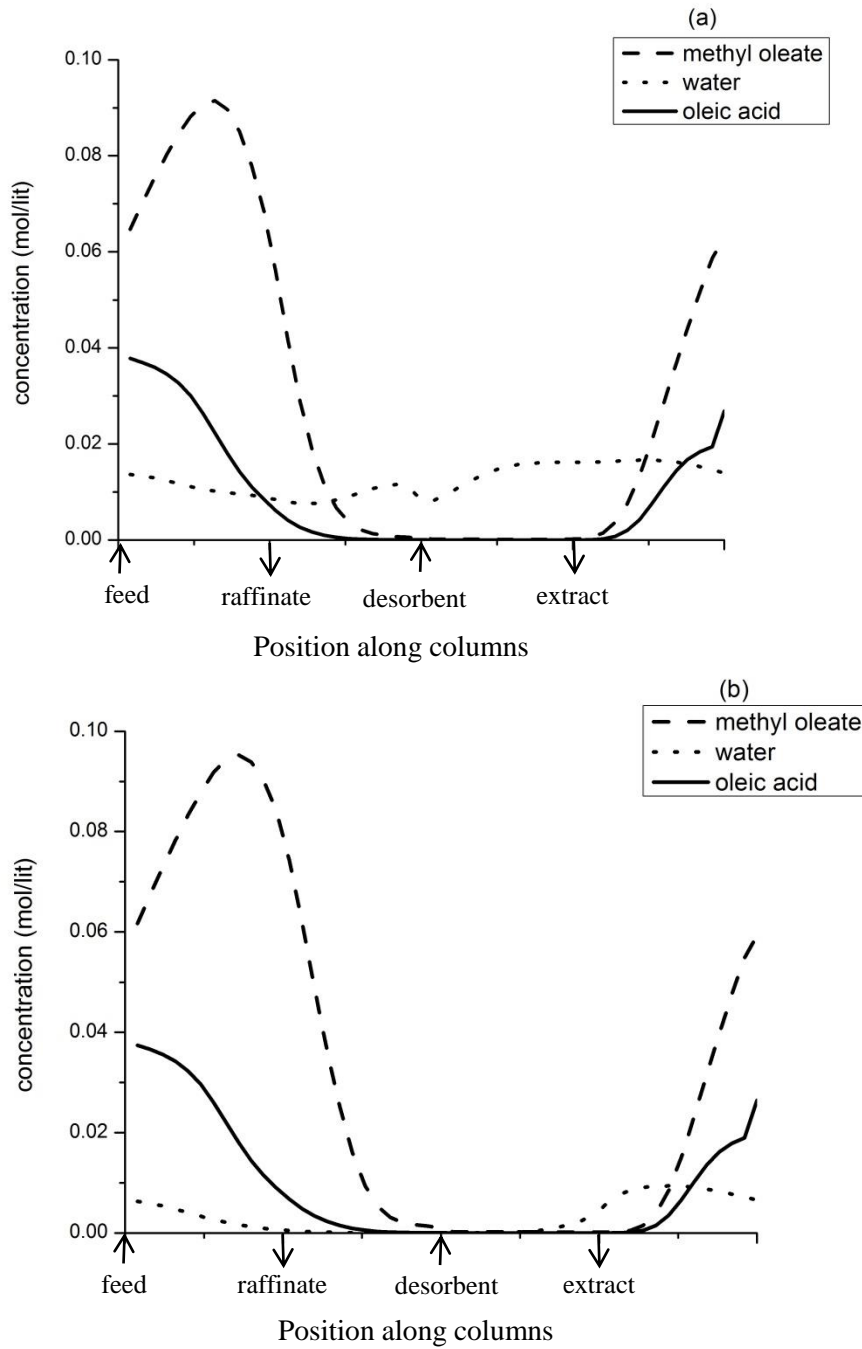


Figure 5.3 Steady state concentration profiles of methyl oleate-water-oleic acid system; (a) corresponding to point 1 & (b) corresponding to point 2 of Figure 5.2a

Case 1.2 Maximization of purity and minimization of desorbent consumption:

This optimization problem attempts to minimize the operational cost by reducing the desorbent flow rate (γ). It can be mathematically described as:

$$\text{Maximize } I_1 = P_{ME} \quad (5.13)$$

$$\text{Maximize } I_2 = 1/(1 + \gamma) \quad (5.14)$$

Subject to constraints:

$$P_{ME} \geq 50\% ; Y_{ME} \geq 50\% \quad (5.15)$$

Decision variables:

$$1(\text{min}) \leq t_s \leq 17(\text{min}); 0.1 \leq \beta \leq 1; 1 \leq \gamma \leq 5 \quad (5.16)$$

Fixed conditions:

$Q_P = 1.66 \text{ ml/min}$, $\alpha = 0.1$, Feed concentration = 0.21 mol/lit , Column length (L_{col}) = 25 cm , Number of columns (N_{col}) = 4 (1 column in each section)

Figure 5.4a represents the Pareto set for desorbent consumption compared to product purity. At low values of γ , it has a linear correlation with P_{ME} ; increasing γ from 1 to 1.5 results in increase of purity from 80 % to 87%. However, after that even a slight increase in P_{ME} (88% to 90%) results in exponential increase of γ (1.5 to 3.5). Hence minimization of desorbent consumption conflicts with improvement of purity.

Figure 5.4b represents correlation between raffinate flow rate (β) and P_{ME} . Unlike the previous optimization problem, the purity is not significantly influenced by β when one of the objectives is minimization of γ . The only significant observation which can be made is that that for high purity, a low value of β (around 0.1) is desired. This is congruent with the fact that a low raffinate flow rate is required for increased residence time in section P of the SMBR to increase product purity. Once again, the switch time is

relatively constant at around 5 minutes, as is represented by Figure 5.4c. This optimization problem results in the conclusion that when desorbent minimization is one of the objective functions, then after a certain threshold value an exponential increase in γ will result only in a slight improvement of purity. Hence to obtain high purity, γ has to be kept high just above the threshold value; a further increase is not required.

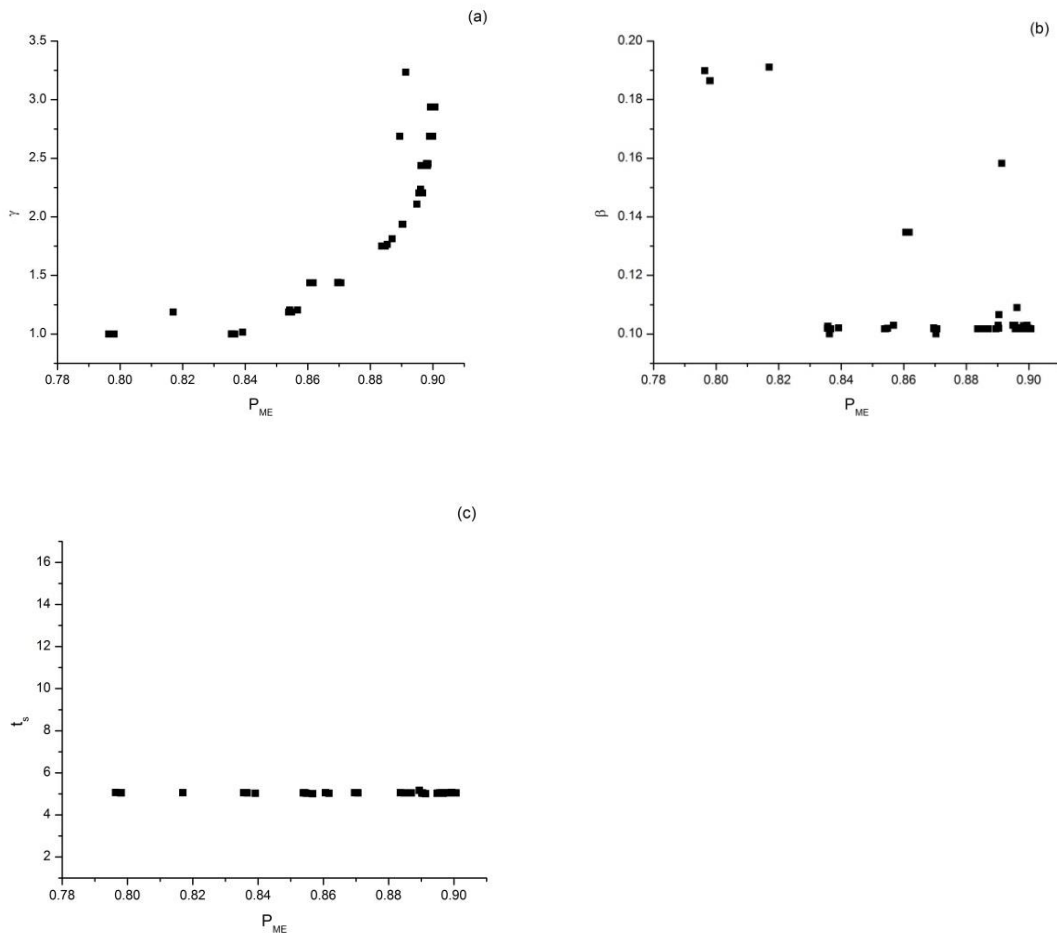


Figure 5.4 Pareto optimal solutions and corresponding operating variables for maximizing purity and minimizing desorbent consumption

5.7 Design stage optimization

This problem involves optimization of SMBR performance by allowing its design parameters such as length of the column to be selected optimally. It is worthwhile to consider this problem for industrial application. The parameter which has been considered for this is column length (L_{col}). Two optimization problems were once again considered for design-stage optimization:

Case 2.1 Simultaneous maximization of yield and purity:

The objective functions, constraints and decision variables for this problem are the same as those of Case 1.1, with the addition of another decision variable; column length [$0.2(m) \leq L_{col} \leq 0.5(m)$]. The Pareto optimal solutions are shown in Figure 5.5.

Figure 5.5a shows the Pareto set for yield and purity of biodiesel. Once again, it is observed that they act in conflicting manner. But a much higher value of purity (97%) can be obtained as compared to case 1.1 where the highest purity value obtained was 87%. Also, the highest yield value obtained in case 1.1 was 79% against a purity value of 76%. The yield in this case is 90% corresponding to value of purity being marginally more than 90% (point 1 in Figure 5.5a). Hence a drastic improvement is achieved when column length is introduced as a decision variable. The purity also acts in conflicting manner against raffinate flow rate, as is evident from Figure 5.5b. A very low value of β (≈ 0.1) is required to achieve 97% purity, indicating the requirement of a higher residence time in section P. Figure 5.5c represents that a high value of desorbent flow rate ($\gamma \approx 3.5$) to achieve a purity in the range of 94% to 97%. Just as in case 1.1, γ has to be kept above a threshold value; further increase in γ will not improve purity. An increase in column length also improves purity, as represented by Figure 5.5d. Larger column length means that the reactants will have more residence time, hence improving the conversion, purity and yield. As far as switch time is concerned, it has increased to about 11 minutes as compared to 5 minutes in Case 1.1. This is due to the introduction of column length as a decision variable. A higher L_{col} value means indicates requirement of a higher residence time before a switch is made.

This optimization problem asserts that SMBR performance can be improved if design parameters are also optimized along with operating parameters. A high value of both yield and purity were obtained when column length was also introduced as a decision variable

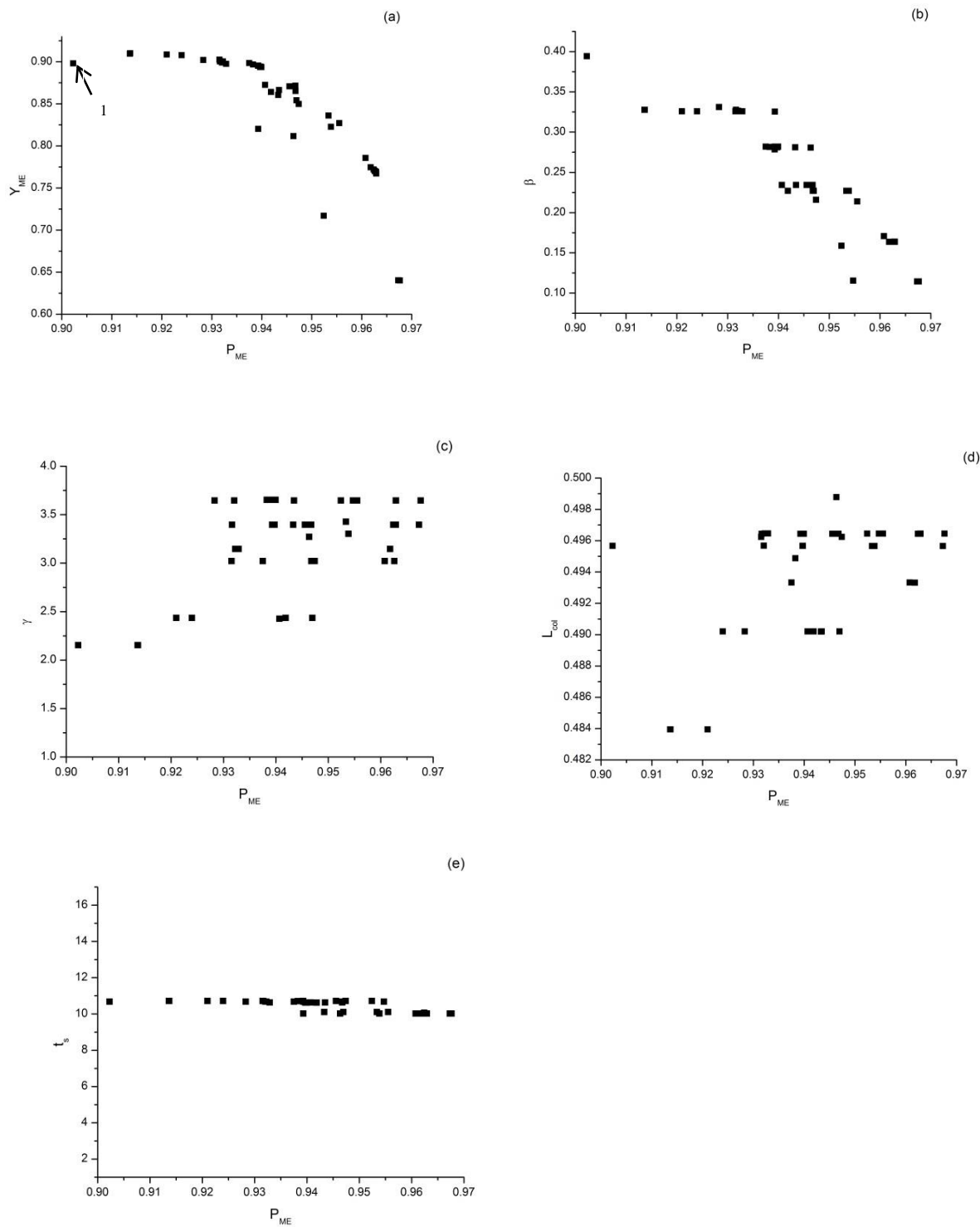


Figure 5.5 Pareto solutions for maximizing yield and purity with column length as a design stage parameter

Case 2.2 Maximization of purity and minimization of desorbent consumption:

The objective functions, constraints and decision variables for this problem are the same as those of Case 1.2, with the addition of another decision variable; column length [$0.2(m) \leq L_{col} \leq 0.5(m)$]. The Pareto optimal solutions are shown in Figure 5.6.

Figure 5.6a shows the relation between γ and purity. At lower values of γ , a linear relation exists with purity. However after that, the graph becomes exponential; indicating that a slight increase in purity would require a very high desorbent consumption, just as in case 1.2. Hence, γ should be just high enough above a threshold value (≈ 2 in this case). Further increase is not necessary.

Figure 5.6b shows the dependence of purity on raffinate flow rate. β is fairly constant at a low value (≈ 0.1). Hence purity is not sensitive to it when column length is a decision variable and minimization of desorbent consumption is an objective. The same trend is shown by switch time; it is fairly constant at around 9 minutes (Figure 5.6c). The dependence of purity on column length is fairly uniform, showing requirement of a high column length for high purity (Figure 5.6d).

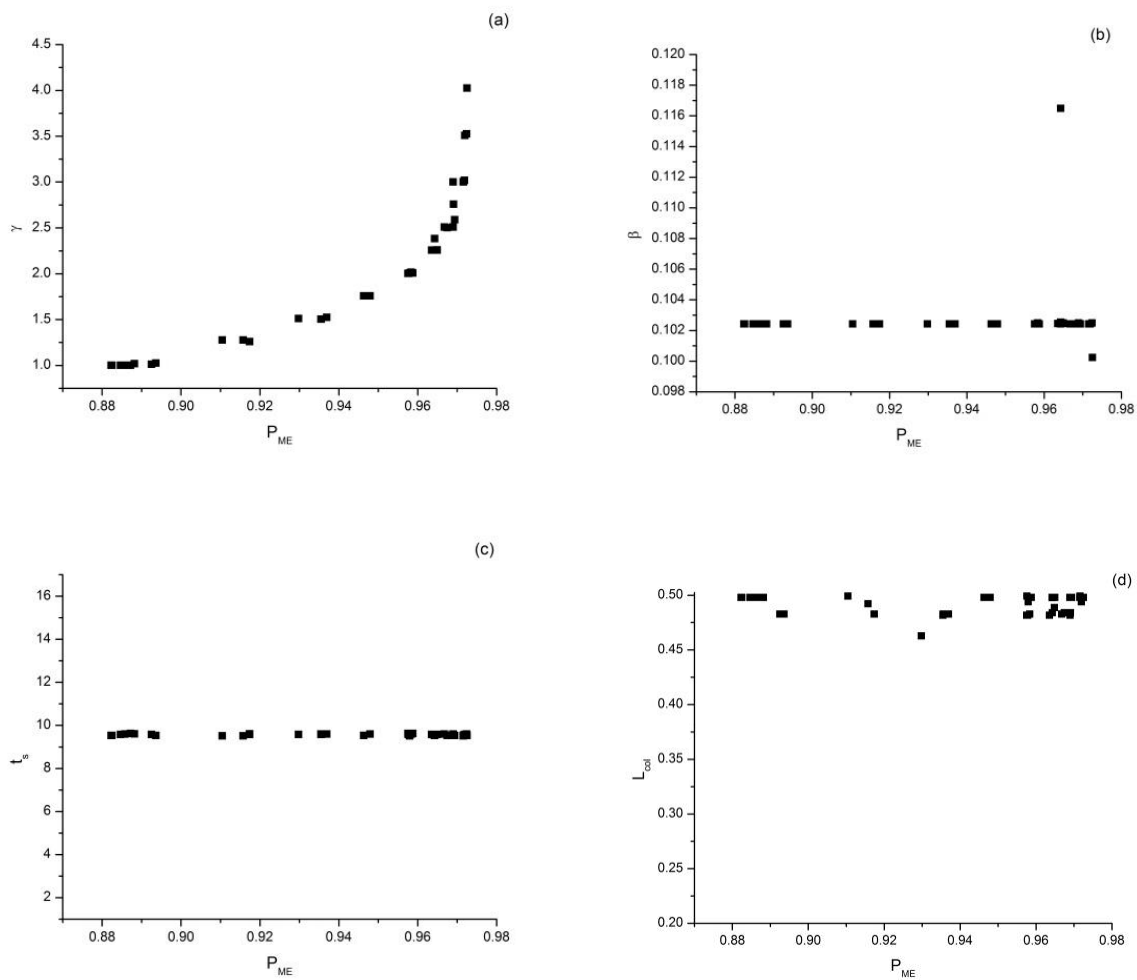


Figure 5.6 Pareto solutions for maximizing purity and minimizing desorbent consumption

5.8 Conclusions

Multi-objective optimization studies were carried out on the performance of a reactive SMB for synthesis of biodiesel. The NSGA algorithm was used to obtain the Pareto optimal solutions. Optimization of both existing set-up and design-stage were studied. Two multi-objective optimization problems were solved involving two objective functions for each mode of operation. Simultaneous maximization of yield and purity as well as maximization of purity and minimization of desorbent consumption were considered as objective functions. It was observed that a yield and purity of above 90% can be achieved by optimizing both operating and design stage parameters. This study extols the usefulness of multi-objective optimization for improvement of design and operation of reactive SMB system for its practical application and successful implementation on industrial scale.

5.9 References

1. Bhaskar V, Gupta SK, Ray AK. Applications of multiobjective optimization in chemical engineering. *Rev Chem Eng.* 2000;16:1-54.
2. Yu W, Hidajat K, Ray AK. Application of Multiobjective Optimization in the Design and Operation of Reactive SMB and Its Experimental Verification. *Ind Eng Chem Res.* 2003;42:6823-6831. doi:10.1021/ie030387p.
3. Rajesh JK, Gupta SK, Rangaiah GP, Ray AK. Multiobjective Optimization of Steam Reformer Performance Using Genetic Algorithm. *Ind Eng Chem Res.* 2000;39:706-717. doi:10.1021/ie9905409.
4. Bhaskar V, Gupta SK, Ray AK. Multiobjective optimization of an industrial wiped film poly(ethylene terephthalate) reactor: Some further insights. *Comput Chem Eng.* 2001;25:391-407. doi:10.1016/S0098-1354(00)00665-7.

5. Tarafder A, Rangaiah GP, Ray AK. Multiobjective optimization of an industrial styrene monomer manufacturing process. *Chem Eng Sci.* 2005;60:347-363. doi:10.1016/j.ces.2004.07.120.
6. Yee AKY, Ray AK, Rangaiah GP. Multiobjective optimization of an industrial styrene reactor. *Comput Chem Eng.* 2003;27:111-130. doi:10.1016/S0098-1354(02)00163-1.
7. Sankararao B, Gupta SK. Multiobjective optimization of the dynamic operation of an industrial steam reformer using the jumping gene adaptations of simulated annealing. *Asia-Pacific J Chem Eng.* 2006;1:21-31. doi:10.1002/apj.4.
8. Mazumder J, Zhu J, Bassi AS, Ray AK. Multiobjective optimization of the operation of a liquid-solid circulating fluidized bed ion-exchange system for continuous protein recovery. *Biotechnol Bioeng.* 2009;103:873-890. doi:10.1002/bit.22328.
9. Wang B, Gebreslassie BH, You F. Sustainable design and synthesis of hydrocarbon biorefinery via gasification pathway: Integrated life cycle assessment and technoeconomic analysis with multiobjective superstructure optimization. *Comput Chem Eng.* 2013;52:55-76. doi:10.1016/j.compchemeng.2012.12.008.
10. Sankararao B, Gupta SK. Multi-objective optimization of an industrial fluidized-bed catalytic cracking unit (FCCU) using two jumping gene adaptations of simulated annealing. *Comput Chem Eng.* 2007;31:1496-1515. doi:10.1016/j.compchemeng.2006.12.012.
11. Zhang Y, Hidajat K, Ray AK. Multi-objective optimization of simulated moving bed and Varicol processes for enantio-separation of racemic pindolol. *Sep Purif Technol.* 2009;65:311-321. doi:10.1016/j.seppur.2008.10.050.
12. Holland JH. *Adaptation in Natural and Artificial Systems: An Introductory Analysis with Applications to Biology, Control, and Artificial Intelligence.*; 1975:1-228. doi:10.1086/418447.

13. John H. Holland, Adaptation in natural and artificial systems. *Ann Arbor MI Univ Michigan Press*. 1992;Ann Arbor:1-200?
<http://www.citeulike.org/group/664/article/400721> \n<http://scholar.google.com/scholar?hl=en&btnG=Search&q=intitle:Adaptation+in+Natural+and+Artificial+Systems#1>.
14. Nandasana AD, Ray AK, Gupta SK. Applications of the Non-Dominated Sorting Genetic Algorithm (NSGA) in Chemical Reaction Engineering Applications of the Non-Dominated Sorting Genetic Algorithm (NSGA) in Chemical Reaction Engineering. *Int J Chem React Eng*. 2003;1.
15. Srinivas N, Deb K. Multiobjective Optimization Using Nondominated Sorting in Genetic Algorithms. *Evol Comput*. 1994;2:221-248. doi:10.1162/evco.1994.2.3.221.
16. Atadashi IM, Aroua MK, Aziz a. A. High quality biodiesel and its diesel engine application: A review. *Renew Sustain Energy Rev*. 2010;14(7):1999-2008.
doi:10.1016/j.rser.2010.03.020.
17. Canakci M, Gerpen JH Van. The Performance and Emissions of a Diesel Engine Fueled with Biodiesel from Yellow Grease and Soybean Oil. 2001;0300(xx):1-17.

Chapter 6

6 Conclusion and future recommendations

6.1 Conclusions

A comprehensive and systematic study of free fatty acid esterification with methanol to produce biodiesel in a simulated moving bed system is presented in this doctoral thesis dissertation. The adsorption constants, kinetic parameters and dispersion coefficients were determined for synthesis reaction of methyl oleate (biodiesel) with methanol as the solvent. Thereafter, an equilibrium-dispersive mathematical model for the multi-column SMB was used to describe the dynamic behaviour of SMBR and the mathematical model was experimentally verified at various operating conditions. Finally, a multi-objective optimization study of SMBR for synthesis of methyl oleate was performed using the validated model for both at the operating-stage (existing set-up) and at design-stage. This was done to determine the optimal design and operating parameters for SMBR to ensure high purity and productivity of the biodiesel formed. Pareto-optimal solutions were obtained. The optimization study was done using non-dominated sorting genetic algorithm (NSGA) in order to obtain equally-good non-dominated solutions.

Determination of adsorption isotherm parameters for biodiesel production by carrying out experiments in single column:

Adsorption and kinetic parameters were determined for the esterification reaction of oleic acid with methanol to produce methyl oleate (biodiesel) and water. This was carried out in a single column packed bed reactor; the column being packed with Amberlyst 15 ion exchange resin which served as both catalyst and adsorbent. Since methanol was present in large excess, a quasi-homogenous kinetic model coupled with a linear adsorption isotherm was followed. The elution profiles of the reactant and products were experimentally determined and compared with those obtained by a mathematical model. The adsorption and kinetic parameters were determined by minimizing an error function

so as to fit the experimentally obtained curves with the model predicted values. Experiments were conducted at room temperature under varying conditions to establish the validity of the obtained parameters. The kinetic parameters obtained were determined to be free from internal and external mass transfer resistances. The model predicted the experimental outcome reasonably well.

Modeling and experimental verification of SMBR for biodiesel synthesis:

The synthesis of biodiesel from the transesterification reaction of free fatty acid and alcohol was investigated in a Simulated Moving Bed Reactor. A four column SMBR set-up with one column in each section was used. Experiments were carried out at different switch times, feed and raffinate flow rates. A rigorous mathematical model was used to predict the dynamic behaviour of the system. The adsorption and kinetic parameters obtained from single column experiments were used by the model to predict the experimental outcome. It was observed that the model predicted the experimental results reasonably well. The highest yield and purity obtained were 56% and 32% respectively; corresponding to 12mins switch time, 0.1ml/min feed flow rate, 1.66ml/min raffinate flow rate and 4ml/min desorbent flow rate. A parametric sensitivity analysis was carried out on the verified model to further investigate the influence of operating conditions on the SMBR performance. It was observed that switch time and raffinate flow rate significantly affected SMBR performance for the current setup. To further improve the performance and successfully implement the SMBR on an industrial scale, a multi-objective optimization must be carried out.

Multi-objective optimization of SMBR for biodiesel synthesis using NSGA:

Multi-objective optimization studies were carried out on the SMBR for biodiesel synthesis. The NSGA algorithm was used to obtain the Pareto set of solutions. Optimization of both existing set up and design stage were studied. The improvement of two objective functions was considered for each optimization study; simultaneous maximization of yield and purity as well as maximization of purity and minimization of

desorbent consumption. It was observed that a yield and purity of above 90% can be achieved by optimizing both operating and design stage parameters. This study proves that multi-objective optimization for improvement of design and operation of reactive SMB system is paramount for its practical application and successful implementation on industrial scale.

6.2 Major contributions of this research

- Investigation of reaction-separation process involving formation of biodiesel from free fatty acid esterification was studied in a Simulated Moving Bed Reactor using both modeling and experimental verification of the model.
- Adsorption isotherm parameters and kinetic parameters were determined for the free fatty acid esterification reaction carried out in a single column packed bed reactor using both modeling and experiments.
- Theoretical and experimental studies were carried out in SMBR for biodiesel production followed by parametric sensitivity analysis to further verify the robustness of the model.
- Multiobjective optimization studies were carried out for both existing and design stage of the SMBR to further improve its performance

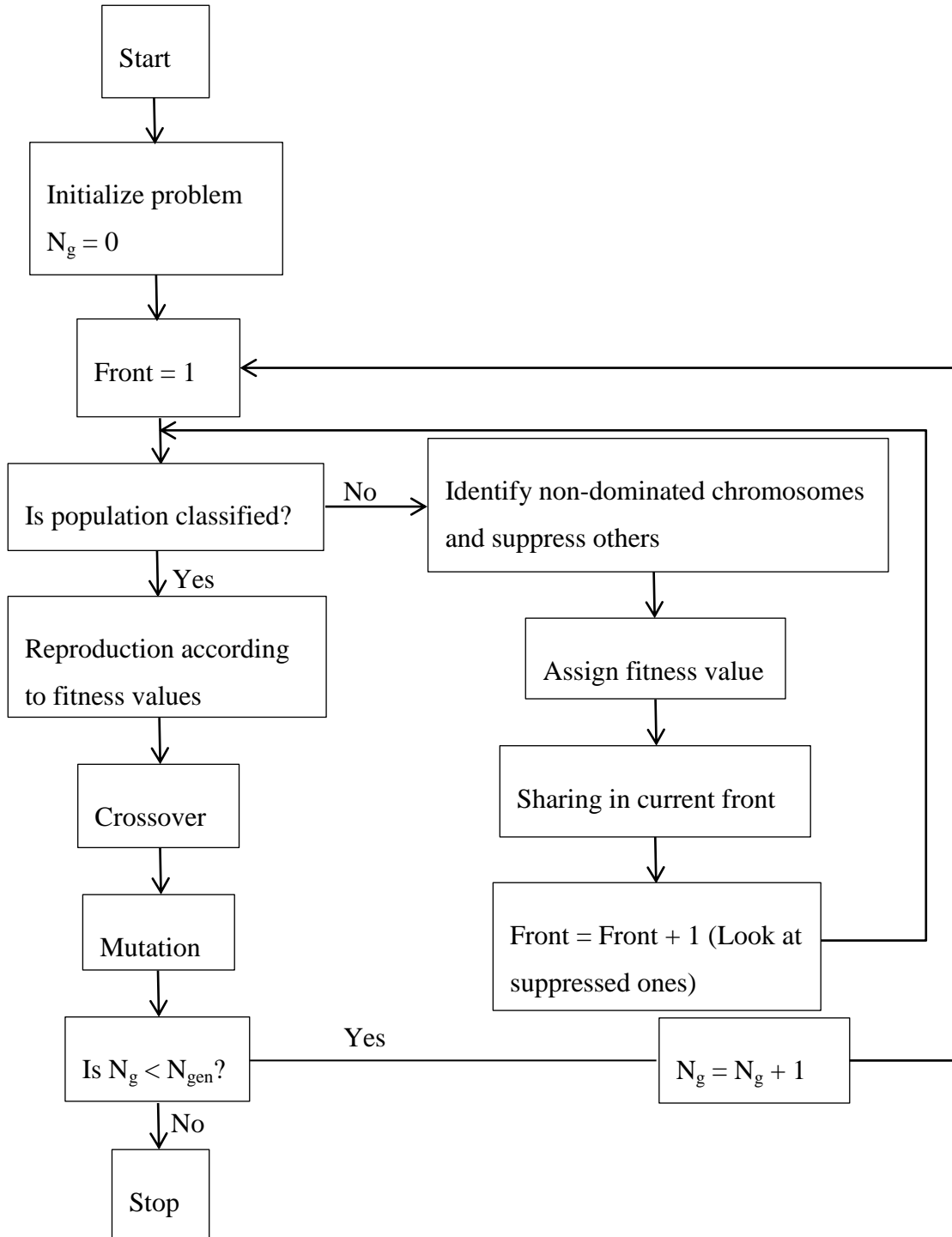
6.3 Recommendations for future work

To determine the adsorption and kinetic constants, a linear adsorption isotherm was assumed. This holds true at low reactant concentrations. On increasing the concentration, the isotherm would deviate from linear behaviour. Hence, it is suggested that a non-linear isotherm model be used to determine the constants that would be valid at higher reactant concentrations. A simple SMB set-up was used in this investigation involving a total of four columns; one column in each section. Putting more number of columns, especially in the zone responsible for reaction can improve the SMBR performance. The optimization problems in this investigation were solved by numerical simulation. However to validate

the multi-objective optimization results, experiments must be carried out. The performance can be further improved by carrying out VARICOL operation, which involves non-synchronous shifting of the feed and desorbent ports during a switching time in contrast to synchronous switching adopted in traditional simulated moving bed operation.

Appendices

Appendix A: A schematic representation of NSGA



Appendix B: Raw data for non-reactive breakthrough experiments

Data points Corresponding to Fig 3.1a

Time mins	Concentration (mol/lit)			
	Methyl Oleate (experimental)	Methyl Oleate (model predicted)	Water (experimental)	Water (model predicted)
2.25	0	0	0	0
4.25	0	0	0	0
6.25	0	0	0	0
8.25	0	0	0	0
10.25	0.003025	0.003001	0	0
12.25	0.037401	0.024897	0	0
14.25	0.096348	0.076248	0	0
16.25	0.139004	0.123280	0	0
18.25	0.128299	0.121150	0	0.002180
20.25	0.086715	0.077567	0	0.004189
22.25	0.045573	0.034930	0	0.006897
24.25	0.021535	0.011903	0	0.010112
26.25	0.009206	0.003255	0.002133	0.013555
28.25	0.003920	7.47E-04	0.009358	0.016947
30.25	0.001750	0	0.013932	0.020047
32.25	0.002334	0	0.021137	0.022688
34.25	0	0	0.021668	0.024765
36.25	0	0	0.023229	0.026247
38.25	0	0	0.036391	0.027145
40.25	0	0	0.030372	0.027504
42.25	0	0	0.028752	0.027387
44.25	0	0	0.025147	0.026874
46.25	0	0	0.024656	0.026041
48.25	0	0	0.022377	0.024961
50.25	0	0	0.020177	0.023703
52.25	0	0	0.018872	0.022324
54.25	0	0	0.017013	0.020880
56.25	0	0	0.014799	0.019402
58.25	0	0	0.010948	0.017930
60.25	0	0	0.010583	0.016490
62.25	0	0	0.008756	0.015100
64.25	0	0	0.005772	0.013773

66.25	0	0	0.005598	0.012519
68.25	0	0	0	0.011344
70.25	0	0	0	0.010251
72.25	0	0	0	0.009239
74.25	0	0	0	0.008308
76.25	0	0	0	0.007456
78.25	0	0	0	0.006679
80.25	0	0	0	0.005973

Data points corresponding to Fig 3.1b

Time mins	Concentration mol/lit			
	Methyl Oleate (experimental)	Methyl Oleate (model predicted)	Water (experimental)	Water (model predicted)
2.25	0	0	0	0
4.25	0	0	0	0
6.25	0	0	0	0
8.25	0	0	0	0
10.25	0.005424	0.005376	0	0
12.25	0.037009	0.033477	0	0
14.25	0.067794	0.070093	0	0
16.25	0.049937	0.068726	0	0
18.25	0.040377	0.039251	0	0.001370
20.25	0.023029	0.015238	0.001287	0.002489
22.25	0.013225	0.004452	0.002778	0.003914
24.25	0.006127	0.001050	0.003619	0.005531
26.25	0.003395	0	0.006619	0.007202
28.25	0.002819	0	0.007222	0.008801
30.25	0.001158	0	0.008148	0.010229
32.25	0	0	0.009328	0.011417
34.25	0	0	0.014370	0.012332
36.25	0	0	0.011667	0.012966
38.25	0	0	0.010793	0.013328
40.25	0	0	0.010117	0.013444
42.25	0	0	0.006670	0.013346
44.25	0	0	0.006609	0.013068
46.25	0	0	0.006111	0.012648

48.25	0	0	0.005556	0.012118
50.25	0	0	0.00500	0.011509
52.25	0	0	0.004722	0.010845
54.25	0	0	0.004419	0.010153
56.25	0	0	0.004121	0.009448
58.25	0	0	0.002731	0.008746
60.25	0	0	0	0.008058
62.25	0	0	0	0.007393
64.25	0	0	0	0.006760
66.25	0	0	0	0.006159
68.25	0	0	0	0.005595
70.25	0	0	0	0.005069
72.25	0	0	0	0.004580
74.25	0	0	0	0.004132
76.25	0	0	0	0.003718
78.25	0	0	0	0.003341
80.25	0	0	0	0.002997

Data points corresponding to Fig 3.1c

Time mins	Concentration mol/lit			
	Methyl Oleate (experimental)	Methyl Oleate (model predicted)	Water (experimental)	Water (model predicted)
2.25	0	0	0	0
4.25	0	0	0	0
6.25	0.036539	0.016056	0	0
8.25	0.126080	0.135160	0.006540	0
10.25	0.176075	0.185720	0.010941	0
12.25	0.115973	0.121970	0.016854	0.003499
14.25	0.046359	0.016870	0.034582	0.011280
16.25	0.015878	5.48E-04	0.051513	0.024753
18.25	0.004745	6.79E-06	0.060706	0.041108
20.25	0.001213	0	0.066542	0.055584
22.25	0	0	0.064968	0.064481
24.25	0	0	0.064602	0.066652
26.25	0	0	0.055134	0.063085
28.25	0	0	0.049480	0.055780

30.25	0	0	0.048157	0.046748
32.25	0	0	0.032687	0.037543
34.25	0	0	0.028957	0.029135
36.25	0	0	0.022067	0.021987
38.25	0	0	0.019037	0.016213
40.25	0	0	0.015275	0.011731
42.25	0	0	0.009902	0.008350
44.25	0	0	0.008183	0.005864
46.25	0	0	0.007191	0.004073
48.25	0	0	0.005444	0.002801
50.25	0	0	0.003001	0.001911
52.25	0	0	0.002138	0.001292
54.25	0	0	1.00E-03	0
56.25	0	0	0	0
58.25	0	0	0	0
60.25	0	0	0	0
62.25	0	0	0	0
64.25	0	0	0	0
66.25	0	0	0	0
68.25	0	0	0	0
70.25	0	0	0	0
72.25	0	0	0	0
74.25	0	0	0	0
76.25	0	0	0	0
78.25	0	0	0	0
80.25	0	0	0	0

Data points corresponding to Fig 3.1d

Time mins	Concentration			
	mol/lit			
	Methyl Oleate (experimental)	Methyl Oleate (model predicted)	Water (experimental)	Water (model predicted)
2.25	0	0	0	0
4.25	0	0	0	0
6.25	0	0	0	0
8.25	0	0	0	0
10.25	0.003025	0.003644	0	0

12.25	0.027401	0.025796	0	0
14.25	0.076348	0.070105	0	0
16.25	0.090000	0.102430	0	0
18.25	0.082600	0.090913	0	0.001359
20.25	0.060500	0.052550	0	0.002686
22.25	0.045573	0.021435	0	0.004534
24.25	0.021535	0.006629	0	0.006791
26.25	0.006206	0.001653	0.002133	0.009281
28.25	0.003000	3.48E-04	0.009358	0.011803
30.25	1.75E-04	0	0.013932	0.014181
32.25	0	0	0.021137	0.016276
34.25	0	0	0.021668	0.018000
36.25	0	0	0.023229	0.019307
38.25	0	0	0.02089	0.020191
40.25	0	0	0.020000	0.020671
42.25	0	0	0.019780	0.020789
44.25	0	0	0.018000	0.020591
46.25	0	0	0.017880	0.020130
48.25	0	0	0.017000	0.019460
50.25	0	0	0.016770	0.018630
52.25	0	0	0.01487	0.017684
54.25	0	0	0.01287	0.016664
56.25	0	0	0.01099	0.015598
58.25	0	0	0.01052	0.014519
60.25	0	0	0.00876	0.013445
62.25	0	0	0.006756	0.012393
64.25	0	0	0.005772	0.011378
66.25	0	0	0.005598	0.010409
68.25	0	0	0	0.009491
70.25	0	0	0	0.008629
72.25	0	0	0	0.007825
74.25	0	0	0	0.007077
76.25	0	0	0	0.006388
78.25	0	0	0	0.005754
80.25	0	0	0	0.005175

Appendix C: Raw data for non-reactive breakthrough experiments

Data points corresponding to Fig 3.2a

Time	Concentration					
mins	mol/lit					
	Methyl Oleate (experimental)	Water (experimental)	Oleic Acid (experimental)	Methyl Oleate (model predicted)	Water (model predicted)	Oleic Acid (model predicted)
2.25	0	0	0	0	0	0
4.25	0	0	0	0	0	0
6.25	0	0	0	0	0	0
8.25	0	0	0	0	0	0.001037
10.25	0	0	0.010389	0.001946	0	0.017096
12.25	0	0	0.045372	0.011623	0.001287	0.065542
14.25	0.030076	0.003215	0.095073	0.028541	0.003408	0.111270
16.25	0.040496	0.003957	0.10568	0.038814	0.005680	0.104690
18.25	0.034003	0.004474	0.071904	0.032534	0.007043	0.057636
20.25	0.027698	0.004895	0.04755	0.018119	0.007491	0.020219
22.25	0.016462	0.005718	0.023691	0.007249	0.007529	0.004986
24.25	0.00965	0.005889	0.011894	0.002245	0.007440	0
26.25	0.005308	0.006301	0.005894	0	0.007300	0
28.25	0.002484	0.006333	0.002779	0	0.007113	0
30.25	0.001162	0.006381	0.001482	0	0.006876	0
32.25	0	0.010352	0	0	0.006599	0
34.25	0	0.008906	0	0	0.006286	0
36.25	0	0.008758	0	0	0.005948	0
38.25	0	0.007292	0	0	0.005592	0
40.25	0	0.006833	0	0	0.005223	0
42.25	0	0.006333	0	0	0.004852	0
44.25	0	0.006101	0	0	0.004486	0
46.25	0	0.006039	0	0	0.004128	0
48.25	0	0.004898	0	0	0.003784	0
50.25	0	0.004333	0	0	0.003455	0
52.25	0	0.004142	0	0	0.003145	0
54.25	0	0.003255	0	0	0.002853	0
56.25	0	0.003234	0	0	0.002581	0
58.25	0	0.003051	0	0	0.002329	0
60.25	0	0.002206	0	0	0.002096	0
62.25	0	0	0	0	0.001883	0

64.25	0	0	0	0	0.001686	0
66.25	0	0	0	0	0.001511	0
68.25	0	0	0	0	0.001352	0
70.25	0	0	0	0	0.001205	0
72.25	0	0	0	0	0.001075	0
74.25	0	0	0	0	0	0
76.25	0	0	0	0	0	0
78.25	0	0	0	0	0	0
80.25	0	0	0	0	0	0

Data points corresponding to Fig 3.2b

Time mins	Concentration (mol/lit)					
	Methyl Oleate (experimental)	Water (experimental)	Oleic Acid (experimental)	Methyl oleate (model predicted)	Water (model predicted)	Oleic Acid (model predicted)
2.25	0	0	0	0	0	0
4.25	0	0	0	0	0	0
6.25	0	0	0	0	0	0
8.25	0	0	0	0	0	0.00111
10.25	0	0	0.007564	0.001227	0	0.018339
12.25	0.004567	0	0.059705	0.006813	0	0.061908
14.25	0.012806	0	0.087400	0.013349	0.001698	0.073946
16.25	0.015715	0.001167	0.063681	0.012764	0.002298	0.042891
18.25	0.011843	0.002438	0.032299	0.007353	0.002488	0.015018
20.25	0.008491	0.002684	0.017146	0.002937	0.002496	0.003650
22.25	0.005257	0.002833	0.008952	0	0.002457	0
24.25	0.002895	0.003294	0.004039	0	0.002401	0
26.25	0.001359	0.003389	0.002318	0	0.002335	0
28.25	0	0.003689	0.001129	0	0.002254	0
30.25	0	0.004056	0	0	0.002162	0
32.25	0	0.004593	0	0	0.002057	0
34.25	0	0.004669	0	0	0.001945	0
36.25	0	0.005201	0	0	0.001830	0
38.25	0	0.005611	0	0	0.001709	0
40.25	0	0.007253	0	0	0.001586	0
42.25	0	0.004454	0	0	0.001468	0

44.25	0	0.004359	0	0	0.001350	0
46.25	0	0.004293	0	0	0.001238	0
48.25	0	0.004171	0	0	0.001128	0
50.25	0	0.004117	0	0	0.001028	0
52.25	0	0.004101	0	0	0	0
54.25	0	0.003778	0	0	0	0
56.25	0	0.003500	0	0	0	0
58.25	0	0.003389	0	0	0	0
60.25	0	0.003278	0	0	0	0
62.25	0	0.003222	0	0	0	0
64.25	0	0.003167	0	0	0	0
66.25	0	0.003157	0	0	0	0
68.25	0	0.002944	0	0	0	0
70.25	0	0.002833	0	0	0	0
72.25	0	0.002401	0	0	0	0
74.25	0	0.001761	0	0	0	0
76.25	0	0.001611	0	0	0	0
78.25	0	0.001167	0	0	0	0
80.25	0	0	0	0	0	0

Data points corresponding to Fig 3.2c

Time mins	Concentration					
	mol/lit					
	Methyl Oleate (experimental)	Water (experimental)	Oleic Acid (experimental)	Methyl Oleate (model predicted)	Water (model predicted)	Oleic Acid (model predicted)
2.25	0	0	0	0	0	0
4.25	0	0	0	0	0	0
6.25	0	0	0.028060	0.002082	0	0.017122
8.25	0.008600	0	0.152718	0.018368	0.001569	0.134190
10.25	0.020771	0.002342	0.202108	0.025591	0.004490	0.179850
12.25	0.022335	0.003987	0.146747	0.017046	0.007019	0.113580
14.25	0.017297	0.007947	0.074597	0.002413	0.007603	0.014470
16.25	0.009801	0.010511	0.029820	0	0.007389	0
18.25	0.004974	0.007877	0.012051	0	0.006944	0
20.25	0.001915	0.006678	0.004151	0	0.006275	0
22.25	0	0.006659	0.001382	0	0.005447	0

24.25	0	0.006610	0	0	0.004547	0
26.25	0	0.006272	0	0	0.003664	0
28.25	0	0.005745	0	0	0.002863	0
30.25	0	0.005651	0	0	0.002180	0
32.25	0	0.005077	0	0	0.001621	0
34.25	0	0.003187	0	0	0.001182	0
36.25	0	0.002606	0	0	0	0
38.25	0	0.001856	0	0	0	0
40.25	0	0.001073	0	0	0	0
42.25	0	0	0	0	0	0
44.25	0	0	0	0	0	0
46.25	0	0	0	0	0	0
48.25	0	0	0	0	0	0
50.25	0	0	0	0	0	0
52.25	0	0	0	0	0	0
54.25	0	0	0	0	0	0
56.25	0	0	0	0	0	0
58.25	0	0	0	0	0	0
60.25	0	0	0	0	0	0
62.25	0	0	0	0	0	0
64.25	0	0	0	0	0	0
66.25	0	0	0	0	0	0
68.25	0	0	0	0	0	0
70.25	0	0	0	0	0	0
72.25	0	0	0	0	0	0
74.25	0	0	0	0	0	0
76.25	0	0	0	0	0	0
78.25	0	0	0	0	0	0
80.25	0	0	0	0	0	0

Data points corresponding to Fig 3.2d

Time mins	Concentration					
	mol/lit					
	Methyl Oleate (experimental)	Water (experimental)	Oleic Acid (experimental)	Methyl Oleate (model predicted)	Water (model predicted)	Oleic Acid (model predicted)
2.25	0	0	0	0	0	0
4.25	0	0	0	0	0	0
6.25	0	0	0	0	0	0
8.25	0	0	0	0	0	0
10.25	0	0	0.01	0	0	0.005243
12.25	0.006000	0	0.038000	0.005714	0	0.029119
14.25	0.020000	0.002930	0.078000	0.016589	0.001710	0.065215
16.25	0.024000	0.003300	0.065000	0.025695	0.003325	0.079919
18.25	0.016000	0.003800	0.045000	0.024238	0.004601	0.058766
20.25	0.011000	0.004100	0.034000	0.014985	0.005191	0.027859
22.25	1.00E-04	0.004200	0.023000	0.006548	0.005324	0.009280
24.25	0	0.004700	0.012000	0.002168	0.005277	0.002340
26.25	0	0.005000	0	0	0.005167	0
28.25	0	0.004300	0	0	0.005024	0
30.25	0	0.004000	0	0	0.004850	0
32.25	0	0.003300	0	0	0.004648	0
34.25	0	1.00E-03	0	0	0.004422	0
36.25	0	0	0	0	0.004180	0
38.25	0	0	0	0	0.003925	0
40.25	0	0	0	0	0.003665	0
42.25	0	0	0	0	0.003404	0
44.25	0	0	0	0	0.003144	0
46.25	0	0	0	0	0.002893	0
48.25	0	0	0	0	0.002649	0
50.25	0	0	0	0	0.002419	0
52.25	0	0	0	0	0.002199	0
54.25	0	0	0	0	0.001997	0
56.25	0	0	0	0	0.001804	0
58.25	0	0	0	0	0.001628	0
60.25	0	0	0	0	0.001466	0
62.25	0	0	0	0	0.001315	0
64.25	0	0	0	0	0.001180	0
66.25	0	0	0	0	0.001055	0
68.25	0	0	0	0	0	0
70.25	0	0	0	0	0	0

72.25	0	0	0	0	0	0
74.25	0	0	0	0	0	0
76.25	0	0	0	0	0	0
78.25	0	0	0	0	0	0
80.25	0	0	0	0	0	0

Curriculum Vitae

Name: Nillohit Mitra Ray

Post-secondary Education and Degrees:

The University of Calcutta
Calcutta, West Bengal, India
2002-2005 B.Sc. in Microbiology

University of Burdwan
Burdwan, West Bengal, India
2005-2007 M.Sc. in Biotechnology

West Bengal University of Technology
Calcutta, West Bengal, India
2007-2009 M.Tech. in Biotechnology

The University of Western Ontario
London, Ontario, Canada
2009-2015 PhD Candidate at the Department of Chemical and Biochemical Engineering

Honours and Awards: Western Engineering Scholarship
2009-2015

Related Work Experience

Graduate Research Assistant
The University of Western Ontario
2009-2015

Graduate Teaching Assistant
The University of Western Ontario
2010-2015